DEMOCRATIC AND POPULAR REPUBLIC OF ALGERIA
Ministry of Higher Education and Scientific Research

N° Série: ……./2021

University Kasdi Merbah Ouargla

Faculty of Hydrocarbons and renewable energies and science of the earth and the universe

Hydrocarbon Production Department

MEMOIRE

To obtain the Master's degree
Option: Academic Production

Presented by:

Akram Aouarib, Mohammed Tedjini

- TOPIC-

Evaluation of the injection performance in the inter-zone 17-19 of HMD field

Presented on: 23 /06 / 2021 in front of the review committee

Judges:

President :	BELMILOUD Fatima Zohra	M.A.A	Univ. Ouargla
Reporter :	ARBAOUI Mohamed Ali	M.A.A	Univ. Ouargla
Reviewers:	LEBTAHI Hamid	M.C.B	Univ. Ouargla

Acknowledgement

First of all, we thank "Allah" Almighty who gave us the courage, the will and the strength to accomplish this modest work. Thank you for lighting the way to success.

We would like to thank especially our parents.

Special thanks to our supervisor Mr. ARBAOUI Med ALI for his participation and his prodigious advices to the realization of this work.

We thank Mr. BOUGAA Lakhdar for his encouragement and valuable advice

We would also like to thank all the teachers of the hydrocarbon department who have contributed in some way to our training during the whole university course.

Finally, we cannot mention all those who have contributed in any way to the elaboration of this work, that all those who have helped us with a simple encouragement find here the expression of our sincerest gratitude.

DEDICATION

I have the great honor to dedicate this modest work:

To the love of my life my dear mother to whom I owe what I am,

She who has always been there for me and who has never stopped praying for my happiness.

To the one who made me a man,

My dear father, for all the advice he gave me, the support he showed me and the sacrifices he made to see me succeed.

My dearest brothers.

My dearest sister.

All my big family.

My best friend Ramzi.

My friends since childhood.

My friends who have accompanied me in this university stage.

To all those whom I love and respect

AOUARIB AKRAM

DEDICATION

It is my great pleasure to dedicate this modest work:

To my dearest father for his encouragement, support, love and sacrifice so that nothing hinders the progress of my studies.

To my dearest mother who has never stopped praying for me in the hope that this one can bring a little more joy to their lives.

To all my brothers, sisters and all my family and especially my grandfather.

To all my friends, each one in his own name.

To all those I love and respect.

TEDJINI MOHAMMED

Abstract:
The recovery of hydrocarbons is done through stages: primary, secondary and EOR, the primary recovery uses the natural energy of the reservoir to produce hydrocarbons, the secondary recovery comes after that and it depends on injecting, water and gas into the reservoir to energize it.
in order to study the efficiency of injection, we have chosen the inter-zone 17-19 which located in the South-East of the Hassi -Messaoud field.

There are two different methods for estimating the quantities of hydrocarbons: The volumetric method which is used to calculate reserves at the beginning of the Development of the reservoir. and the dynamic method which depend on the material balance equation.

After analyzing the VRR and the HCPVI curves we find that the withdrawal-injection balance is established in our zone and the recovery factor reaches 36% after the injection of 57.9% of the pore volume.

Keywords: VRR, HCPVI, MBAL software, Injection patterns, Forecast.

Résumé :
La récupération des hydrocarbures se fait par étapes : primaire, secondaire et RAP, la récupération primaire utilise l'énergie naturelle du réservoir pour produire des hydrocarbures, la récupération secondaire vient ensuite et elle dépend de l'injection d'eau et de gaz dans le réservoir pour le maintien de pression.

Afin d'étudier l'efficacité de l'injection, nous avons choisi l'inter-zone 17-19 qui est située au sud-est du champ de Hassi-Messaoud.

Il existe deux méthodes différentes pour estimer les quantités d'hydrocarbures : La méthode volumétrique qui est utilisée pour calculer les réserves au début du développement du réservoir. Et la méthode dynamique qui dépend de l'équation du bilan matière.

Après l'analyse des courbes VRR et HCPVI, on a constaté que l'équilibre soutirage-injection est établi dans notre zone et le facteur de récupération atteint 36% après l'injection de 57,9% du volume poreux.

Mots-clés : VRR, HCPVI, logiciel MBAL, patterns d'injection, prévisions.

الملخص:
يتم استخلاص الهيدروكربونات عبر مراحل: أولية، ثانوية والاستخلاص المعزز للنفط ، الاستخلاص الأولي يستخدم الطاقة الطبيعية للخزان لإنتاج الهيدروكربونات ثم يأتي الاستخلاص الثانوي بعد ذلك والذي يعتمد على حقن المياه والغاز في الخزان لتزويده بالطاقة .
من أجل دراسة كفاءة الحقن اخترنا المنطقة البينية 17-19 التي تقع في الجنوب الشرقي من حقل حاسي مسعود.

هناك طريقتان مختلفتان لتقدير كميات الهيدروكربونات: الطريقة الحجمية التي تستخدم لحساب الاحتياطيات في بداية تطوير المكمن. والطريقة الديناميكية التي تعتمد على معادلة توازن المواد.

بعد تحليل منحنيات VRR و HCPVI ، وجد أن توازن السحب والحقن قد تم إنشاؤه في منطقتنا وأن عامل الاسترداد يصل إلى 36٪ بعد حقن 57.9٪ من حجم المسام.

الكلمات المفتاحية: VRR، HCPVI ، برنامج MBAL ، أنماط الحقن ، التنبؤ.

Contents

Figure list

Tables list

Symbols / Abbreviations

Δ**p** Change in reservoir pressure = pi − p, bar.

μ_o = Oil viscosity, cp.

μ_w = water viscosity, cp.

A = well or reservoir drainage area, m^2**.**

B_g = Gas Formation Volume Factor, m^3/STm^3

B_{gi} = Initial gas formation volume factor, m^3/STm^3

B_o = Oil Formation Volume Factor, m^3/STm^3

B_{oi} = Initial oil Formation Volume Factor, m^3/STm^3

B_w = Water Formation Volume Factor, m^3/STm^3

c_f = Formation (rock) compressibility, bar^{-1}

c_w = Water compressibility, bar^{-1}

F = withdrawal of fluids in reservoir conditions, Rm^3.

F_w = fractional water flow, fraction

G = Initial gas-cap gas, STm^3

Ginj = Cumulative gas injected, STm^3

GOR = Gas Oil Ratio, m^3/m^3

G_p = Cumulative gas produced, STm^3

HCPVi = Hydrocarbon Pore Volume Injection, fraction.

I_g = Gas Injection flow rate, km^3/month

I_w = Water Injection flow rate, km^3/month

k = absolute permeability, fraction.

k_o = effective permeability to oil for a given oil saturation, fraction.

k_{ro} = relative permeability to oil, fraction.

k_{rw} = relative permeability to water, fraction.

k_w = effective permeability to water at some given water saturation, fraction.

M = mobility ratio, fraction

M = Ratio of initial gas-cap-gas reservoir volume to initial reservoir oil volume, m^3/m^3

N = Initial (original) oil in place, STm^3

N_p = Cumulative oil produced, STm^3

P = Volumetric average reservoir pressure

P.V = Pore volume, m^3

P_b = Bubble point pressure, bar

P_i = Initial reservoir pressure, bar

Q_g = Gas flow rate, STm^3/ month

Q_o = Oil production flow rate, STm^3/month

Q_w = Water production flow rate, STm^3/month

R_F = Recovery Factor, Fraction.

R_p Cumulative gas-oil ratio, m^3/m^3

R_S = Solution Gas Oil Ratio, m^3/m^3

R_{si} = Initial solution gas oil ratio, $m^{3/}$ m^3

R_{sw} = Gas solubility in the water, $m^{3/}$ m^3

SOOIP = Original oil in place at surface conditions, m^3

Swi = Initial water saturation, fraction

VRR = Voidage Replacement Ratio, fraction.

WAG = Water alternating gas.

We = Cumulative water influx, m^3

W_{inj} = Cumulative water injected, STm^3

W_p = Cumulative water produced, m^3

λ_o = oil mobility, md/cp

λ_w = water mobility, md/cp

Φ = porosity, fraction.

EOR= enhanced oil recovery.

RAP= récupération assistée du pétrole.

GENERAL INTRODUCTION

The ultimate purpose of oil field development is to recover the maximum amount of reserves in place in the most efficient and economical manner. at the early stages of any oil field life the hydrocarbons are produced by the natural energy of the reservoir which come from expanding of the rock and liquid, releasing and expanding of the gas dissolved in oil, expanding of the gas cap or active aquifer. when these natural mechanisms are no longer able to ensure the goal mentioned above, the use of secondary recovery mechanisms becomes necessary, Gas and water injection remains the most widely used methods of enhanced recovery due to their efficiency and relatively low cost compared to other methods.

The success of any injection project as an enhanced recovery method requires careful monitoring and regular adjustment of its parameters because the knowledge available at the time of implementation of such a project is often limited.

The injection project implemented in the inter-zone 17-19 of the Hassi Messaoud Southeastern field includes both gas and water injection and it has helped, especially in its early years, to improve oil recovery in this zone. However, this relative success has not lasted and oil production has fallen back to its pre-injection levels. This leads us to question the causes of this drop in performance and the solutions to improve this performance and increase the ultimate recovery of oil.

The objectives of the work:

- Evaluate the efficiency of the injection implemented in the inter-zone 17-19.
- Diagnose the problems of the injection project using monitoring and surveillance techniques.
- Guiding the actions to be taken to remedy these problems by setting priorities and focusing on those that can provide the greatest payback.

This work is structured in four chapters followed by a general conclusion and recommendations.
The first chapter discusses the various methods of oil recovery focusing on the secondary ones.
In the second chapter we identified the drainage mechanisms and the different methods of estimating the reserves in place. The third, chapter deal with the estimation of recoverable reserves by the material balance method based on production data using the MBAL simulation software.
The fourth chapter discuss the different problems causing the production decline and give a hint on the future of the zone.

CHAPTER I: GENERALITY ABOUT THE OIL RECOVERY

I.1. Introduction:

The recovery of hydrocarbons is done through stages: primary recovery which is the volume of hydrocarbons produced using the natural energy of the reservoir and/or artificial lift through a single wellbore, after this energy gets exhausted, secondary recovery comes in play, and it refers to volume of hydrocarbons produced using external energy add to the reservoir such as injecting fluids to maintain or increase the initial energy in the reservoir.

Enhanced Oil Recovery comes after the above and aims to increase oil retrieval from the oil reservoir.

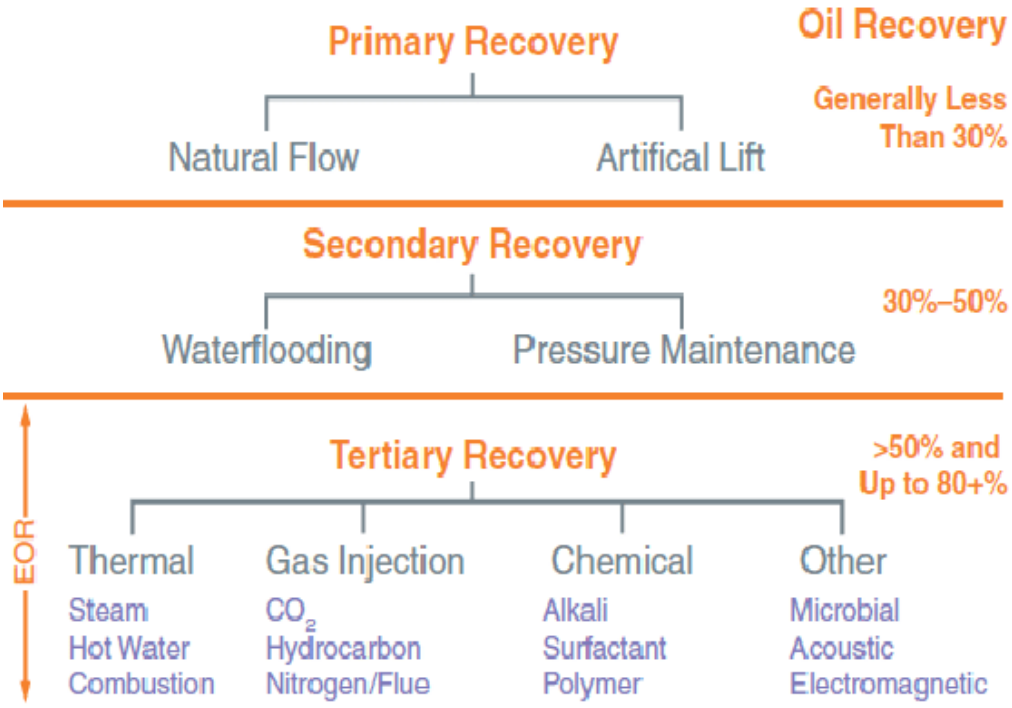

Figure I. 1: The different oil recovery stages and the corresponding oil recovery factor [14].

I.2. Primary recovery:

Primary recovery, is the initial stage in extracting hydrocarbons when natural energy is used to move oil through reservoir into the production well this energy comes from gravity forces, expanding rock and liquid, releasing and expanding gas dissolved in oil while reducing reservoir pressure (depletion drive), expanding the gas cap or active aquifer, or a combination of these factors [11].

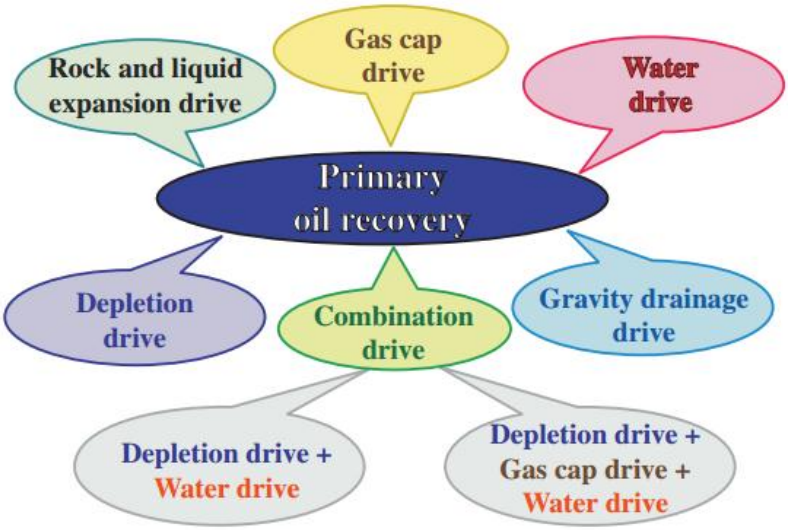

Figure I. 2: Driving processes for the primary oil recovery stage [22].

I.3. Secondary recovery:

The secondary recovery of hydrocarbons involves the introduction of an external energy from the outside into the reservoir via one wellbore and production of oil and/or gas from another wellbore. Secondary oil recovery methods include water injection, immiscible gas injection, and immiscible water alternating gas injection to energize the reservoir or sweep oil to increase production. however the most common fluid injected is water because of its availability, low cost, and high specific gravity which facilitates injection [16].

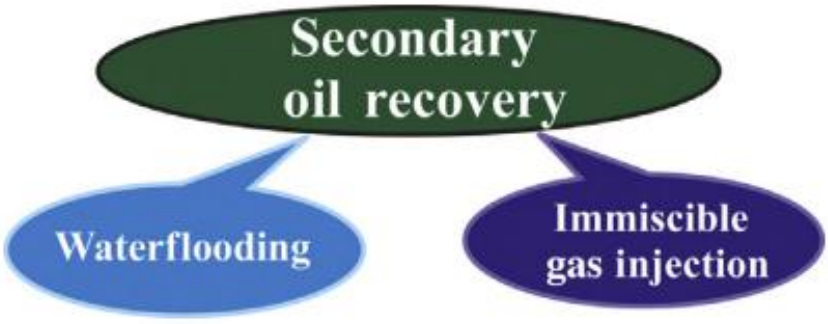

Figure I. 3: Driving processes for the secondary oil recovery stage [22].

I.3.1. Waterflooding:

Waterflooding is one of the major oil production techniques. It is estimated that almost half of all produced oil is produced by use of waterflooding. Waterflooding is carried out by pumping water into a series of injection wells and hydrocarbons production through the production wells. In general, waterflooding is carried out to achieve any of the following goals, or combinations thereof:

- Reservoir pressure maintenance.
- Disposal of connate water after separation from hydrocarbons.
- Creation of a water-pressure regime for displacing hydrocarbons from injection wells to producing wells.
- Balance the voidage replacement ration [13].

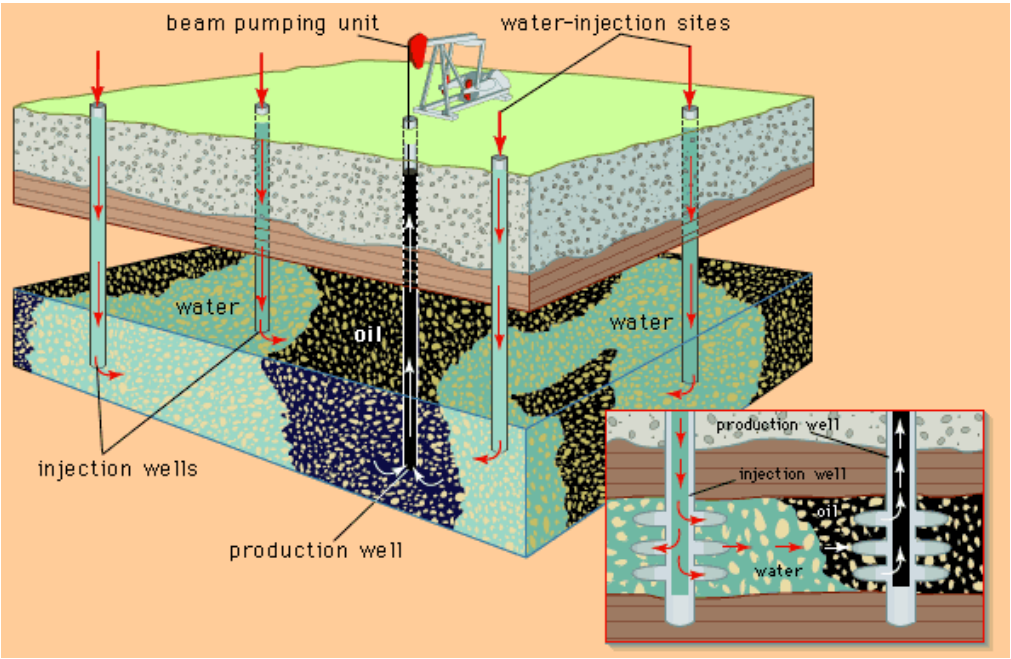

Figure I. 4:waterflooding technique [26].

I.3.2. Gas Flooding:

Gas Flooding or sometimes called pressure maintenance is carried out to maintain reservoir pressure, slow down the production decline rate in the natural regimes of the reservoir and, sometimes, to support the gravity regime. The gas injected into the well behaves in the same way as the gas in gas cap drive mode: the gas expands acting as a compressed spring, displacing oil to the producing wells. The implementation of gas injection requires the use of high pressure

compressors. According to miscibility between gas injected and oil displaced, gas injection can be classified into two major types: miscible gas injection and immiscible gas injection.

I.3.2.1. Miscible gas injection:

the gas is injected at or above minimum miscibility pressure (MMP) which causes the gas to be miscible in the oil.

I.3.2.2. Immiscible gas injection:

flooding by the gas is conducted below MMP. This low pressure injection of gas is used to maintain reservoir pressure to prevent production cut-off and thereby increase the rate of production [1].

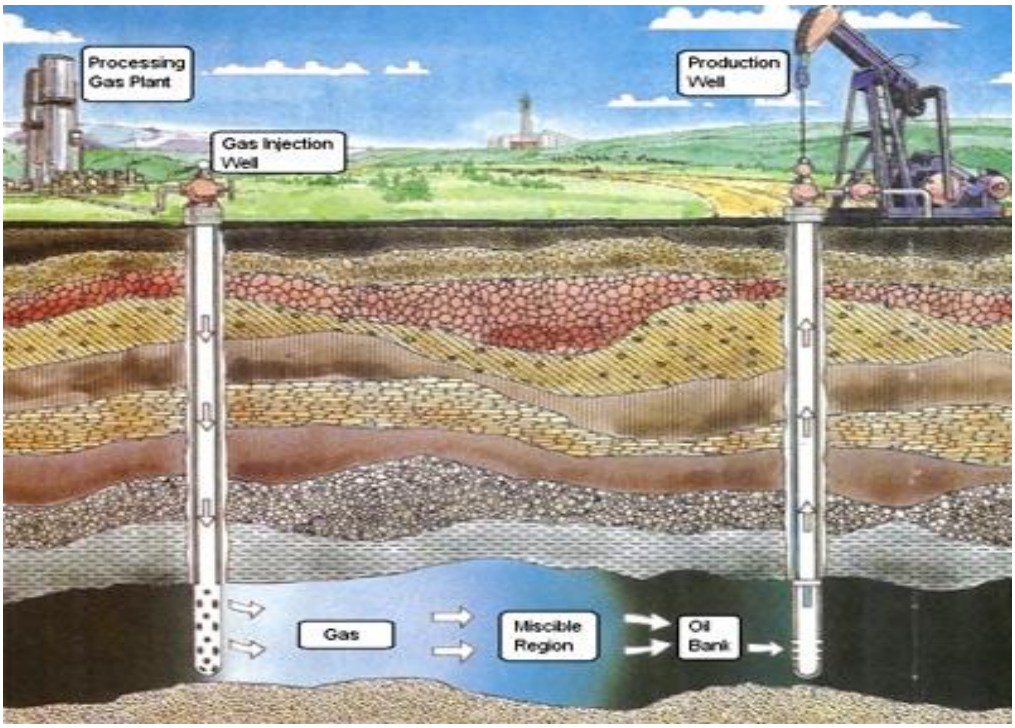

Figure I. 5: Gas injection [27].

I.3.3. Water alternating gas (WAG):

The WAG process was initially proposed as a method to increase sweep efficiency during gas injection. In practice the WAG process consists of the injection of water and gas as alternate slugs by cycles, with the objective of improving the sweep efficiency of waterflooding and miscible or immiscible gas-flood projects by reducing the impact of viscous fingering The gas pumped into

the reservoir, which is a non-wetting phase, moves into large pores and into top layers of the formation under the action of gravitational forces. The water on the contrary, under the influence of capillary forces occupies small pores of the hydrophilic reservoir and generally concentrates at the lower strata [10].

The WAG methods can be classified into miscible WAG (MWAG), immiscible WAG (IWAG), hybrid WAG (HWAG), Simultaneous WAG (SWAG), Selective Simultaneous WAG (SSWAG) and WAG after water flooding (WAG a.WF) injection methods [7].

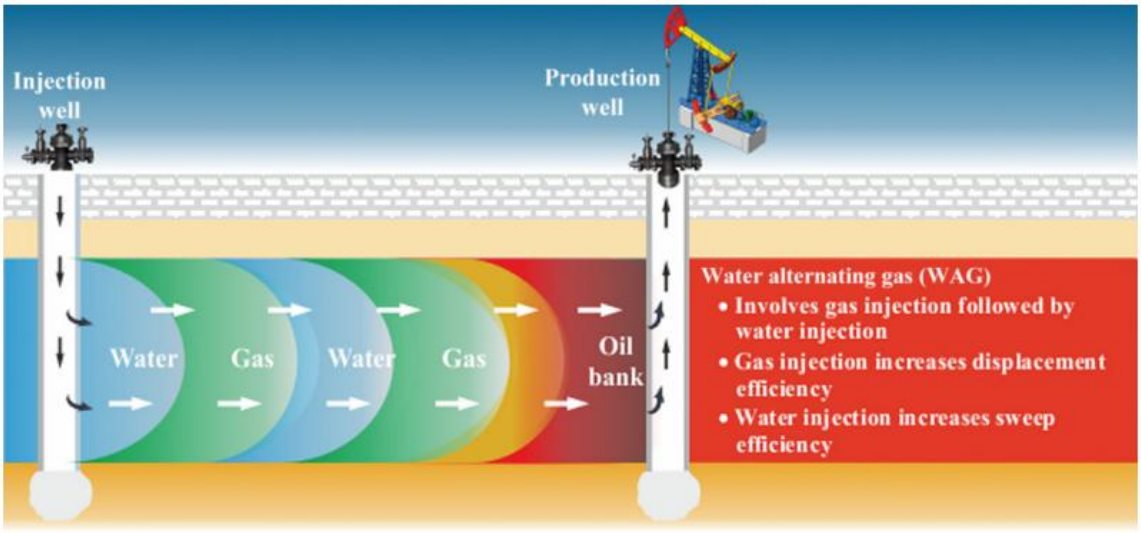

Figure I. 6: Water alternating gas (WAG) process [23].

I.4. Tertiary oil recovery (Enhanced Oil Recovery, EOR):

Secondary oil recovery methods increase volumes of recovered oil. Nevertheless, despite the increase in oil recovery rate as a result of the use of secondary oil recovery methods, in particular the most effective oil flooding, a significant amount of residual oil remains in the reservoir, the purpose of the EOR methods is to decrease this amount of residual oil by:

- Increase in sweep efficiency due to:
  - ❖ reducing the ratio of the mobility of the injected and displaced fluids,
  - ❖ blocking of the washed highly permeable water-saturated zones and the re-direction of the injected fluid into the low-permeable oil-saturated zones of the reservoir.
- Surface forces modification in the reservoir due to:
  - ❖ reducing the interfacial surface tension between the oil and the displacing fluid,

- ❖ reduce the effect of capillary forces,
- ❖ changes in reservoir rock wettability,
- ❖ disjoining pressure changes.

- Combinations of the above processes [22].

EOR methods are mainly categorized into four major techniques:

- ✓ thermal method, which incorporates heat transfer to bring up the viscous crude oil
- ✓ gas injection, which uses nitrogen and carbon dioxide in both miscible and immiscible approaches
- ✓ chemical techniques, which are used not only to improve the waterflood sweep efficiency, but also to reduce the oil surface tension
- ✓ other methods like microbial EOR [5].

I.5. Factors to consider in injection process:

I.5.1. Reservoir Geometry:

The areal geometry of the reservoir will influence the location of wells and, if offshore, will influence the location and number of platforms required. The reservoir's geometry will essentially dictate the methods by which a reservoir can be produced through injection practices.

I.5.2. Reservoir Depth:

Maximum injection pressure will increase with depth. The costs of lifting oil from very deep wells will limit the maximum economic water–oil ratios that can be tolerated, thereby reducing the ultimate recovery factor and increasing the total project operating costs. On the other hand, a shallow reservoir imposes a restraint on the injection pressure that can be used, because this must be less than fracture pressure

I.5.3. Reservoir dip:

In the inclined layer, in the two-phase flow zone, the fractional flow F_w is expressed by the equation:

$$F_w = \frac{\frac{\mu_o}{kro} - \frac{Ak}{qt}(\rho w - \rho O) g \sin \alpha}{\frac{\mu_w}{k_{rw}} + \frac{\mu_o}{k_{ro}}} \quad \textbf{(I.1)}$$

I.5.4. Heterogeneity degree:

Substantial reservoir uniformity is one of the major physical criterions for successful flooding. Some of the following issues regarding reservoir characteristic must be considered and evaluated to study their impacts on the success of a secondary recovery process must be evaluated:

- If the formation contains a layer of limited thickness with a very high permeability (i.e., thief zone), rapid channeling and bypassing will develop unless this zone can be located and shut off.
- The lower depletion pressure that may exist in the highly permeable zones will also increase the water-channeling tendency due to the high-permeability variations.

Interference tests are performed before any enhanced recovery project to verify the communication between the wells.

I.5.5. Petrophysical characteristics:

Porosity: the greater the porosity, the greater the residual oil saturation S_{or} at the end of the primary phase that it is interesting to try to recover.

Permeability: the permeability is a favorable factor for recovery. However, there is an upper limit beyond which the secondary recovery becomes uneconomical.

The capillary pressure: capillary phenomena sometimes have a useful effect. It is the case when they allow a regularization of the advance of the front separating two immiscible fluids in heterogeneous porous medium (the imbibition). But sometimes they have a negative effect. They are responsible for the trapping of oil in the pores.

I.5.6. Fluid characteristics:

Fluid viscosity: the viscosity of the crude oil "μ_o" is considered the most important fluid property that affects the degree of success of a waterflooding project. The oil viscosity has a significant impact of the mobility of the oil "λ_o" which, in turn, impact the mobility ratio "M"

The oil mobility is defined by the ratio: $\boldsymbol{\lambda_o = k_o / \mu_o}$ **(I.2)**

While the mobility ratio is defined as the ratio of the displacing fluid mobility, e.g. "λ_w", to that of the displaced fluid, e.g λ_o

$\boldsymbol{M = \lambda_w / \lambda_o = (k_w / k_o)(\mu_o / \mu_w)}$ **(I.3)**

Fluid Saturations: a high oil saturation that provides a sufficient supply of recoverable oil is the primary criterion for successful flooding operations. Note that higher oil saturation at the beginning of flood operations increases the oil mobility "λo" which contributes to obtaining a higher recovery efficiency [3].

I.6. Monitoring techniques of injection performance:

I.6.1. Voidage Replacement Ratio (VRR):

Voidage Replacement (VR) is the process of replacing oil, gas and water in the reservoir by fluid injection. Voidage Replacement Ratio (VRR) cen be defined as the ratio of reservoir volume of injected fluid to reservoir volume of produced fluids.

$$VRR = \frac{injected\ reservoir\ volume}{produced\ reservoir\ volume} = \frac{I_w B_w + I_g B_g}{Q_o B_o + (GOR - R_s) Q_o B_g + Q_w B_w} \quad \textbf{(I.4)}$$

Where:

B_w = Water Formation Volume Factor (m^3/STm^3)

I_w = Water Injection flow rate (STm^3/month)

B_g = Gas Formation Volume Factor (m^3/STm^3)

I_g = Gas Injection flow rate (STm^3/month)

B_o = Oil Formation Volume Factor (m^3/STm^3)

Q_o = Oil production flow rate (STm^3/month)

R_S = Solution Gas Oil Ratio (m^3/m^3)

Q_w = Water production flow rate (STm^3/month)

GOR = Gas Oil Ratio (m^3/m^3)

The VRR is the key parameter that defines the injection/withdrawal balance and thus allows us to judge the effectiveness of this injection. This balance significantly affects the pressure distribution in the reservoir, which in turn affects the production of the field.

Thus the VRR is represented in the same graph with the pressure trend. When the VRR is greater than 1 and the reservoir pressure does not increase, we suspect the loss of injection outside the zone. Similarly, when the VRR is less than 1 and the reservoir pressure does not decrease, we suspect fluid influx (vertical or horizontal influx) in the investigated zone [20].

I.6.2. Impact of the injection on the recovery factor:

In order to evaluate the effect of injection on recovery, the RF versus HCPVI (Recovery Factor Vs Hydrocarbon Pore Volume injected) curve is useful to fully understand the drainage mechanisms and the maturity of the studied zone.

RF and HCPVI are defined as follows:

$$RF = \frac{N_p}{N} \quad \textbf{(I.5)}$$

$$HCPVI = \frac{W_{ing}B_w + G_{ing}B_g}{NB_{oi}} \quad \textbf{(I.6)}$$

Where:

W_{ing} = Cumulative water injection km^3

G_{ing} = Cumulative gas injection km^3

B_w = Water Formation Volume Factor (m^3/STm^3)

B_g = Gas Formation Volume Factor (m^3/STm^3)

N = original oil in place $kSTm^3$

B_{oi} = Initial oil Formation Volume Factor (m^3/STm^3) [21].

I.7. Breakthrough problem in the injection process:

During the life of most wells, reservoirs exhibit high oil recovery due to the injection of water or gas, the percentage of water and gas (breakthrough) in the produced fluid is constantly increasing, this breakthrough represents a technical and economic problem in the exploitation of oil fields. It is generally responsible for both a rapid decrease in productivity or even the closure of wells and an increase in operational costs related to the need to transport, separate and store large quantities of water and gas. The problems of water and gas breakthroughs have become a major concern for oil operators and a key component of operating costs. In order to improve production and well life, several techniques are being used to understand the sources, causes and mechanisms of breakthrough.

I.7.1. Breakthroughs source:

- The presence of gas cap or an aquifer in the reservoir
- The injected fluids in the reservoir during the secondary recovery process

I.7.2. Breakthroughs causes:

I.7.2.1. Permeability effect:

High permeability zones accelerates injection fluid flow and leads to premature production at producing wells.

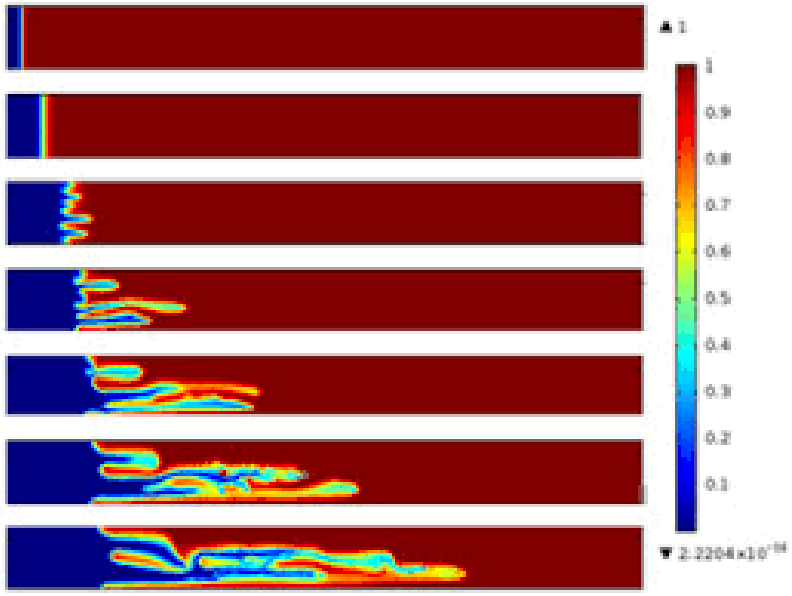

Figure I. 7: Permeability effect [25].

I.7.2.2. Perforation locations of injector and producer:

The perforation locations decide the flow path and sweep area. If the perforation locations are adaptable to the formation, breakthrough will be late; otherwise breakthrough will be early.

I.7.2.3. Injection rate:

Generally, the injection rate is adaptable to the production rate to keep the formation pressure to be balanced. But as the sweep area increases, the practical injection rate is difficult to be controlled. If the injection rate is too high, gas will channel along the direction of higher pressure gradient.

I.7.2.4. Production rate:

Hydrocarbon production is achieved by creating a pressure gradient across the formation. However, flowing into a partially penetrated or perforated well creates a vertical pressure

gradient. Also, the pressure gradient increases with increasing flow rate. As a result, large flow rates cause the withdrawal to accelerate and result in excessive production of injected fluids.

I.7.2.5. Reservoir fissures and faults:

Their nature is tectonic. The faults and fissures represent a preferential path for gas or water between the injector wells and the producer wells. In these cases, the production of this last one puts the well in danger [24].

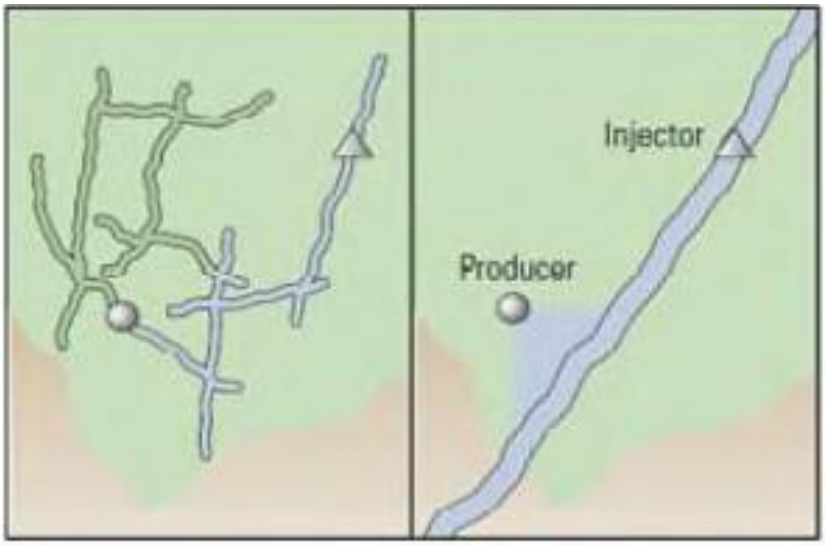

Figure I. 8: Reservoir fissures and faults effect [6].

CHAPTER II: OIL RECOVERY MECHANISMS AND MATERIAL BALANCE EQUATION

II.1. Introduction

Each one of the sub surface hydrocarbons reservoir compose a unique combination of geometric form, geological rock properties, fluid characteristics, and primary driving mechanism. Two reservoirs may not be totally identical, they can be grouped according to the primary production mechanism where each drive mechanism has its typical performance (recovery rate, pressure drop, GOR and water production).

Natural oil recovery drainage mechanism refers to production without the use of any process to make up the natural energy of the reservoir.

The main objectives of this chapter is to:

1. Introduce the various principal recovery methods and their impacts on the overall performance of oil reservoirs.
2. Explain the fundamentals of the material balance equation and other governing relationships that can be applied to forecast oil reservoir volumetric performance.

II.2. Primary recovery mechanisms:

Knowledge of the driving processes that influence the behavior of fluids within reservoirs is required for a proper understanding of reservoir behavior and forecasting future performance. The type of the energy and the driving mechanism, have a big impact on the overall performance of oil reservoirs, available for moving oil to the wellbore. The natural energy required for oil recovery is provided by six major driving mechanisms: [18] [4].

• Rock and liquid expansion drive
• Depletion drive
• Gas cap drive
• Water drive
• Gravity drainage drive
• Combination drive

II.2.1 Rock and Liquid Expansion:

When oil initially exists at a pressure Pi > Pb, the reservoir is called under saturated. Crude oil, connate water, and rock are the only materials that exist. When the pressure decreases, the fluids and the rock expand due to their compressibilities. The reservoir rock expands as a result of individual rock grains expansion and formation compaction.

Both of the above two factors are the results of a decrease of fluid pressure within the pore spaces, which allows to reduce the pore space, so the porosity is reduced.

As the expansion of the fluids and reduction in the pore volume occur with decreasing reservoir pressure, the crude oil and water will be forced out of the pore space to the wellbore.

This mechanism is characterized by a constant GOR and has the lowest recovery factor [15].

II.2.2 The Depletion Drive Mechanism:

This type of drainage occurs when the reservoir pressure drops below the bubble pressure due to the production. Under the effect of this pressure drop the gas dissolved in the oil is liberated. it becomes able to move and carries the Oil with it, and the GOR of production increase [8] [4].

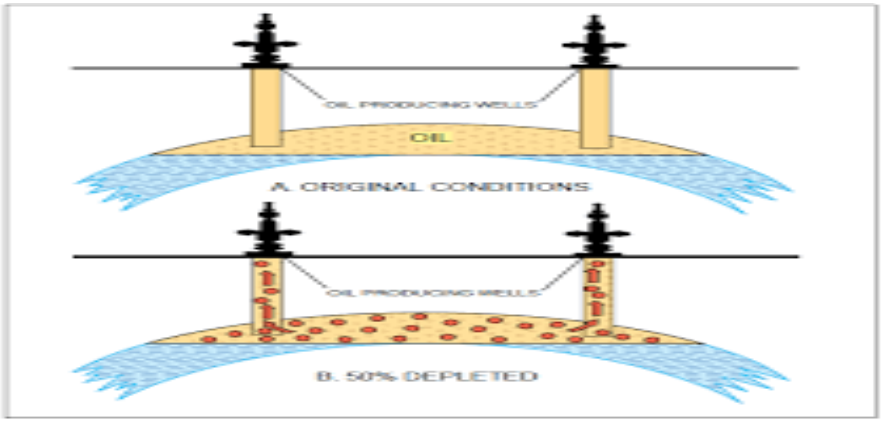

Figure II. 1: Solution gas drive reservoir [28].

II.2.3 Gas Cap Drive:

Gas-cap-drive reservoirs can be identified by the presence of a gas cap and have an initial pressure equal to the bubble pressure.

Generally, more gradual pressure and oil rate decline than for solution gas drive can be expected, which is called cap drive. Oil recovery due to gas cap drive is typically around 30% but could be as much as 40% [12] [15].

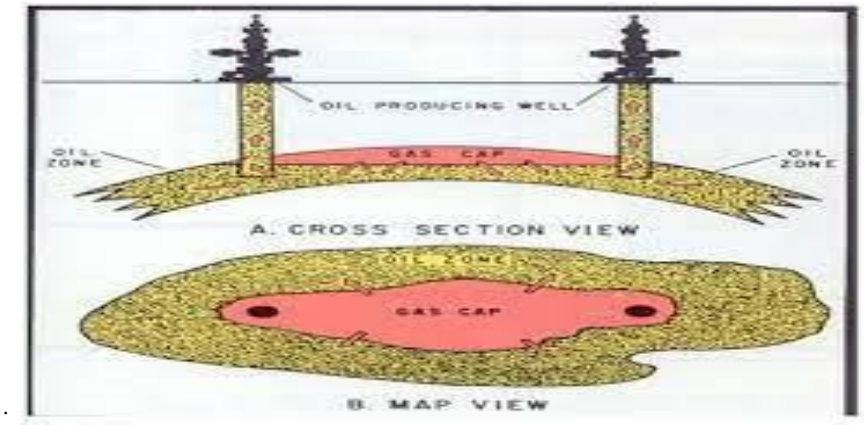

Figure II. 2: Gas-cap-drive reservoir [29].

II.2.4 The Water-Drive Mechanism:

In a reservoir where the oil is in contact with an active aquifer, which has a significant dimension, the energy that allows the expulsion of the oil, is provided by the push of the water, as a result of that, the production rate increase next to the water- oil contact (WOC). The water that displaces the oil must come from either:

- An aquifer whose volume is very large compared to the oil (ten times larger or more), in this case the pressure drop is compensated by the expansion of water, which replaces the expelled oil.
- An aquifer that is connected to the surface, so it has a high energy, and the water that replaces the oil is recharged from the surface.

In correctly operated water drive reservoirs, oil recovery from the reservoir might reach 45 percent. Hydrostatic pressure, reservoir water expansion, or a combination of both could be the driving mechanism behind the water drive [18] [4].

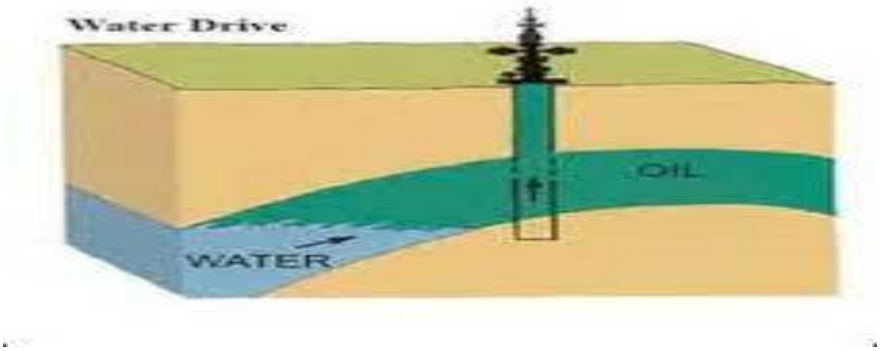

Figure II. 3:water drive reservoir [30].

II.2.5 The Gravity-Drainage-Drive Mechanism:

Gravity drainage occurs in petroleum reservoirs due to changes in reservoir fluid densities. These forces maintain fluid equilibrium, which allows to define the WOC, GOC. The gravitational segregation of the fluids in place contributes significantly to the recovery of oil from the reservoir [4].

II.2.6 The Combination-Drive Mechanism:

The driving mechanism most commonly encountered is one in which both water and free gas are available in some degree to displace the oil toward the producing wells. Combination-drive reservoirs can be recognized by:

- Relatively rapid pressure decline.
- The evolution of the GOR. The GOR will continue to rise in the structurally high wells.
- The evolution of the water cut. Structurally low-producing wells will gradually increase their water production rates [4].

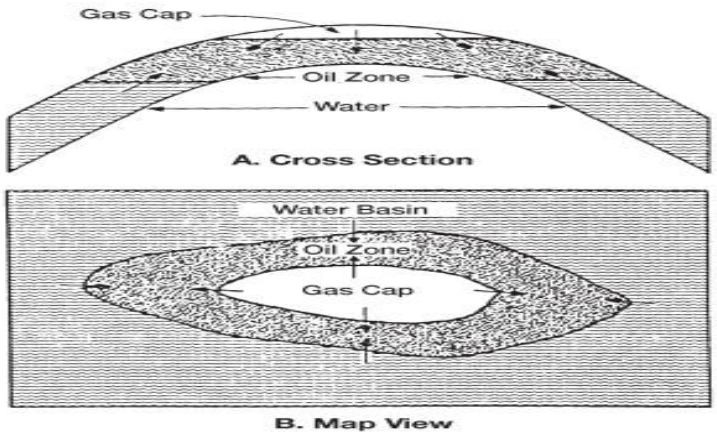

Figure II. 4: Combination-drive reservoir [4].

II.3. Performance of drainage mechanisms:

To evaluate the performance of one drainage regime over another, the behavior and evolution of some key parameters of the produced fluids and the reservoir must be observed. To do so, a summary table (II.1) of the different regimes and the parameters influencing their performance (GOR, WC, and P) as well as the recovery factor of each regime has been drawn up.

Table II. 1: Performance of different drainage regimes [19].

drainage mechanisms	Origin of the energy	reservoir performance	Rate of Recovery
Rock and Liquid Expansion	Compressibility of rock and pore water	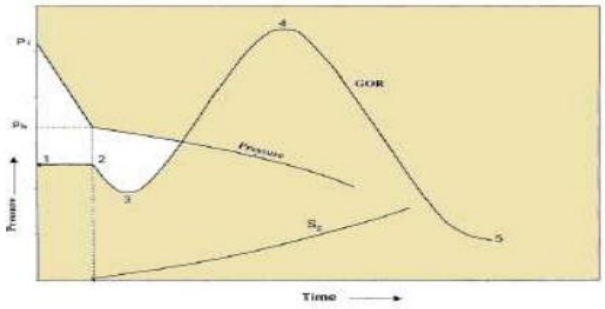	(5 ÷10) %
Depletion Drive	Compressibility of gas dissolved in oil	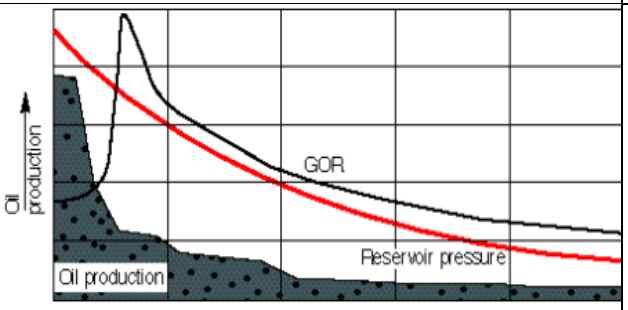	(5 ÷ 30) %
Gas Cap Drive	the gas-cap expands	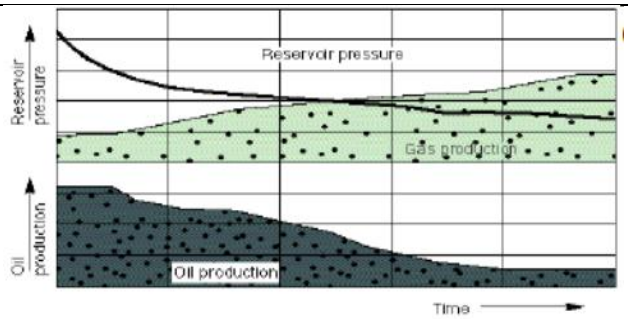	(20 ÷ 40) %
Water-Drive	an active aquifer	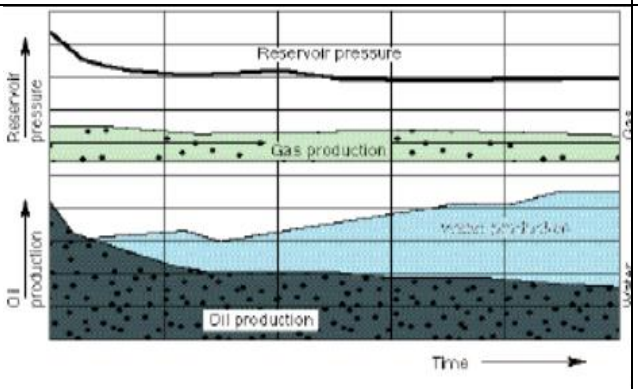	(30 ÷ 60) %

Gravity-Drainage-Drive	difference in the densities of the fluids in place		Varies with the degree of depletion

II.4. Methods of estimating reserves in place:

There are two different methods for estimating the quantities of hydrocarbons in the reservoirs and each method has its own basis and interest:

II.4.1 The volumetric method:

II.4.1.1 Principe:

The development of accumulations is made delicate by the complicity of reservoir, it only takes into account the geology it allows to give the reserves in static place (is not affected by the pressure difference), it is used in most cases in the phase of development of reservoir, this evaluation is done from data from two different sources.

The seismic: it provides the external geometry of the reservoir in the form of map. Isobaths, which allows to calculate the volume of the impregnated rock.

Drilling: which allow to reach the reservoir and evaluate the average characteristics either from the logs that are recorded, or from the measurements made in the laboratory on cores. The difficulty lies in determining the parameters characterizing the volume of hydrocarbons in place rather than in calculating this volume, which is reduced to the following simple operations:

$$SOOIP = H_u . A . \emptyset (1 - S_{wi}) . \frac{1}{B_o} \quad \text{(II.1)}$$

SOOIP: original oil in place at surface conditions (m^3).

H_u: net thickness (m).

A: the area of the zone (m^2).

$\emptyset$: porosity (fraction).

S_{wi}: initial water saturation (fraction).

B_o: oil formation volume factor m^3/stm^3

The volumetric method takes into consideration all the reserves contained in the pores (connected and unconnected), which does not reflect the true potential of the reservoir, which is the recoverable reserves.

II.4.2. The Material Balance Equation:

The material balance equation (MBE) has long been considered one of reservoir engineers most important tools for analyzing and forecasting reservoir performance. The MBE, when properly applied, can be used to:

- Estimate initial hydrocarbon volumes in place
- Predict future reservoir performance
- Predict ultimate hydrocarbon recovery under various types of primary driving mechanisms

II.4.2.1 Principe:

The equation is structured to simply keep inventory of all materials entering, leaving, and accumulating in the reservoir. The concept of the material balance equation was presented by Schilthuis in 1941. In its simplest form, the equation can be written on volumetric basis as:

Initial volume =volume remaining +volume removed.

Several of the material balance calculations require the total pore volume (P.V) as expressed in terms of the initial oil volume N and the volume of the gas cap. The expression for the total pore volume can be derived by conveniently introducing the parameter (m) into the relationship as follows: [9] [4].

Defining the ratio (m) as:

$$\mathrm{m} = \frac{\text{Initial volume of gas cap}}{\text{Volume of oil initially in place}} = \frac{G\,B_{gi}}{N\,B_{oi}} \qquad \text{(II.2)}$$

Solving for the volume of the gas cap gives:

Initial volume of the gas cap $= G\,B_{gi} = \mathrm{m}\,N\,B_{oi}$

The total volume of the hydrocarbon system is then given by:

$$N\,B_{oi} + \mathrm{m}N\,B_{oi} = (\mathrm{P.V})\,(1 - S_{wi})$$

$$\text{Or} \quad \mathrm{P.V} = \frac{N\,B_{oi}(1+m)}{(1-S_{wi})} \qquad \text{(II.3)}$$

Where Swi= initial water saturation

N= initial oil in place,

P.V= total pore volume,

m= ratio of initial gas-cap-gas reservoir volume to initial reservoir oil volume.

Treating the reservoir pore as an idealized container as illustrated in Figure (II.5), volumetric

balance expressions can be derived to account for all volumetric changes which occur during the natural productive life of the reservoir.

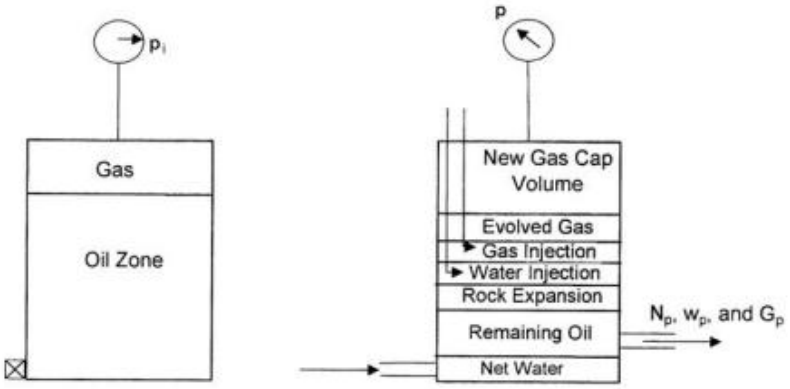

Figure II. 5: Tank-model concept [19].

a) Pore Volume Occupied by the Oil Initially in Place at Pi

$$\text{Volume occupied by initial oil in place} = N\,B_{oi} \tag{II.4}$$

b) Pore Volume Occupied by the Gas in the Gas Cap

$$\text{Volume of gas cap} = GB_{gi} = mNB_{oi} \tag{II.5}$$

c) Pore Volume Occupied by the Remaining Oil

$$\text{Volume of the remaining oil} = (N - N_p)B_o \tag{II.6}$$

d) Pore Volume Occupied by the Gas Cap at Reservoir Pressure P

As the reservoir pressure drops to a new level P, the gas in the gas cap expands and occupies a larger volume. Assuming no gas is produced from the gas cap during the pressure decline, the new volume of the gas cap can be determined as:

$$\text{Volume of the gas cap at P} = \left[\frac{\text{m}\,N\,B_{oi}}{B_{gi}}\right] B_g \tag{II.7}$$

e) Pore Volume Occupied by the Evolved Solution Gas

This volumetric term can be determined by applying the following material balance on the solution gas:

[volume of the evolved solution gas] = [volume of gas initially in solution]
- [volume of gas produced]
- [volume of gas remaining in solution]

$$[\text{volume of the evolved solution gas}] = \left[NR_{si} - N_pR_p - \left(N - N_p\right)R_s\right]B_g \quad \text{(II.8)}$$

f) Pore Volume Occupied by the Net Water Influx

$$\text{net water influx} = W_e - W_pB_w \quad \text{(II.9)}$$

g) Change in Pore Volume Due to Initial Water and Rock Expansion

The compressibility coefficient c, which describes the changes in the volume (expansion) of the fluid or material with changing pressure, is given by:

$$c = \frac{1}{V}\frac{\partial V}{\partial_p} \quad \text{Or} \quad \Delta V = V.c.\Delta P \quad \text{(II.10)}$$

The reduction in the pore volume due to the expansion of the connate water in the oil zone and the gas-cap is given by:

$$\text{Connate water expansion} = [(\text{PV})\ S_{wi}]c_w\ \Delta P \quad \text{(II.11)}$$

Substituting for the pore volume (P.V) with Equation gives:

$$\text{Expansion of connate water} = \frac{N\ B_{oi}(1+m)}{(1-S_{wi})}\ S_{wi}\ c_w\ \Delta P \quad \text{(II.12)}$$

Similarly, the reduction in the pore volume due to the expansion of the reservoir rock is given by:

$$\text{Change in pore volume} = \frac{N\ B_{oi}(1+m)}{(1-S_{wi})}\ \ c_f\ \Delta P \quad \text{(II.13)}$$

Combining the expansions of the connate water and formation as represented by Equations (II.12) and (II.13) gives:

$$\text{Total changes in the pore volume} = \ N\ B_{oi}(1+m)\left(\frac{S_{wi}C_w+C_f}{1-S_{wi}}\right)\ \Delta P \quad \text{(II.14)}$$

h) Pore Volume Occupied by the Injection Gas and Water

$$\text{Total volume} = G_{inj}B_{gi} + W_{inj}B_w \quad \text{(II.15)}$$

The MBE can be written in a generalized form as follows:

$$\text{(a) + (b) = (c) + (d) + (e) + (f) + (g) + (h)} \quad \text{(II.16)}$$

Replacing (a), (b), (c), by their equations we obtain the following equation:

$$N\left[B_{oi} - B_o + B_g(R_s - R_{si}) + mB_{oi}\left(1 - \left(\frac{B_g}{B_{gi}}\right)\right) - (1+m)\left(\frac{S_{wi}C_w+C_f}{1-S_{wi}}\right)B_o\Delta P\right] +$$

$$N_p\left[B_o + B_g(R_p - R_s)\right] = W_p - W_pB_w + W_{inj}B_w + G_{inj}B_g \quad \text{(II.17)}$$

This is the general material balance equation. This equation is applicable for a producing field with all natural drainage regimes and water and gas injection.

II.4.2.2 Average pressure calculation:

Establishing an average pressure-decline trend can be possible even if there are large pressure differences across the field under normal conditions. Averaging individual well pressure drops can possibly be used to determine a uniform trend in the entire reservoir, these pressures are determined with respect to the volumes drained by each well, the volumetric average pressure of the entire reservoir can be estimated from: [4]

$$\bar{P}_r = \frac{\sum_i (\bar{P}V)_i}{\sum_i V_i} \tag{II.18}$$

In practice, the V_i values are difficult to determine and, therefore, it is common to use individual wells flow rates, qi, in determining the average reservoir pressure from individual wells average drainage pressure. From the definition of the isothermal compressibility coefficient:

$$\frac{\partial_V}{\partial_t} = \frac{1}{CV}(q) \tag{II.19}$$

With: q= $\frac{\partial_V}{\partial_t}$

The last expression suggests that for a reasonably constant c at the time of measurement:

$$V\alpha\ q/(\partial P/\partial t)$$

The flow rates are measured on a routing basis throughout the lifetime of the field, the average reservoir pressure can be alternatively expressed in terms of the individual wells average drainage-pressure decline rates and fluid-flow rates by:

$$\bar{P}_r = \frac{\sum_i ((\bar{P}q)_i/(\partial \bar{P}/\partial t)_i)}{\sum_i (q_i/(\partial \bar{P}/\partial t)_i)} \tag{II.20}$$

Since the material balance equation is usually applied at regular intervals (i.e., Δt = month), throughout the life of the field, the average field pressure can be expressed in terms of the incremental net change in underground fluid withdrawal, $\Delta(F)$, as

$$\bar{P}_r = \frac{\sum_i ((\bar{P}q)_i/(\partial \bar{P}/\partial t)_i)}{\sum_i (q_i/(\partial \bar{P}/\partial t)_i)} \tag{II.21}$$

Where the total underground fluid withdrawal at times t +Δt are given by:

$$\Delta(F) = \int_0^{r+\Delta t} [Q_o B_o + Q_w B_w + (R_p - R_s) Q_o B_g] \tag{II.22}$$

II.4.2.3 Solution of the material balance equation:

This technique essentially consists of rearranging the equilibrium equation in such a way as to have it in a linear form.

The most important aspect of this solution method is that it gives meaning to the order of the plotted points, the direction in which they plot, and the shape of the resulting plot. A dynamic signification was presented in the image to arrive at the final answer.

$$F = N_p\left[B_o + (R_p - R_s)B_g\right] + \left(W_p - W_{inj}\right)B_w - G_{inj}B_g \quad \text{(II.23)}$$

$$E_o = (B_o - B_{oi}) + B_g(R_{si} - R_s) \quad \text{(II.24)}$$

$$E_{f,w} = B_{oi}(1+m)\left(\frac{S_{inj}C_w + C_f}{1 - S_{wi}}\right) \quad \Delta P \quad \text{(II.25)}$$

$$E_g = B_{oi}\left(\frac{B_g}{B_{gi}} - 1\right) \quad \text{(II.26)}$$

$$W_e = C_s \sum \Delta P \; Q \; (\Delta t_p) \quad \text{(II.27)}$$

Material balance equation will be written:

$$F = N\left[E_o + mE_g + E_{f,w}\right] + W_e \quad \text{(II.28)}$$

For saturated reservoirs, we can neglect the expansion of the rock and water ($E_{f,w}$=0) Equation (II.28) becomes:

$$F = N\left[E_o + mE_g\right] + W_e \quad \text{(II.29)}$$

The above equation is a simplified version of the material balance equation that includes the three production methods of oil expansion, gas expansion, and water drive. The missing of one or two of the above mechanisms requires the deletion of the appropriate limits from the equation.

1st Case:

- No active aquifers
- No gas cap.

Equation (II.29) becomes

$$F = NE_o \quad \text{(II.30)}$$

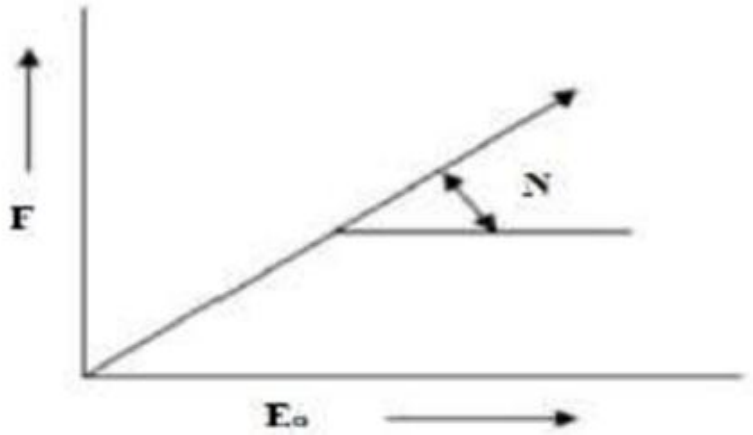

Figure II. 6: Solution of the material balance equation (No active aquifers, No gas cap) [31].

The curve F vs. E_o is a straight line passing through the origin and N its slope.

2nd Case:

- With gas cap.

Equation (II.29) becomes

$$F = N(E_o + mE_g) \tag{II.31}$$

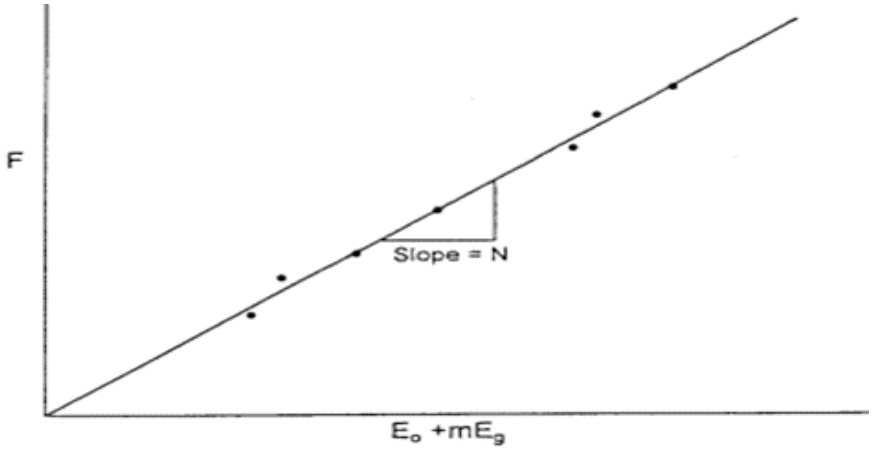

Figure II. 7: Solution of the material balance equation (with gas cap) [31].

The curve F vs. Eo+ mEg is a straight line passing through the origin and N its slope.

3rd Case:

- No aquifers
- N and m unknown

Equation (II.29) becomes:

$$F = N(E_o + mE_g) \quad \text{(II.32)}$$

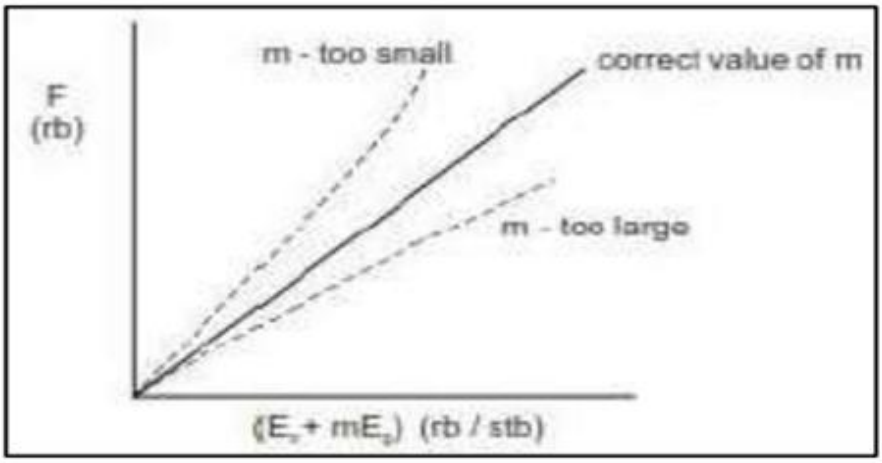

Figure II. 8: Solution of the material balance equation (No aquifers, N and m unknown) [31].

We give some values for m and then we plot: F vs. $E_o + m\,E_g$

- If assumed m is correct, the curve is a straight line passing through the origin and N its slope.
- If assumed m is too small the line will pass through the origin but will curve upwards.
- If assumed m is too large, the line will pass through the origin but will curve down.

4th Case:

- with aquifers
- No gas cap.

Equation (II.29) becomes

$$FE_o = N + W_e E_o \quad \text{(II.33)}$$

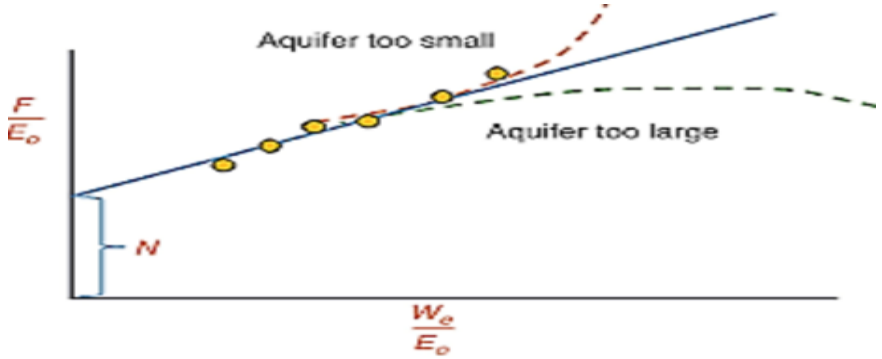

Figure II. 9: Solution of the material balance equation (with aquifers, No gas cap) [31].

In the case where the tank is topped by a gas cap.

Equation (II.29) becomes

$$FE_o + mE_g = N + W_e E_o + mE_g \quad \text{(II.34)}$$

Assuming that the reserves N and the ratio m are known the interpretation is similar to that shown in figure (II.5).

Chapter III: Performance Analysis of the Inter-Zone 17-19 and its Patterns

III.1. Presentation of the Hassi Messaoud field:

III.1.1. Field history:

The Hassi Messaoud reservoir was discovered on January 16th 1956 by the first drilling MD1; implanted following a seismic refraction campaign not far from the camel well of Hassi Messaoud.

On June 15th of the same year, this drilling discovered oil at a depth of 3338 meters in the Cambrian sandstone.

In May 1957 and 7 km North-West of MD1, the OM1 well drilled by the C.F.P.A confirmed the existence of a very important oil quantity in the Cambrian sandstones.

The reservoir was therefore covered by two separate concessions:

- In the North the C.F.P.A.
- In the South the SN. REPAL.

After several years of production, the reservoir pressure has dropped enormously which has led to use secondary recovery methods (injection of gas, water, etc...).

III.1.2. Geographical location:

The Hassi Messaoud field is located in the North-East of the Algerian Sahara, 850 km South-East of Algiers and 350 km from the Algerian-Tunisian border.and on the edge of the great oriental erg. The dimensions of the field reach 2500 Km², it is limited to the North by Touggourt and to the South by Gassi-Touil, and to the West by Ouargla. Its location in geographical coordinates is as follows:

- To the North by the latitude 32°15 N.
- To the South by the latitude 31°30 N.
- To the West by longitude 5°40 N.
- To the East by the longitude 6°35 N

  And Lambert coordinates:

- X= 790,000 to 840,000 East.
- Y= 110.000 to 150.000 North.

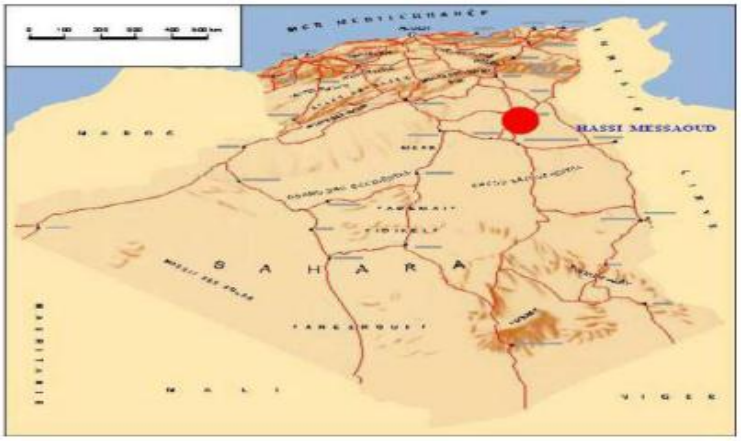

Figure III. 1: Geographical location of Hassi Messaoud field [17].

III.1.3. Geological location:

The Hassi Messaoud field occupies the central part of the North oriental triassic province which, by its surface and its reserves is the largest petrogasic province.

Its delimitations are the following:

- In the West by the depression of oued Mya.
- In the South by the Horst of Amguid.
- To the North by the Djamaa Touggourt structure.
- In the East by the depression of Ghadamès, Rhoude El-Baguel and the highlands of Dahar.

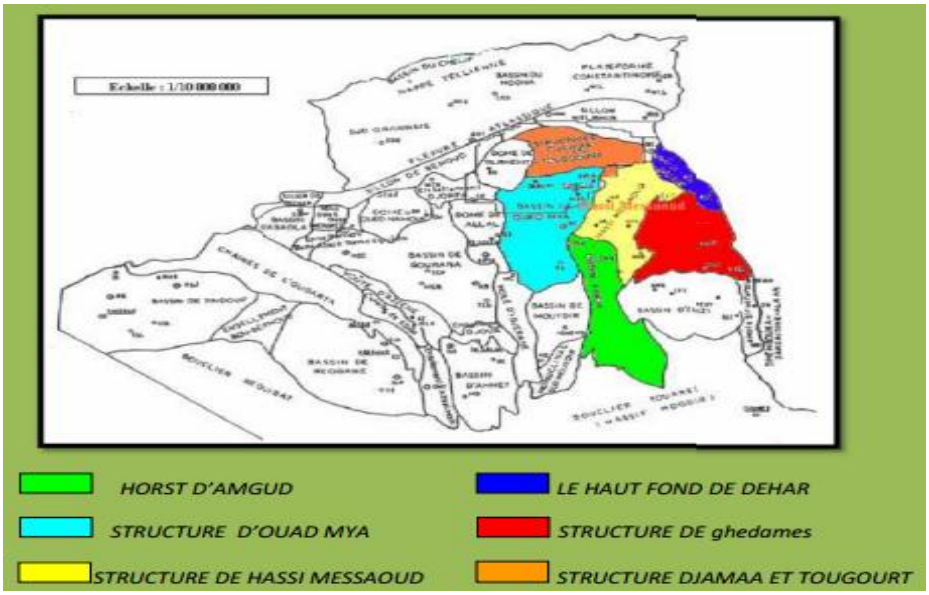

Figure III. 2: Geological location of Hassi Messaoud field [17].

III.1.4. Field organization:

The structure of Hassi Messaoud develops in a large subcircular anticline of 45 km in diameter, direction: North-East / South-West as shown in the figure (III.3).

The structural image of the Hassi Messaoud field is highly complex to analyze and difficult to define because of its dimensions and tectonic phenomena and especially the interference between its structure itself and the Hercynian erosion superimposed on the depositional conditions of the Cambro-Ordovician sandstone.

The Hassi Messaoud topography has been subjected to erosion over a very long period of time which has:

- Made disappear the upper reservoir units in the highest parts in the center of the reservoir.
- The reservoirs have been widely eroded by the creation of deep and narrow valleys major faults. These topographically low zones are filled by volcanic rocks
  The reservoir is deeply divided by very complex fault systems whose directions are:

- North East-South West for regional faults (field scale). East-West, North-West-South-East for smaller scale faults.

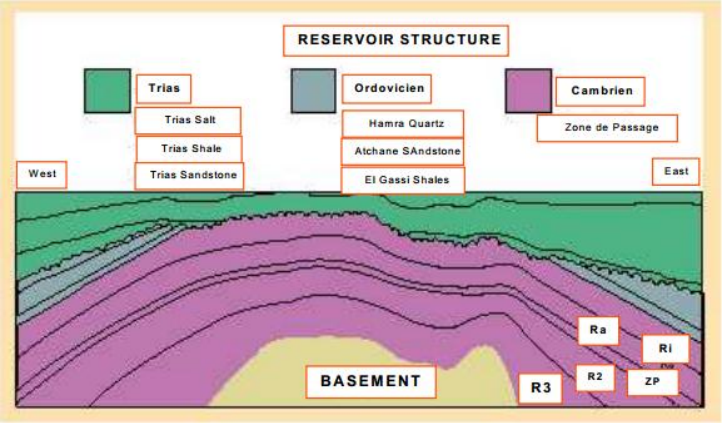

Figure III. 3: Structural map for Hassi Messaoud reservoir. [17].

III.1.5. Reservoir description:

The reservoir of Hassi Messaoud is located at a depth that varies between 3100 and 3380 m. Its thickness goes up to 200 m, it includes three sandstone reservoirs of Cambrian age, resting directly on the granitic base. It is represented by a sandstone series whose Paleozoic post erosion affects a part in the center of the field. It is subdivided from top to bottom as follows:

- Ri: Isometric zone with a thickness of 45 m, essentially fine-grained quartzite and tigillite. It corresponds to the D5 drain.
- Ra: Anisometric zone with an average thickness of about 120 m, composed of silico-clayey cement sandstone of medium to coarse grains. It is subdivided into drains respectively from bottom to top: D1, ID, D2, D3, and D4.
- R2: Clay-cemented sandstone series, with an average thickness of 80 m.
- R3: About 300 m high, it is a very gross to microscale sandstone series, very clayey based on the granitic basement encountered at a depth of over 4000 m deep, it is a rose porphyroid granite.

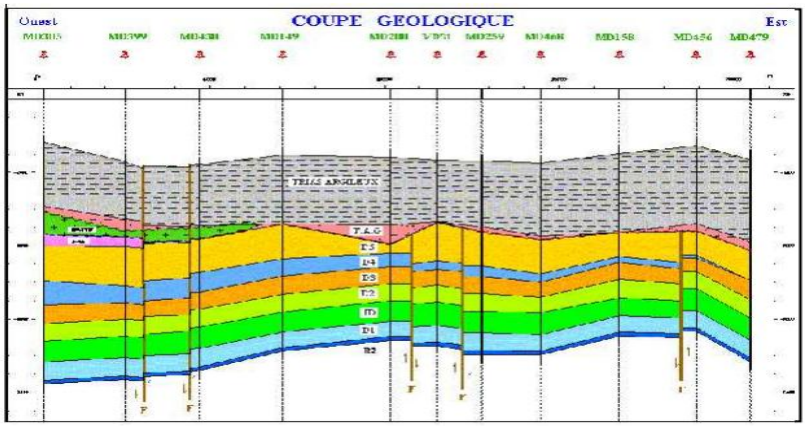

Figure III. 4: Geological section of Hassi Messaoud field [17].

III.1.6. Well zonation and numbering:

The field of Hassi Messaoud is divided into numbered zones as shown in the figure (III.5). This division is deduced naturally from the characteristics of the production and the geology. The evolution of well pressures, according to the production, has made it possible to subdivide the field into 25 producing zones. A production zone is defined as a group of wells that communicate with each other but with little or no communication with neighboring zones. It should be noted that the current subdivision is not satisfactory because the same zone can be subdivided into sub zones. The Hassi Messaoud field is divided from East to West into two distinct parts:

- The South field and the North field, each has its own numbering.
- The North field: It is a geographical numbering completed by a chronological numbering, for example: OMO38, ONM14, OMPZ12.

O: Capital letter, Ouargla license.

M: surface area of the oil zone: 1600 km2.

O: Small letter, oil area of 100 km2,

3: X-axis and 8: Y-axis.

- South field: The numbering of the zones is chronological. Ex: MD1, MD2, MDZ509.

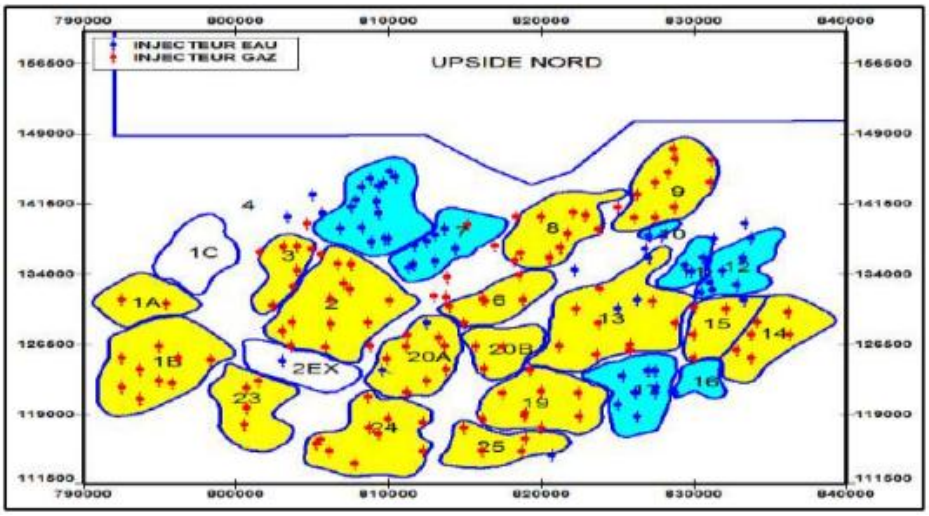

Figure III. 5: Hassi Messaoud field zonation [17].

III.2. Presentation of the inter-zone 17-19:

III.2.1. Location of the inter-zone 17-19:

the inter-zone 17-19 is located in South-East of Hassi-Messaoud field.

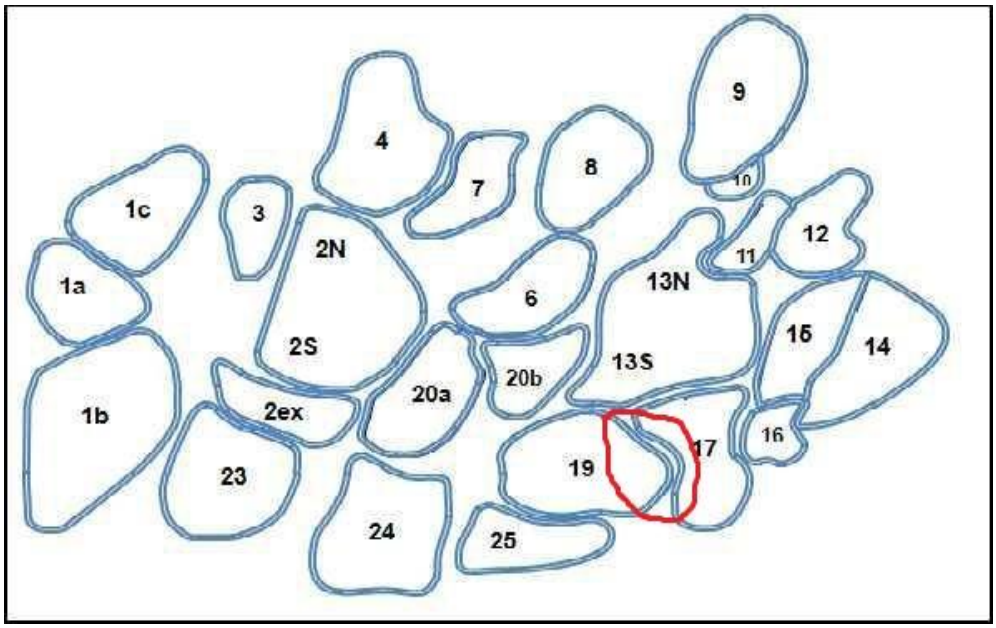

Figure III. 6: location of the inter-zone 17-19 in Hassi-Messaoud field [17].

III.2.2. Location of wells in the inter-zone 17-19:

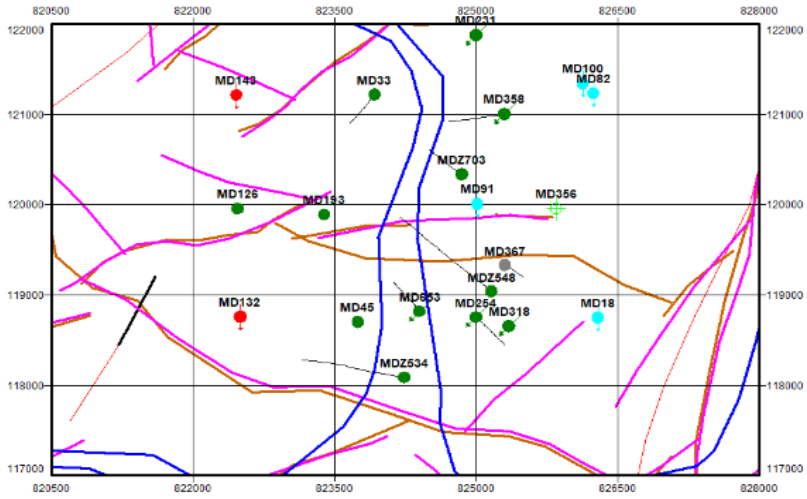

Figure III. 7: location of wells in the inter-zone 17-19 [17].

The inter-zone 17-19 contains a total of 20 wells:

- ✓ 7 oil producing wells
- ✓ 5 gas lift wells
- ✓ 4 water injector wells
- ✓ 2 gas injector wells
- ✓ 2 closed wells

III.2.3. Structure:

Since the reservoir of Hassi-Messaoud is an eroded anticlinal structure, the only horizon the reflect the true structure of the area is the R2.

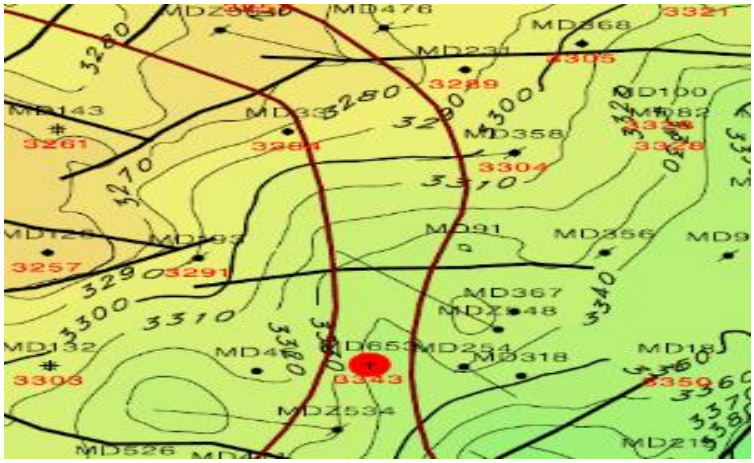

Figure III. 8: Isobath map of the R2 [17].

As shown in the previous figure, the inter-zone 17-19 has a monoclinal structure oriented from northwest to southeast, bounded by faults on all sides and has a major horizontal fault from east to west that has no offset, which divides the zone into two different compartments with some transmissibility between them.

III.2.4. Stratigraphy:

Since this zone is located at the boundary of the reservoir it did not expose to the erosion effect, due to that, all reservoir layers are existing in it, except for the D4 which its extension does not reach this part of the reservoir.

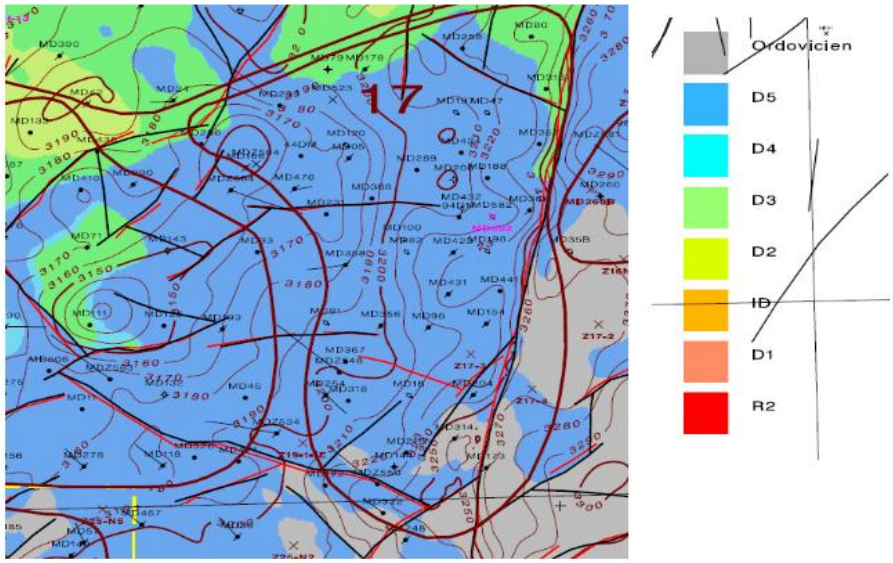

Figure III. 9: Map of the Ecorche under the Hercynian Discordance [17].

III.2.5. Porosity:

The R2 present the highest value of porosity which can reach up to 12%, then it decreases as we go up in reservoir's layers until it reaches its worst value at the D5 which is in the order of 0.001% as shown in the figure (III.10).

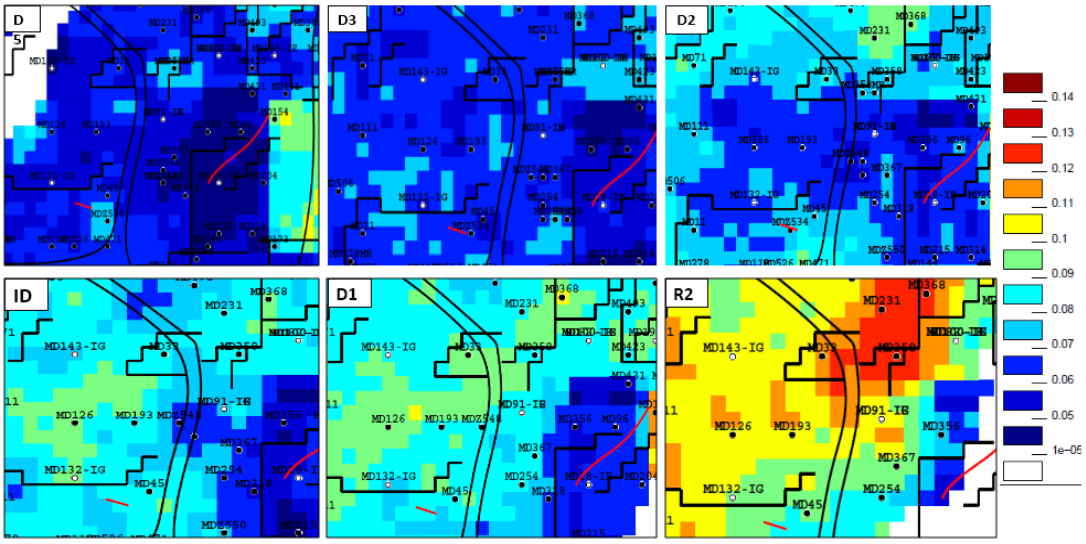

Figure III. 10: Porosity distribution by drain in the inter-zone 17-19 [17].

III.2.6. Permeability:

The figure (III.10) the Ra reservoir present the best quality in term of permeability specially in the D1, D2 and ID.

The D3 and R2 have a low permeability but still better than D5 which has a permeability in the range of 0.1 md.

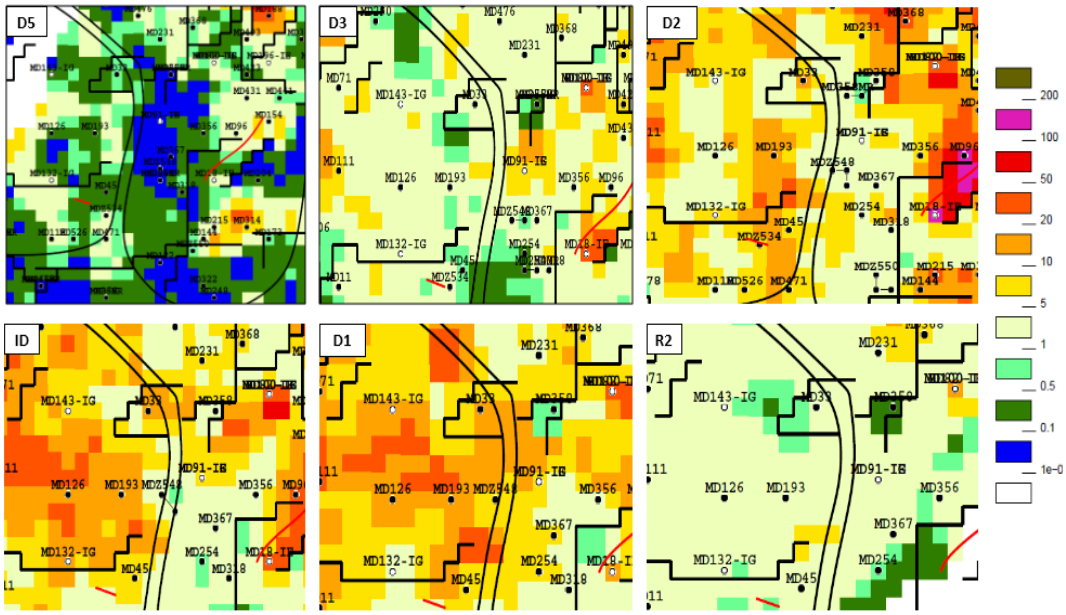

Figure III. 11: Permeability distribution by drain in the inter-zone 17-19 [17].

III.2.7. Pay zones:

The distribution of net pay thickness is shown in the figure (III.12):

The figure shows that the best net to gross ratio is in D1, ID and R2.

The D2 and D3 have an acceptable net thickness between 0.68 and 0.77, while D5 has the worst ratio that does not pass 0.5.

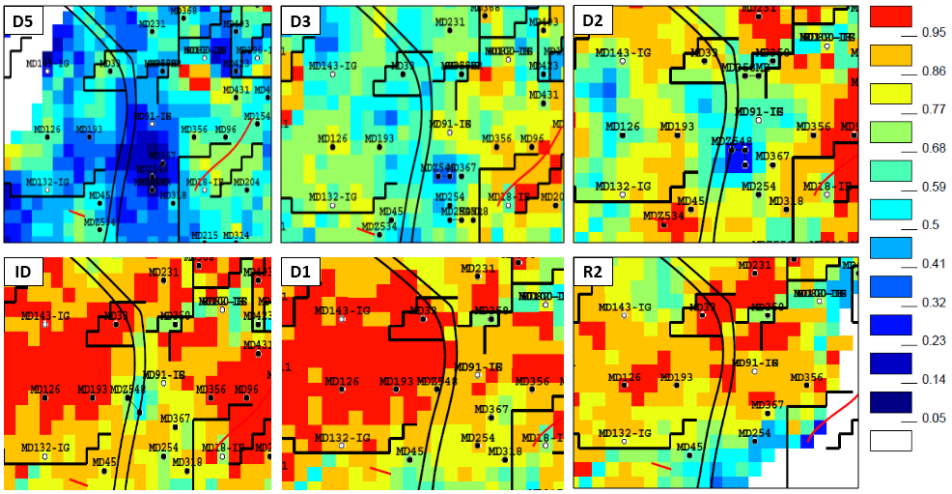

Figure III. 12: net to gross thickness distribution by drain in the inter-zone 17-19 [17].

III.3. Global study of the inter-zone 17-19 performance:

III.3.1. Production history:

III.3.1.1. Oil production history:

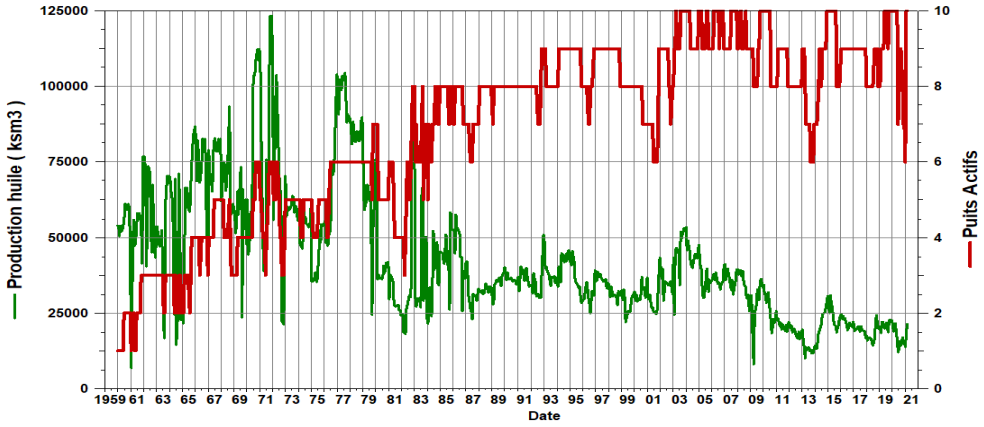

Figure III. 13: Oil production history and the number of active wells in the inter-zone 17-19[17].

The figure (III.13) shows that there is a direct relation between the number of wells and the oil production

First period: 1959-1972: The development of the zone began with the drilling of the first well MD18 in April 1959 then gradually added 8 other wells (MD33, MD45, MD82, MD91, MD100, MD126, MD132 and MD143) in this period.

In this period the zone was depleted naturally which causes the decrease in reservoir pressure from 484 kg/cm^2 to 275 kg/cm^2, at the end of 1972 oil produced was 5 229 260 Stm^3.

Second period: 1972-1983:

The development of the zone continued with the drilling of 7 new wells, but the number of active wells did not pass 8, also a 1.53 Billion Sm^3 of gas and 637 474 Sm^3 of water are injected which allows the production of 5 133 940 Sm^3 of oil.

The pressure decreased slowly from 275 kg/cm^2 to 214 kg/cm^2 due to the start of injection of both gas and water.

Last period: 1983-2021:

the volume of gas injected reaches up to 9.63 Billion Sm^3 and the water to 7 000 010 Sm^3 while the cumulative oil production reached up to 21 868 300 Sm^3 at the same time the pressure is maintained above 196 kg/cm^2.

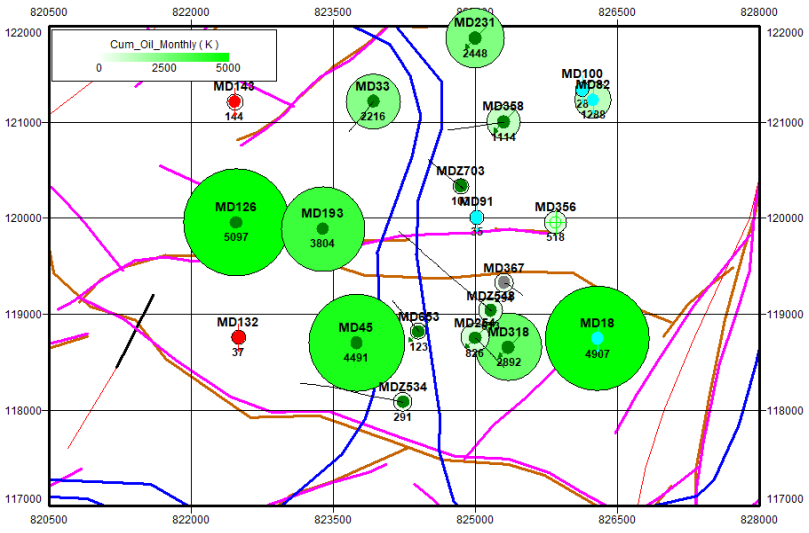

Figure III. 14: Bubble map of cumulative oil production of the inter-zone 17-19 [17].

III.3.1.2. Gas production history:

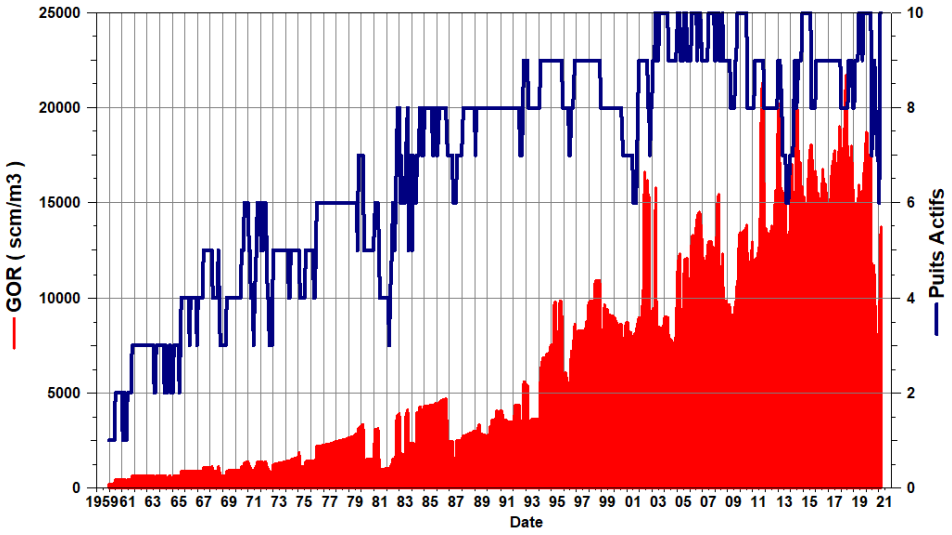

Figure III. 15: GOR and the number of active wells in the inter-zone 17-19 [17].

The GOR is strongly correlated to the number of active wells, also we notice a highly increase in the GOR after 1975 due to gas injection.

III.3.2. Injection history:

III.3.2.1. Water injection history:

The water injection started at 1968 by drilling the first water injector well MD100

Then later on by converting tow oil producing wells MD18 and MD82 on 1972 and 1980 respectively.

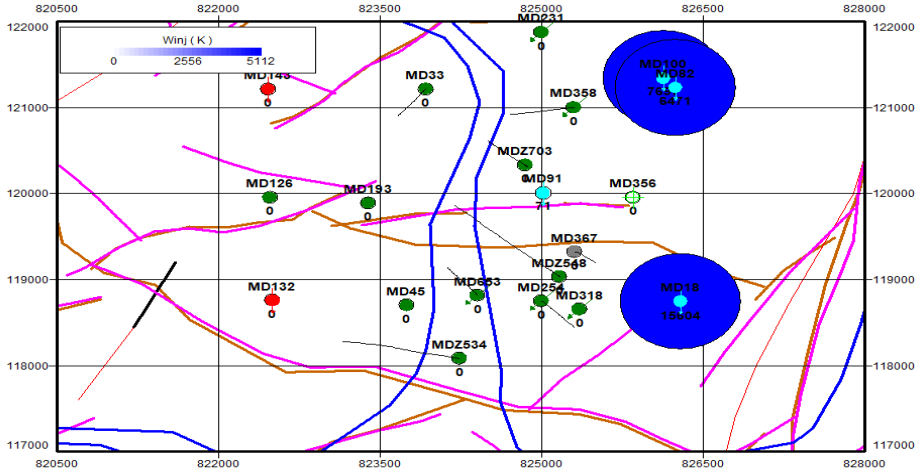

Figure III. 16: Bubble map of cumulative water injection of the inter-zone 17-19 [17].

III.3.2.2. Gas injection history:

The gas injection started in 1972 by converting the tow oil producing wells MD132 and MD143 the cumulative gas injection of the inter-zone 17-19 is shown in the figure (III.17).

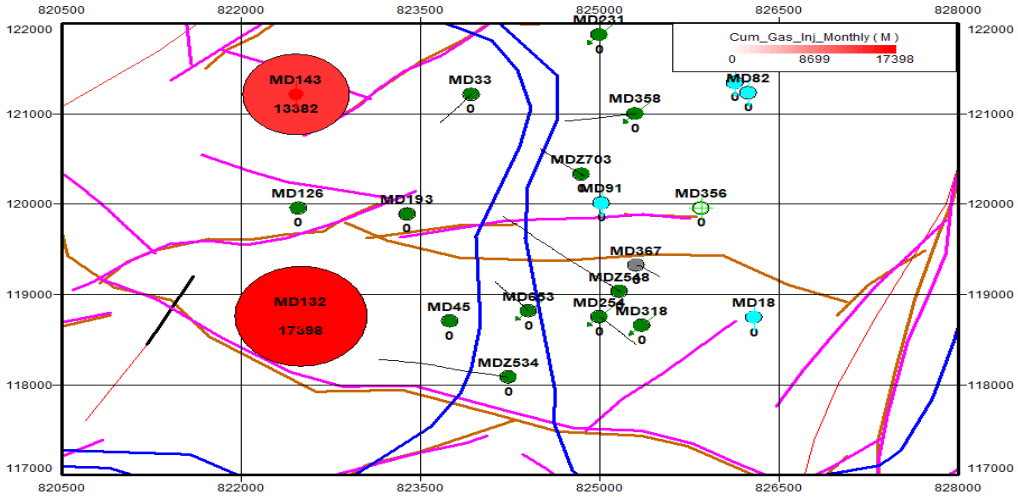

Figure III. 17: Bubble map of cumulative gas injection of the inter-zone 17-19 [17].

III.3.3. Pressure history:

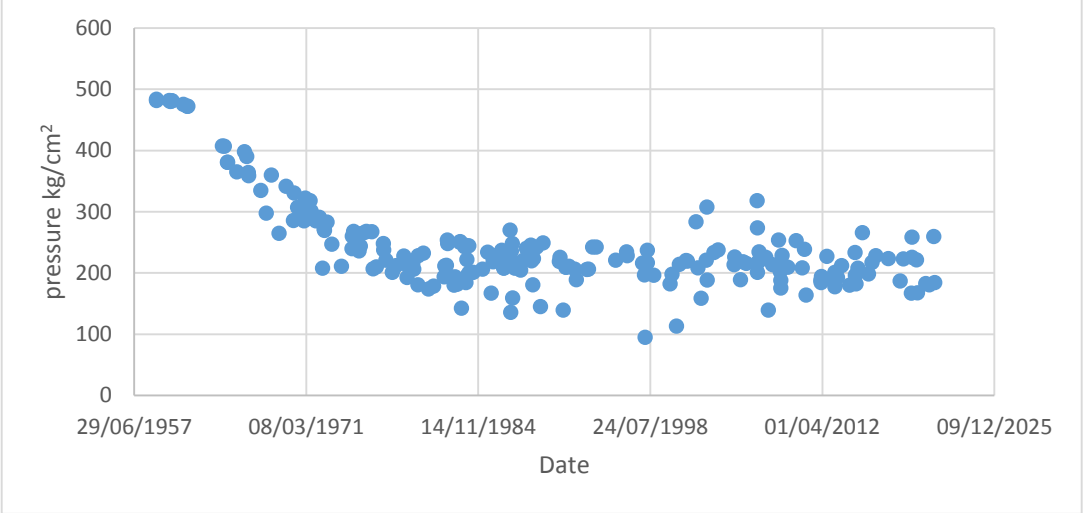

Figure III. 18: Reservoir pressure of the wells in the inter-zone 17-19.

The figure (III.18) shows that the zone's wells has a similar pressure trend, and also shows that the pressure decreases significantly in the period of natural depletion between 1957 and 1972 from 484 kg/cm^2 to around 200 kg/cm^2, then after the start of injection the pressure is maintained around 200 kg/cm^2.

III.3.4. Reserves in place calculation:

III.3.4.1. With volumetric method:

For the sake of calculating the reserves in the inter-zone 17-19 we use the following relations:

$$SOOIP = H_u . A . \emptyset (1 - S_{wi}) . \frac{1}{B_o} \quad \text{(III.1)}$$

SOOIP: original oil in place at surface conditions (m^3).

H_u: net thickness (m).

A: the area of the zone (m^2).

$\emptyset$: porosity (fraction).

S_{wi}: initial water saturation (fraction).

B_o: oil formation volume factor m^3/stm^3

$$H_{uAvr} = \frac{\sum_{i=1}^{n} H_{ui}}{n} \quad \text{(III.2)}$$

$$\emptyset_{Avr} = \frac{\sum_{i=1}^{n} H_{ui}\emptyset_i}{\sum_{i=1}^{n} H_{ui}} \quad \text{(III.3)}$$

$$S_{wAvr} = \frac{\sum_{i=1}^{n} H_{ui}\emptyset_i S_{wi}}{\sum_{i=1}^{n} H_{ui}\emptyset_i} \quad \text{(III.4)}$$

H_{uAvr}: average net thickness (m).

$\emptyset_{Avr}$: average porosity (fraction).

S_{wAvr}: average initial water saturation (fraction).

The reserve in place calculations is summarized in the table (III.1).

Table III. 1:reserve in place calculations with volumetric method

.

	Thickness	porosity	saturation	Reserve in place
D5	11,304	0,067861	0,128967145	5126,264
D3	18,94	0,066719	0,128585665	8448,24
D2	24,128	0,078475	0,100765006	13062,79
ID	29,556	0,078268	0,099523764	15981,29
D1	28,356	0,074084	0,115393432	14257,11
R2	5,836667	0,081793	0,254387341	2730,906
TOTAL				59606,6

The reserve in place estimated by volumetric method is 59 606 600 Stm^3

III.3.4.2. With material balance method:

The parameters Bo, Bg, Rs, are entered into the MBAL software in the form of the table (III.2) that contain the values of these parameters at different pressures and at a constant temperature equal to that of the reservoir (120° C).

the software will look in many correlations and try to find a good match evolution of PVT parameters with respect to pressure.

The most well fit correlation in our case is correlation of Lasater.

Table III. 2: Evolution of PVT parameters with a function of pressure. [17]

Temperature (°c)	**Pressure kg/cm^2**	**Bubble pressure (kg/cm^2)**	**Bo Corrected (m^3/stm^3)**	**Rs Corrected m^3/m^3**	**Bg m^3/stm^3**
120	632,7	180,2	1,805	263,2	
120	562,5	180,2	1,828	263,2	
120	492,2	180,2	1,855	263,2	

120	421,9	180,2	1,886	263,2	
120	381,6	180,2	1,906	263,2	
120	351,5	180,2	1,923	263,2	
120	281,2	180,2	1,970	263,2	
120	210,9	180,2	2,032	263,2	
120	193,3	180,2	2,051	263,2	
120	180,2	180,2	2,063	263,2	
120	147,6	180,2	1,851	203,4	0,008
120	119,5	180,2	1,724	167,9	0,01
120	91,4	180,2	1,603	135,8	0,013
120	63,3	180,2	1,491	107,1	0,019
120	35,2	180,2	1,380	78,1	0,035

III.3.4.2.1. Petrophysical data:

We calculated the reservoir porosity and saturation using the equations (III.3) and (III.4)

Connate water saturation: 13.7 %

Average reservoir porosity: 7.45 %

III.3.4.2.2. Pressure history matching:

The software will calculate the pressure with taking into account the produced and injected volumes. our job is based on matching each well with its correct Geometric Allocation Factor depending on its position and the geological constraints until the calculated pressure match with the pressure which developed by the actual measurements at the wells of the zone.

III.3.4.2.3. Steps of the work:

The execution of the work is carried out according to the following steps:

- ✓ Selection of wells in the zone.
- ✓ Collection of production, injection and measured pressure data from wells in the zone.
- ✓ Calculation of the pressure until we obtain an acceptable match with the measured pressures in the injection period.
- ✓ To match the pressure in the natural depletion period we vary the reserves in place, taking as initial values the volumetric reserves.

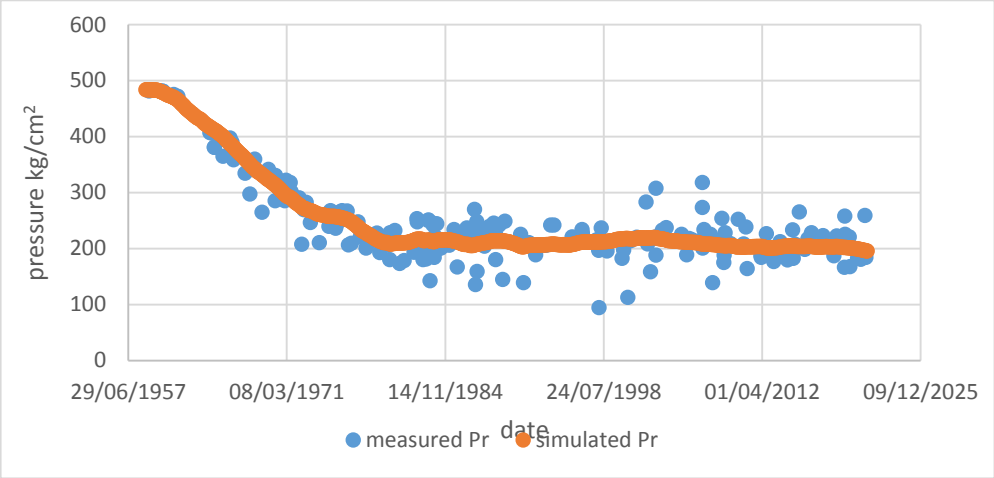

Figure III. 19: Pressure history matching of the inter-zone 17-19

The reserves in place estimated by the MATERIAL BALANCE method in the inter-zone 17-19 is 60 810 000 Stm^3.

III.3.5. Drainage mechanisms:

In the inter-zone 17-19, four drainage mechanisms coexist as shown in the figure (III.20):

During the natural depletion period, the dominating mechanism was the expansion of the oil and its dissolved gas where its drainage index was about 70% the whole period, the other mechanism present was the expansion of the formation but its contribution to production does not exceed 30% as indicated by its index.

The injection began in 1972 and from that year, the gas injection has gradually become the mechanism that ensures the most important part of production with a 65% index, the other mechanisms contribute in the rest 35% as following: fluid expansion 20%, water injection 10%, and formation expansion with 5%.

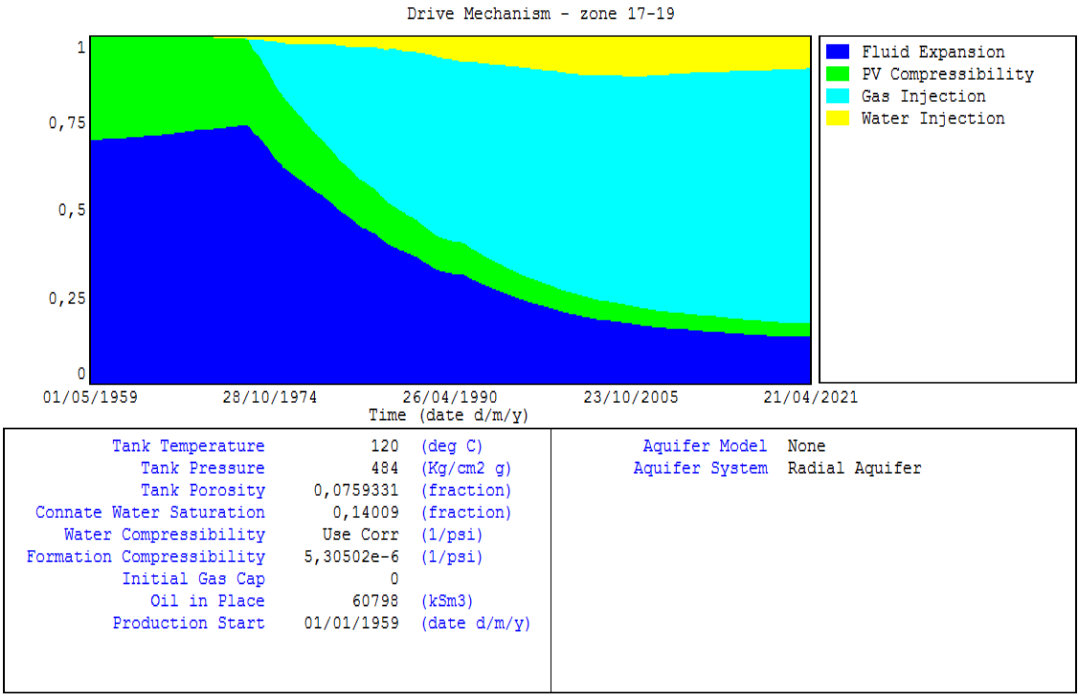

Figure III. 20: Evolution of drainage indices as a function of time in the inter-zone 17-19.

III.3.6. Injection performance in the inter-zone 17-19:

III.3.6.1. VRR (voidage replacement ratio) analysis :

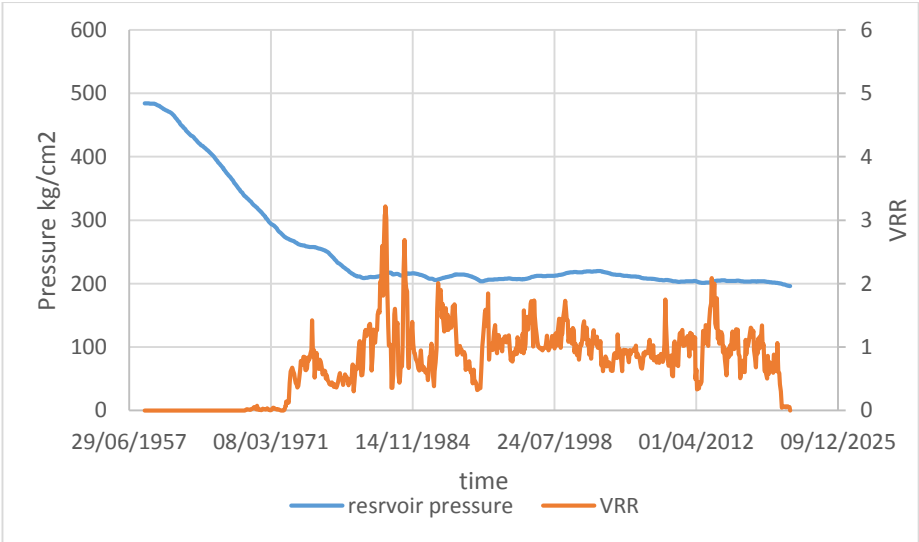

Figure III. 21: VRR and the average pressure curves of the inter-zone 17-19 as a function of time

The figure (III.21) shows the evolution of the VRR and the average pressure curves of the inter-zone 17-19 as a function of time and it shows that the injection in the inter-zone 17-19 could be divided on 3 periods:

The first period: from 1972 to 1981: the VRR was less than 1 which did not prevent the pressure from decreasing

The second period: from 1981 to 1991: in this period a new water injector well (MD82) started injecting and with the periodic closing of the producing wells, the VRR was significantly greater than 1 which allow a pressure maintain.

The third period: from 1991 until now: the VRR fluctuates slightly around unity, which allows us to say that a withdrawal-injection balance is established, and also the pressure was maintained.

III.3.6.2. Impact of the injection on the recovery factor:

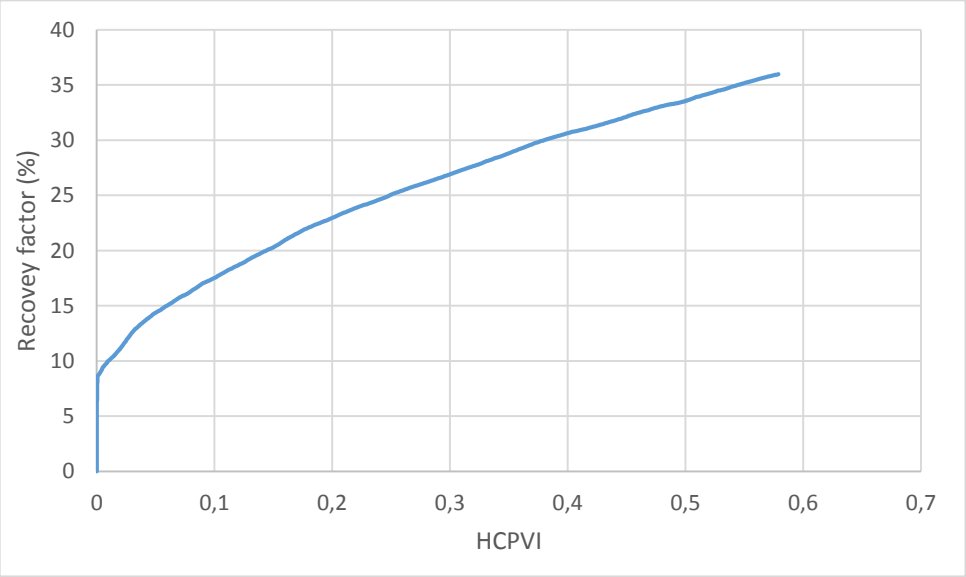

Figure III. 22: Recovery factor versus HCPVI of the inter-zone 17-19 as a function of time

The figure (III.22) shows that the total oil recovery is 36% compared to the reserves in place, 9% of this oil was recovered by natural depletion of the reservoir, while 30.48% of the oil has been recovered since the beginning of injection and after the injecting of 57.9% of the pore volume.

III.4. Analysis of injection patterns in the inter-zone 17-19:

III.4.1. Validation of injection patterns in the inter-zone 17-19:

The choice of the location and the extent of a pattern must satisfy certain recommendations that allow it to be considered closed.

We can mention:

- The corners of the pattern should be occupied by injector wells, leaving the center of the pattern to producers.
- The boundaries of the pattern are marked by the presence of injector wells or by impermeable barriers
- The pattern wells should have a pressure trend as close as possible
- The pattern must have an acceptable pressure calibration by the material balance method

The methodology of the analysis is summarized in the following steps:

- Establish the patterns on reservoir respecting the criteria of choice.
- Plot the pressures of each pattern (pressure trends).
- Assign a volume of hydrocarbons from the geological model (volumetric reserves) as initial reserves of each pattern.
- Assign to each well its appropriate geometric allocation factor
- Calculate the average pressure of each pattern and match it with the actual pressure trend.
- Extract the reserves of each pattern that Correspond to the set pressure profile.
- Estimate the primary and secondary recovery.
- Plot and analyze the VRR curves associated with the pressure and flow rate for each pattern.
- Analyze the curves of recovery factor versus injected pore volume.

The objectives of the analysis in this section will be:

- Optimizing gas and water injection volumes.
- Examine the injection-recovery balance of each pattern.
- Defining the over-injected and under-injected compartments.
- Defining potential zones for the implementation of new producing wells.
- Estimation of the recovery for each pattern.

III.4.2. Defining injection patterns:

After a detailed analysis of the production and injection history, pressures trends and the geological structures (barriers, faults and seismic features) of the inter-zone 17-19, it was possible to assign a pattern configuration that meets all the above criteria

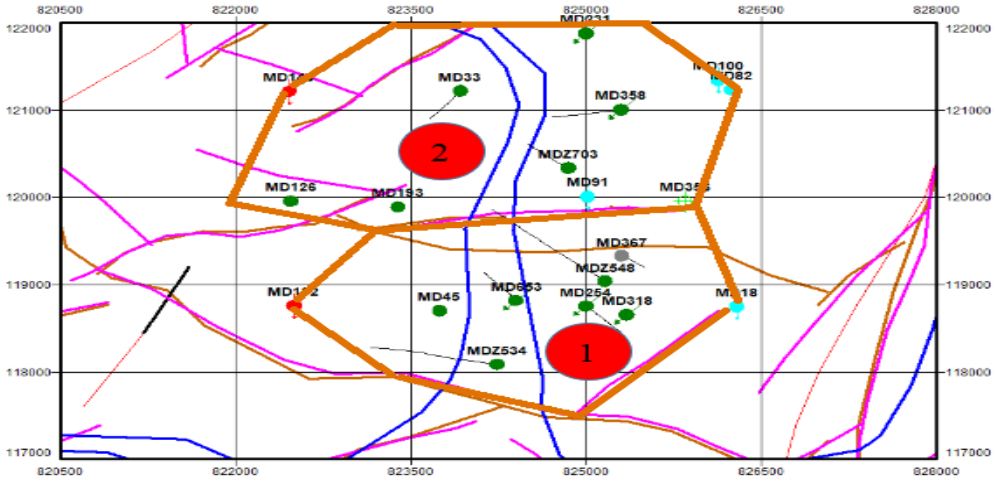

Figure III. 23: The patterns configuration assigned to the inter-zone 17-19**.**

The table (III.3) shows the injector and producer wells for each pattern:

Table III. 3: Well distribution by pattern

pattern	Gas injector wells	water injector wells	Producer wells
Pattern 1	MD132	MD18	MD45, MD653, MD367, MD252, MD318, MDZ534, MDZ548
Pattern 2	MD143	MD82,MD91,MD100	MD33, MD231, MD358, MD356, MD193,MD126, MDZ703

III.5. Patterns Performance Analysis:

III.5.1. Pattern 1:

III.5.1.1. Pressure history matching:

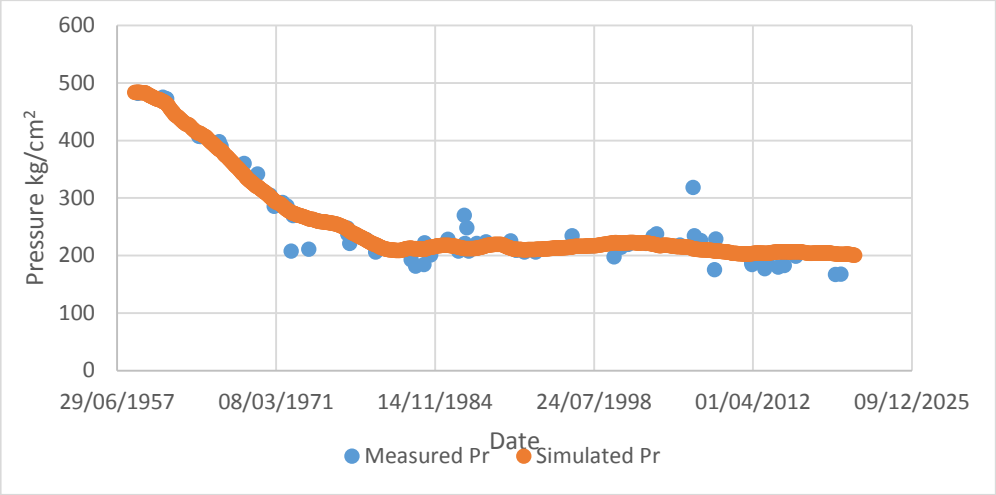

Figure III. 24: pressure history matching of pattern 1

The calculated pressure curve is well matched in the period of natural depletion as well as in the injection period as shown in the figure (III.24). Injection is considered the only energy source that assure the pressure maintenance of this pattern.

III.5.1.2. Drainage index evolution:

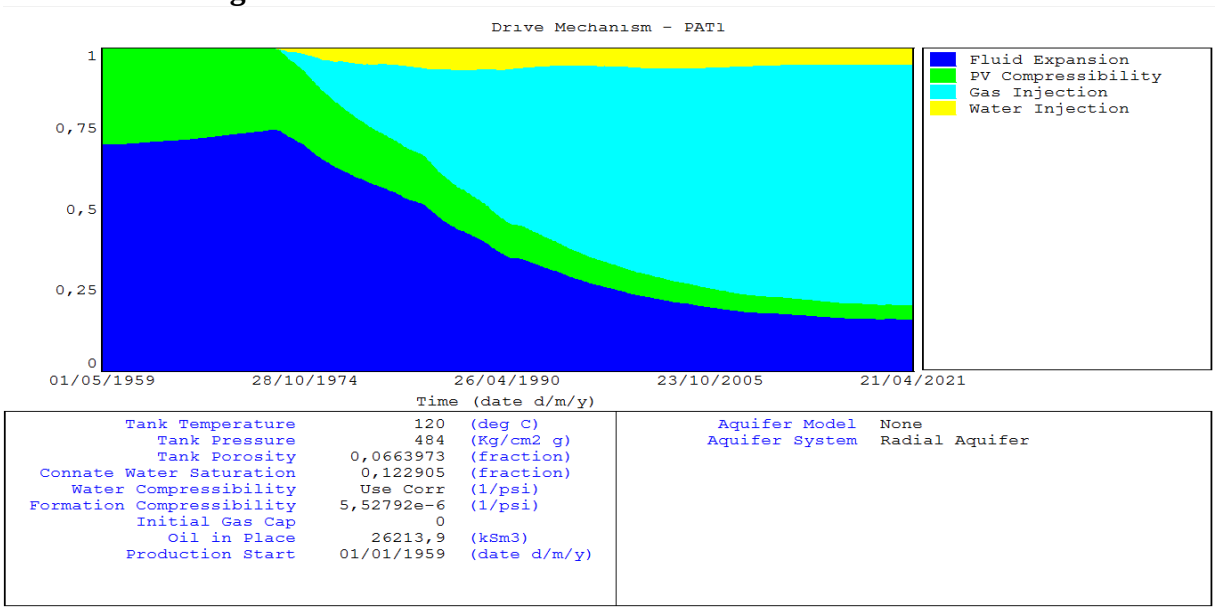

Figure III. 25: Drainage index evolution versus time of pattern 1

The injection began in 1972 and from that year, the gas injection has gradually become the mechanism that ensures the most important part of production with a 70% index, the other mechanisms contribute in the rest 30% as following: fluid expansion 20%, water injection 5%, and formation expansion with 5%.

III.5.1.3. VRR curve analysis:

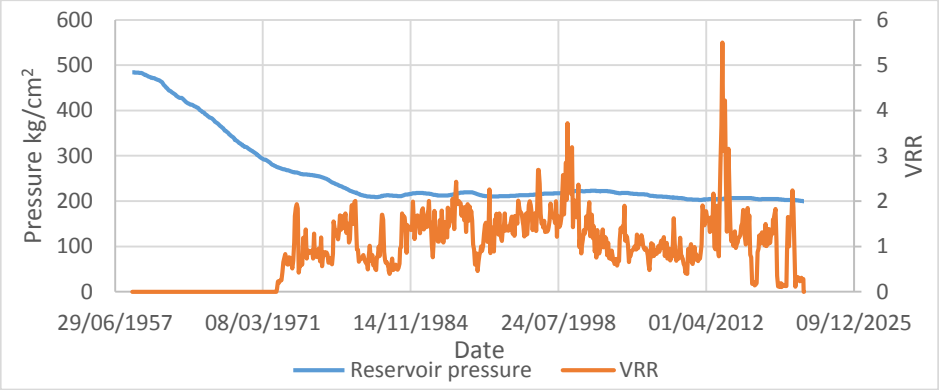

Figure III. 26: VRR and the average pressure curves of the pattern 1

From the beginning of injection in 1972 the VRR fluctuates slightly around unity as shown in the figure (III.26), which allows us to say that a withdrawal-injection balance is established, and also the pressure was maintained.

From the figure (III.27) we notice a strong correlation between the VRR and the oil production except for the period from 2001 to 2012 where new wells were drilled which causes the increase in the oil production and the decrease in the VRR.

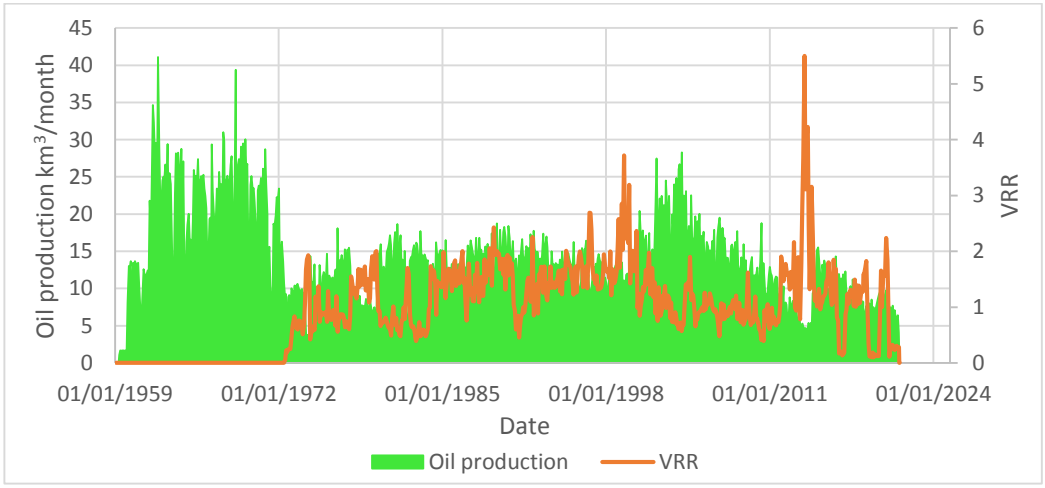

Figure III. 27: VRR and oil flow rate curves of pattern 1

III.5.1.4. Impact of injection on the recovery factor:

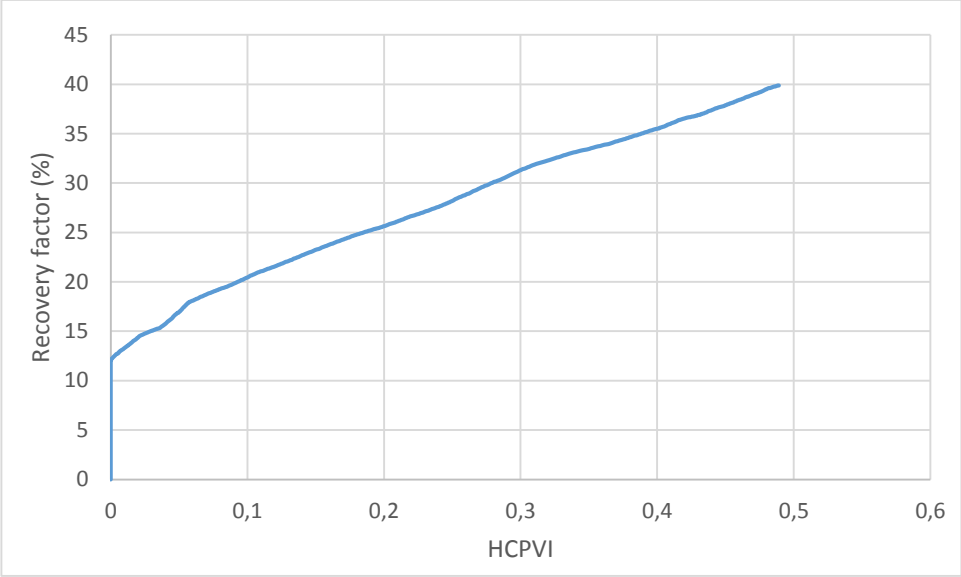

Figure III. 28: Recovery factor versus HCPVI of pattern 1

The figure (III.28) shows that the total oil recovery is 40% compared to the reserves in place, 12% was recovered by natural depletion of the reservoir, while the other 28% has been recovered since the beginning of injection and after the injecting of 49% of the pore volume, also the slope of the curve is still sharp which indicates that there are more hydrocarbons to produces by injecting more in this pattern.

III.5.2. Pattern 2:

III.5.2.1. Pressure history matching:

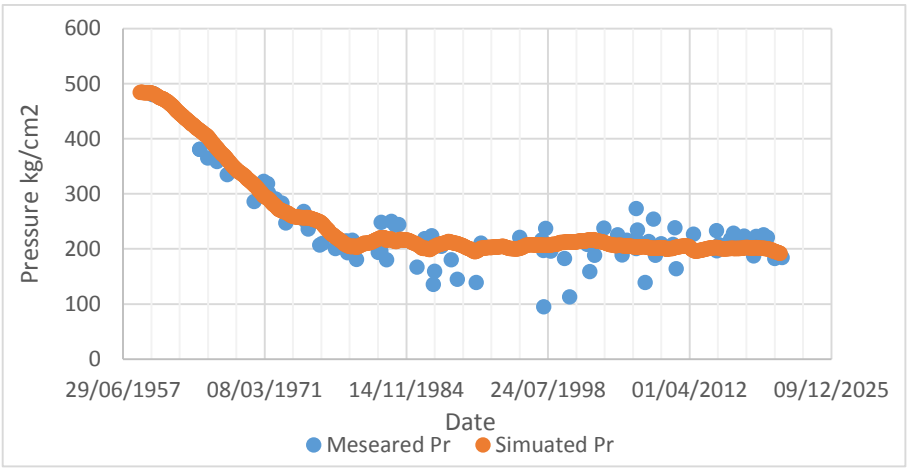

Figure III. 29: pressure history matching of pattern 2

The calculated pressure curve is well matched in both natural depletion and the injection periods. as shown in the figure (III.29) Injection is considered the only energy source that assure the pressure maintenance of this pattern as well as the previous one.

III.5.2.2. Drainage index evolution:

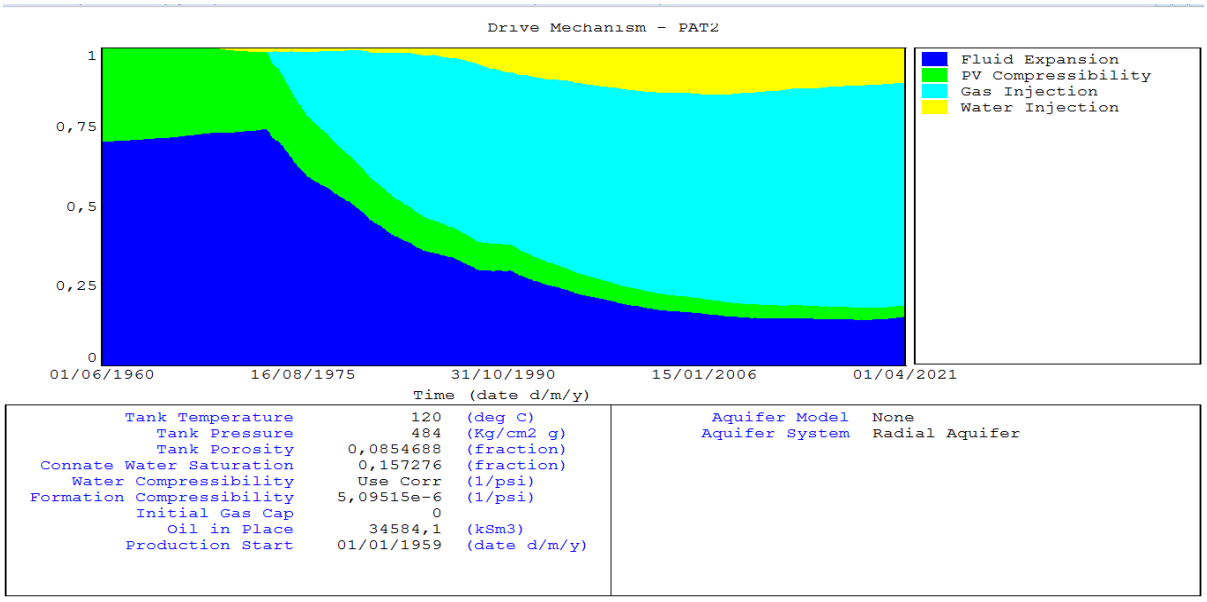

Figure III. 30: Drainage index evolution versus time of pattern 2

As in pattern 1, the gas injection has gradually become the mechanism that ensures the most important part of production since its start of injection with a 65% index, while the fluid expansion contribute with a 20%and the water injection with a 10% and the last one, the formation expansion with only 5%.

III.5.2.3. VRR curve analysis:

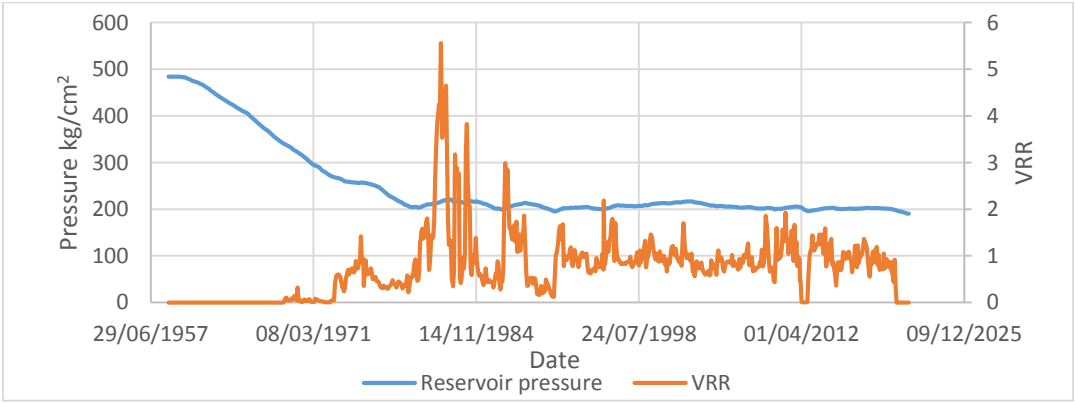

Figure III. 31: VRR and the average pressure curves of the pattern 2

From the beginning of injection until 1981 the VRR was less the 1 due to large number of producer wells compared to injector, this VRR allowed the pressure to drop.

In the period from 1981 to 1991 the VRR was not stable due to opening and closing of the producer wells and also adding new injector wells, the VRR was mostly greater than 1 and the pressure was maintained, from 1991 until now the VRR fluctuates slightly around unity, which allows us to say that a withdrawal-injection balance is established, and also the pressure was maintained. Also the VRR correlate greatly with the oil rate.

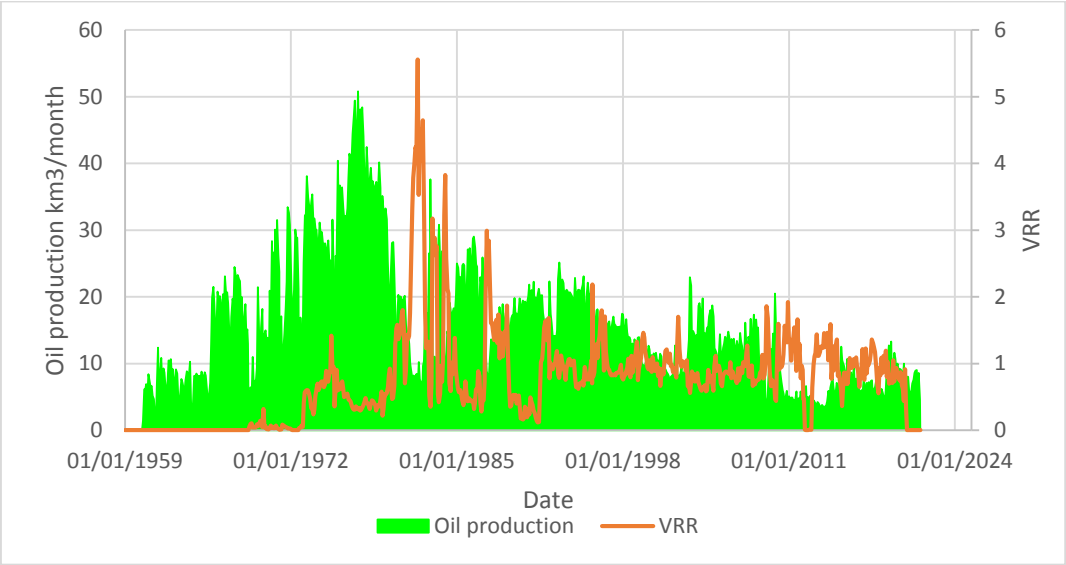

Figure III. 32: VRR and oil flow rate curves of pattern 2

III.5.2.4. Impact of injection on the recovery factor:

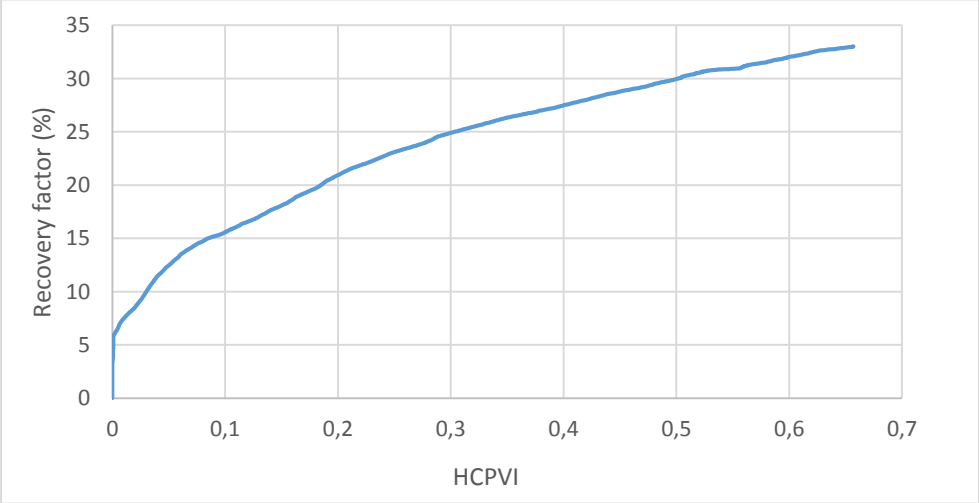

Figure III. 33: Recovery factor versus HCPVI of pattern 2

The figure (III.33) shows that the total oil recovery is 33% compared to the reserves in place, only 6% was recovered by natural depletion of the reservoir, while the other 30% has been recovered since the beginning of injection and after the injecting of 65.66% of the pore volume, the slope of the curve starts to flat horizontally which indicates that there is not much production left in this pattern.

III.6. Conclusion:

The zone:

- The original oil-in-place reserves of the inter-zone 17-19 are estimated to be 60.81 million stm^3.
- The pressure of the reservoir was maintained in the zone since the start of injection and the VRR was kept close to 1 in most of the zone life.
- Before the start of the injection, the oil recovery factor was 5.52%. Currently, it reaches 36% after injection of a volume equivalent to 57.9% of the pore volume.
- The natural drainage mechanisms in this area are the expansion of oil and its dissolved gas (more than 70%) and the expansion of the formation (less than 30%).
- After the initiation of gas injection, it gradually replaces the other mechanisms to become the mechanism that assures the most important part of the production in the zone.
- A good withdrawal-injection balance has been established in the zone.

The patterns:

- The recovery factor is 40% at an HCPVI= 49% in the pattern 1, while it is 33% at an HCPVI =65.66% in second pattern.
- The VRR fluctuates around 1 in both patterns and the pressure is maintained which allow us to say that a withdrawal-injection balance.
- The efficiency of injection is better in pattern 1than 2, where there is more 51% of hydrocarbons left in the first pattern compare to only 35% in the second.

Table III. 4: Summary of recovery factors and HCPVI of injection patterns

	OOIP (KSm^3)	**Primary recovery(%)**	**Actual recovery(%)**	**HCPVI (%)**	**Actual state of injection**
Pattern 1	**26213.9**	**12**	**40**	**49**	**VRR=1**
Pattern 2	**34584.1**	**3**	**33**	**65.66**	**VRR=1**

CHAPTER IV: FORECAST OF THE PRESSURE BEHAVIOR OF THE PATTERNS AND BREAKTHROUGH PROBLEM DIAGNOSTIC

IV.1. Introduction:

The pressure in the inter-zone 17-19 started to decrease after closing most of the injector wells due to either water or gas breakthroughs problems, in this chapter we are going to try to predict the pressure behavior for each pattern for the next 4 years and diagnose the wells that have breakthrough problem.

IV.2. Forecast of the pressure behavior of the patterns:

IV.2.1. Methodology of the analysis:

- Analyze the current state of the zone.
- Perform a decline curve analysis on all the wells (see Annexes).
- Insert the data collected from the decline curve analysis in MBAL software.
- Calculate the average pressure for each pattern.
- Plot and analyze the VRR curves associated with the pressure.
- Try different scenarios to find the optimum one.

IV.2.2. Current state of the zone:

- 2 gas injector wells (MD132, MD143) are closed.
- 3 water injector wells (MD82, MD91, MD100) are closed.
- Only one water injector well is opened (MD18).
- 3 oil producing wells are closed (MD231, MD356, MD367).
- 11 oil producing wells are opened.

After the analysis we managed to forecast four different scenarios until the year 2025:

IV.2.3. First scenario: (continue with the current state):

IV.2.3.1. Pattern 1:

The figures (IV.1) and (IV.2) shows that the well MD18 alone will not achieve the withdrawal-injection balance where the VRR will be only 0.25 which will lead to a pressure drop in this pattern to 183 kg/cm^2.

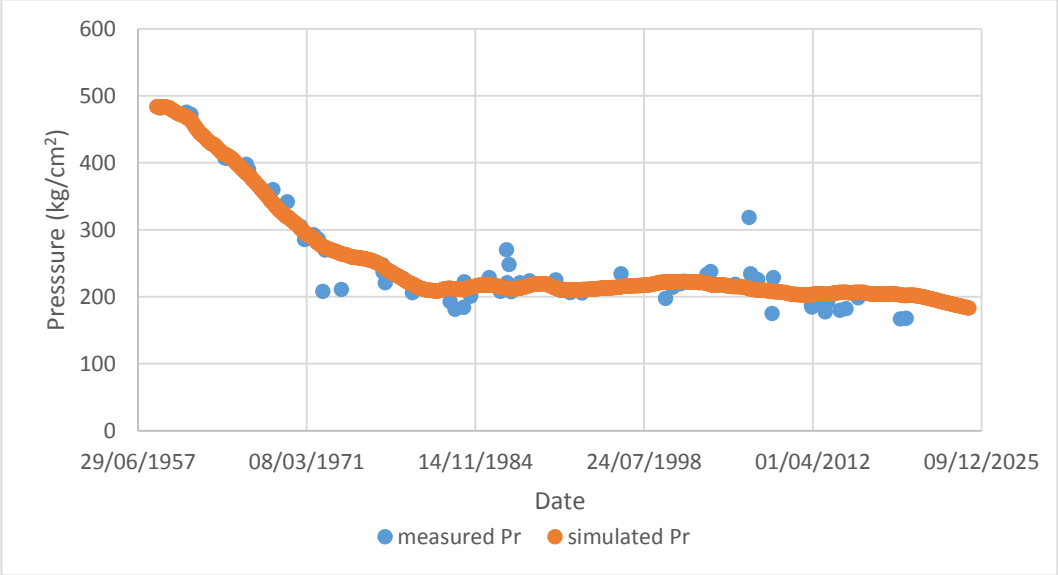

Figure IV. 1: pressure forecast of pattern 1 (first scenario)

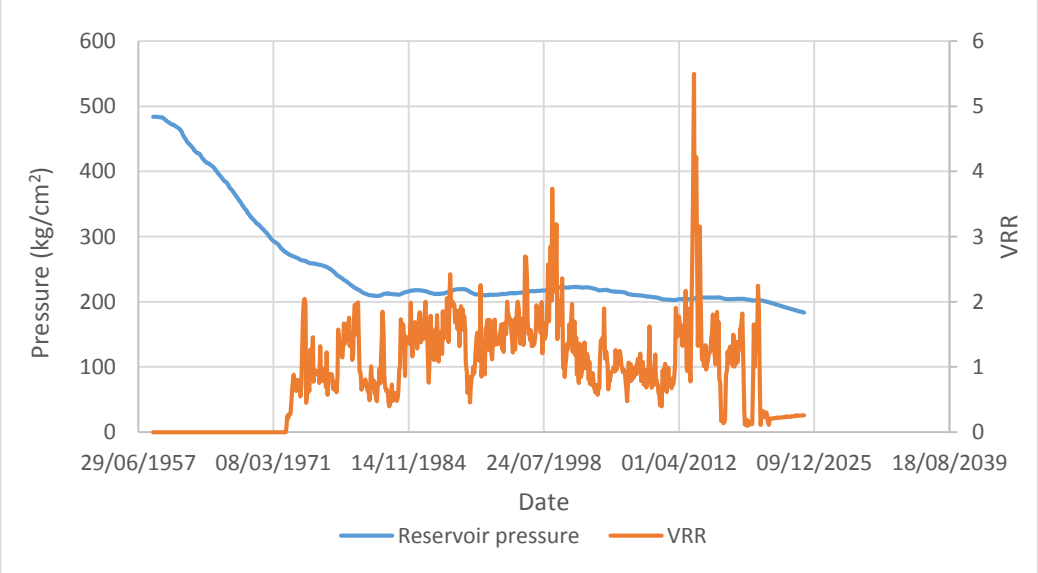

Figure IV. 2: forecast of VRR and the average pressure curves of the pattern 1 (first scenario)

IV.2.3.2. Pattern 2:

Since there are no injector wells open in this pattern the VRR will 0 which will cause a severe drop in the pressure to 171 kg/cm^2 as shown in the figures (IV.3) and (IV.4).

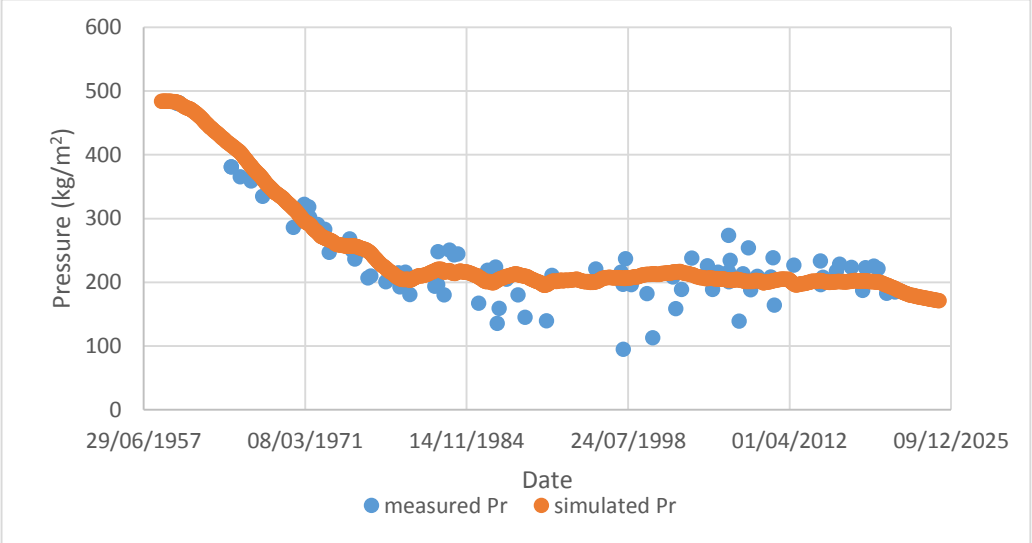

Figure IV. 3: pressure forecast of pattern 2 (first scenario)

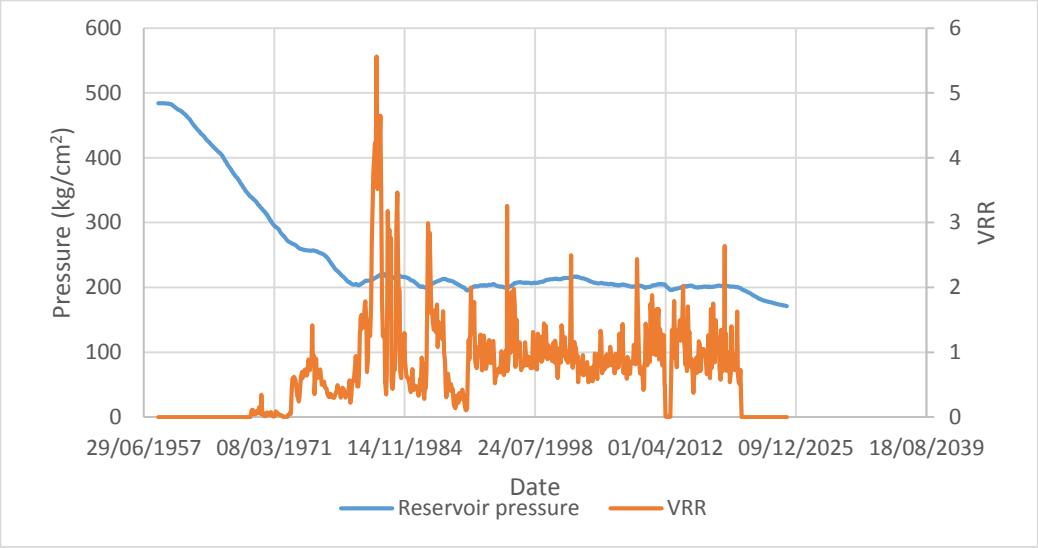

Figure IV. 4: forecast of VRR and the average pressure curves of the pattern 2 (first scenario)

IV.2.4. Second scenario: (opening only the water injector wells):

IV.2.4.1. Pattern1:

Since the water injector is already opened in the previous scenario the behavior will be the same.

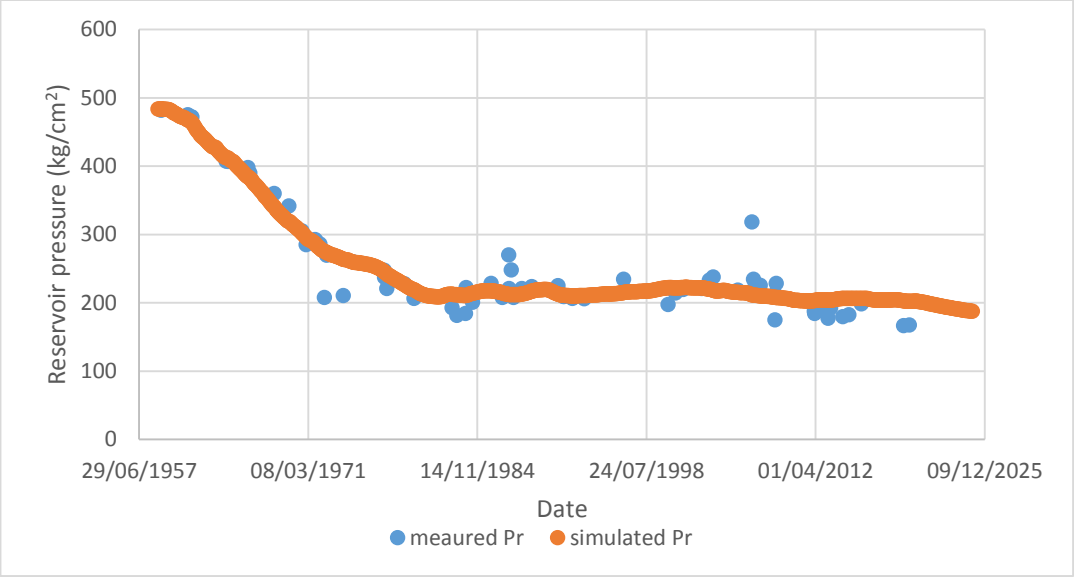

Figure IV. 5: pressure forecast of pattern 1 (second scenario)

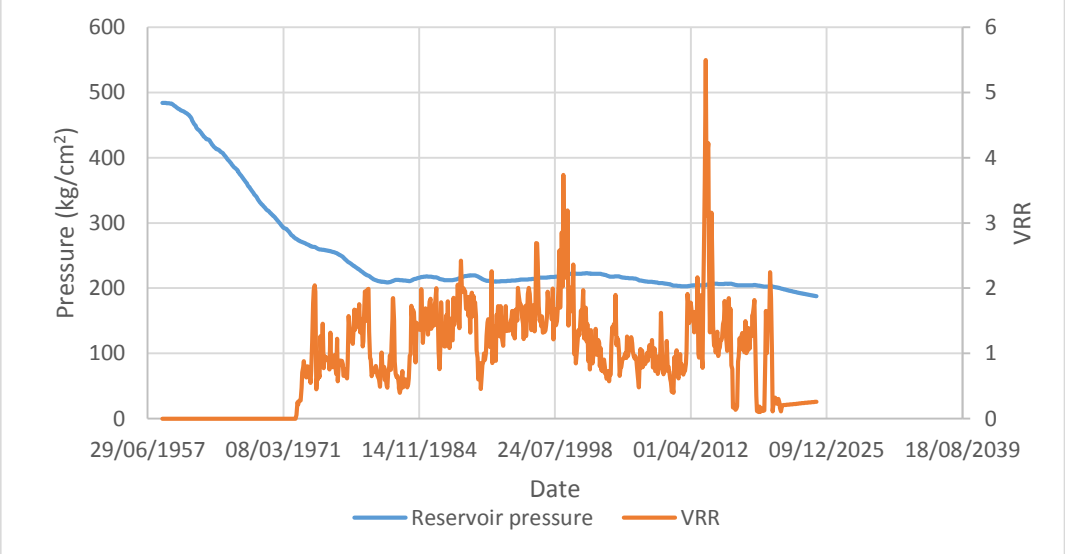

Figure IV. 6: forecast of VRR and the average pressure curves of the pattern 1 (second scenario)

IV.2.4.2. Pattern 2:

The opening of two water injector wells MD82 and MD100 with a rate of 1500 m^3/day each will allow the VRR to reach only 0.64 which will decrease the decline rate of the pressure where it will drop to just 182 kg/cm^2 as shown in the figures (IV.7) and (IV.8).

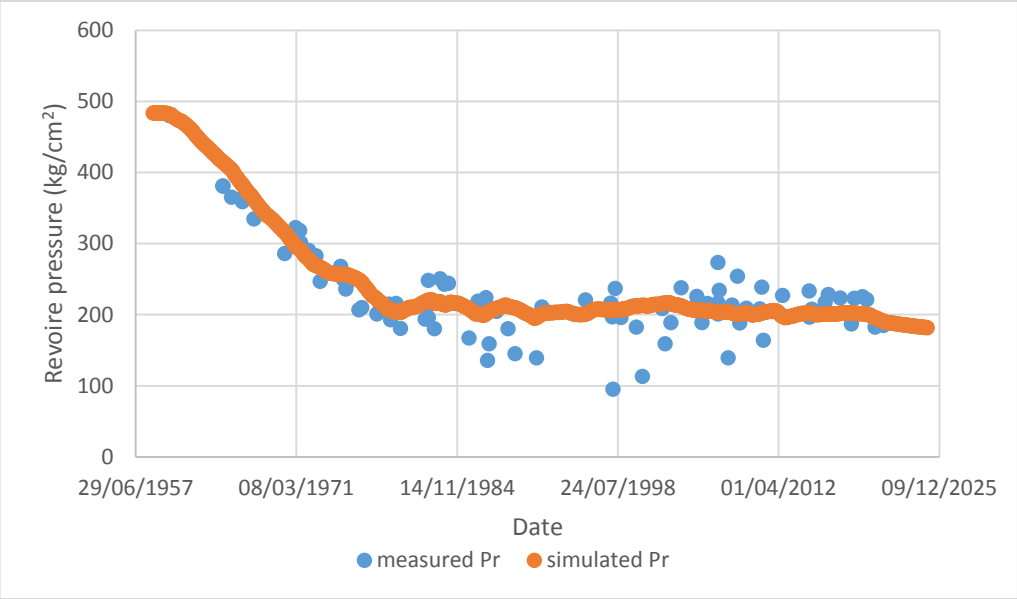

Figure IV. 7: pressure forecast of pattern 2 (second scenario)

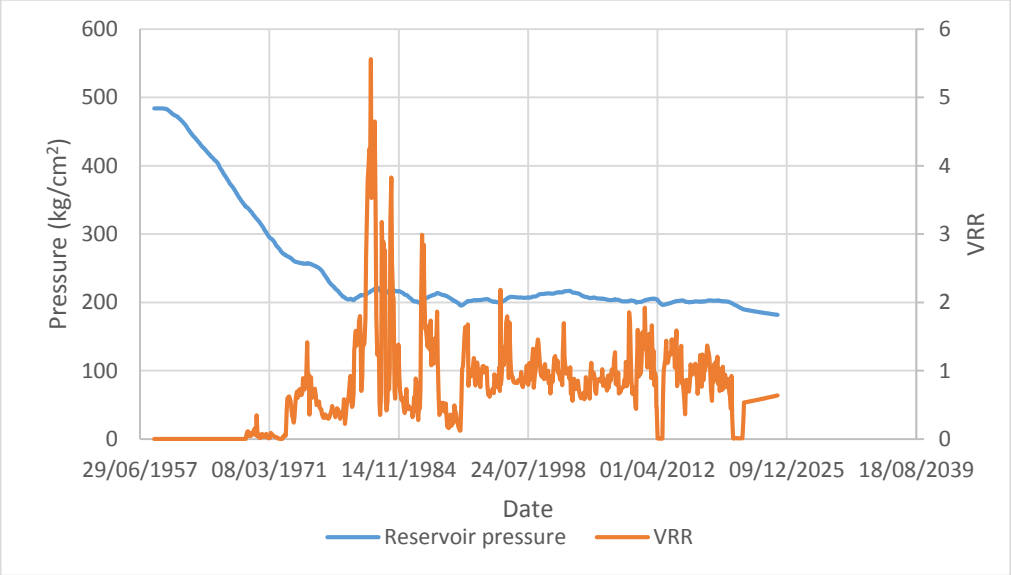

Figure IV. 8: forecast of VRR and the average pressure curves of the pattern 2 (second scenario)

IV.2.5. Third scenario: (opening only the gas injector wells):

IV.2.5.1. Pattern 1:

Injecting gas with a rate of 350 km^3/day from the well MD132 will allow a pressure maintenance and will achieve withdrawal-injection balance.

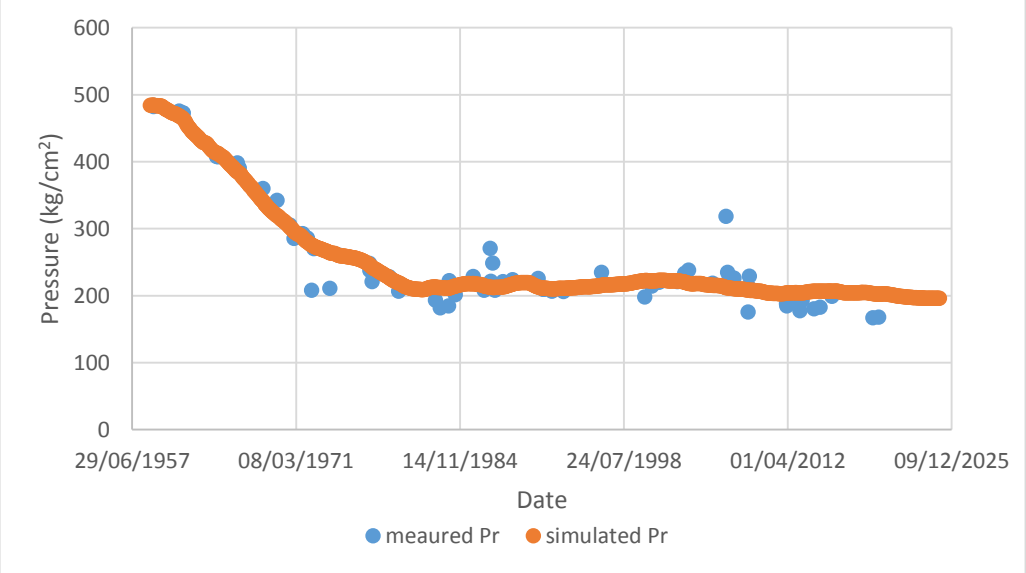

Figure IV. 9: pressure forecast of pattern 1 (third scenario)

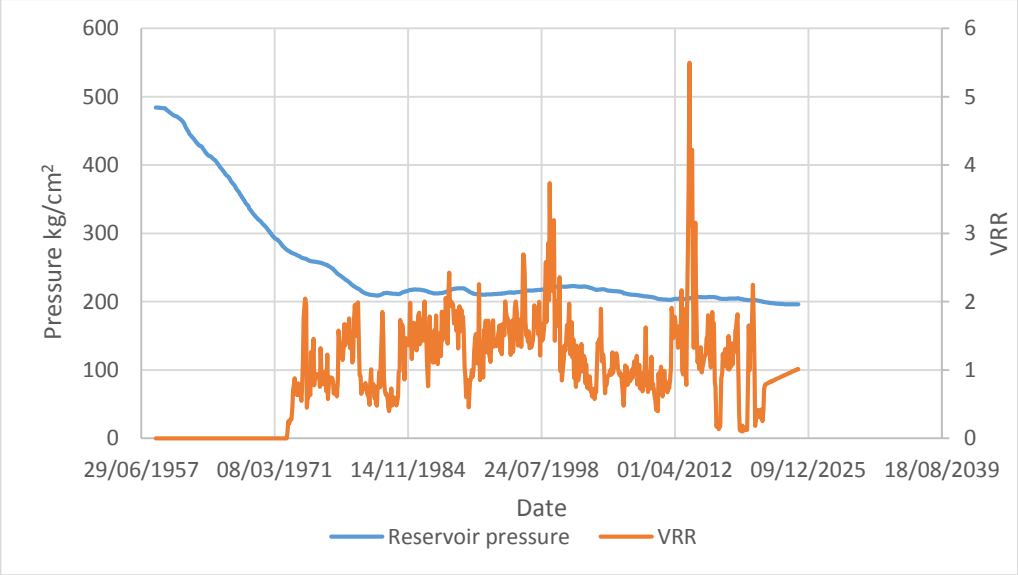

Figure IV. 10: forecast of VRR and the average pressure curves of the pattern 1 (third scenario)

IV.2.5.2. Pattern 2:

To maintain the pressure and achieve a VRR = 1 in this pattern we will need a rate of 500 km^3/day.

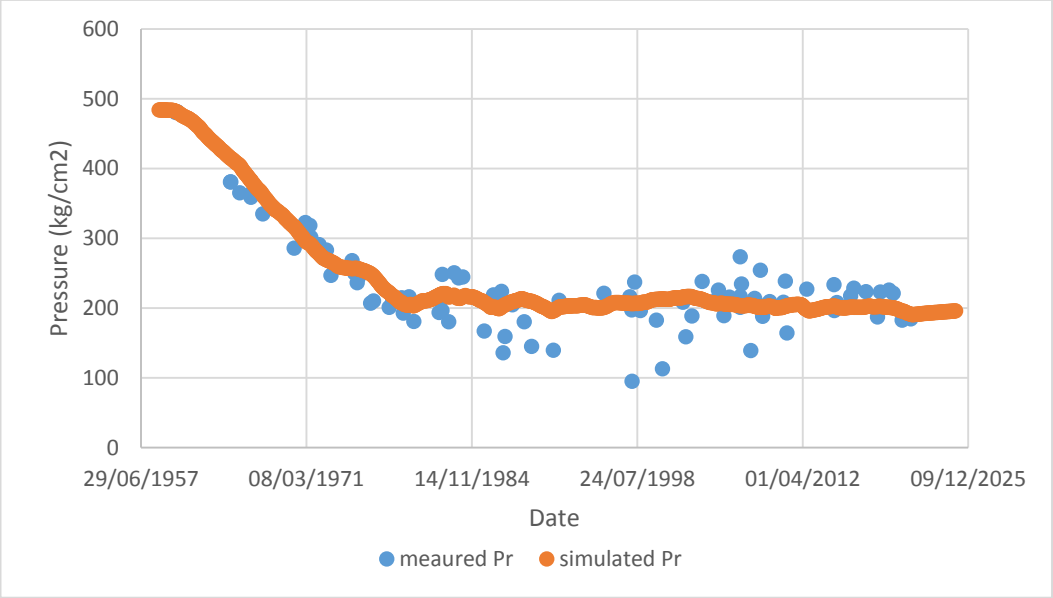

Figure IV. 11: pressure forecast of pattern 2 (third scenario)

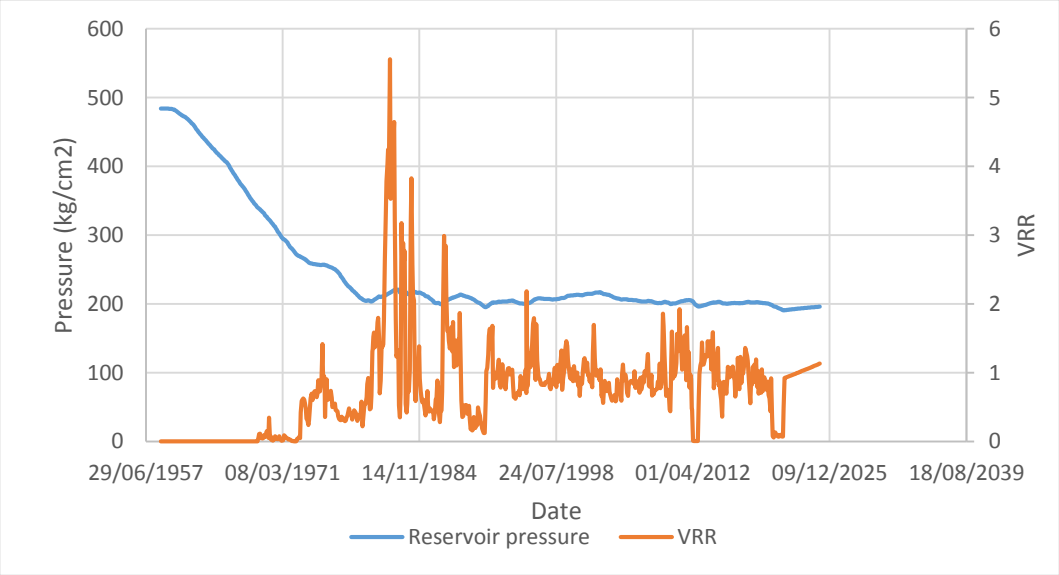

Figure IV. 12: forecast of VRR and the average pressure curves of the pattern 2 (third scenario)

IV.2.6. Fourth scenario: (opening all injector wells):

IV.2.6.1. Pattern 1:

The pressure maintenance and withdrawal-injection balance can be established by injecting a 1300 m^3/day of water and a 250 km^3/day of gas.

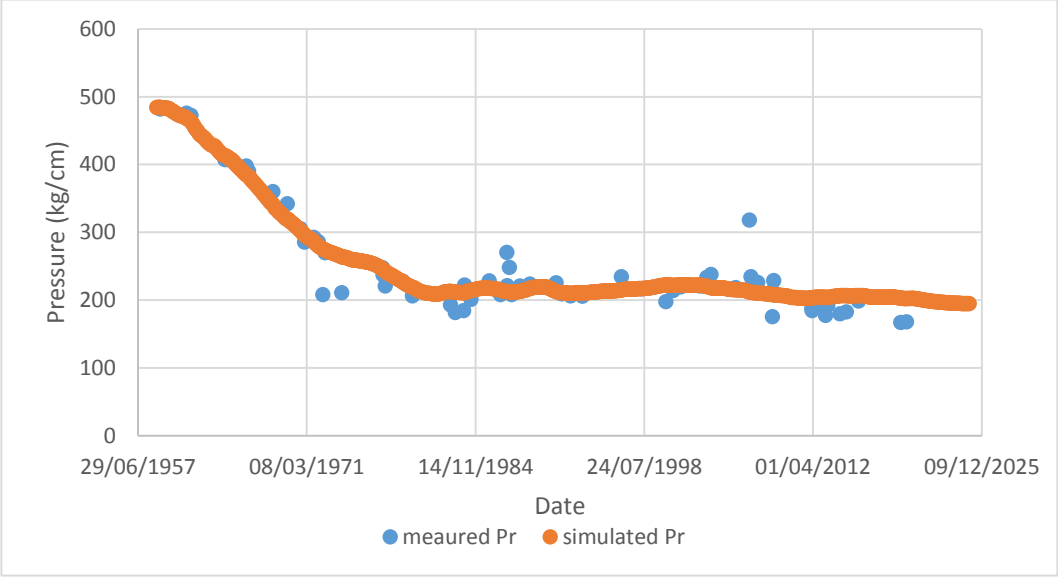

Figure IV. 13: pressure forecast of pattern 1 (fourth scenario)

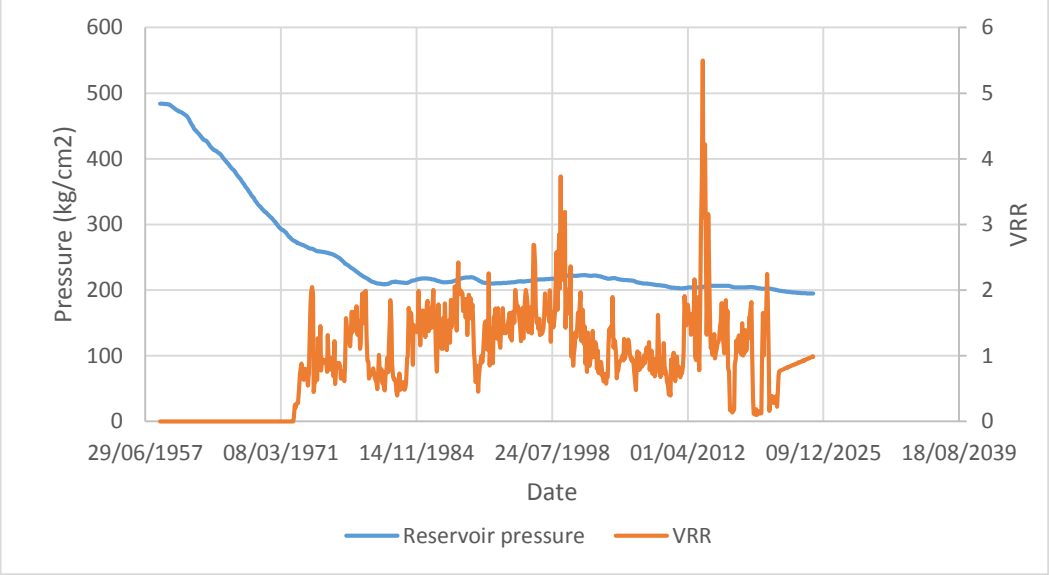

Figure IV. 14: forecast of VRR and the average pressure curves of the pattern 1 (fourth scenario)

IV.2.6.2. Pattern 2:

The pressure will be maintained in this pattern through the injection of 1300 m^3/day of water in both wells MD82 and MD100 and the injection of 200 m^3/day of gas by the well MD143.

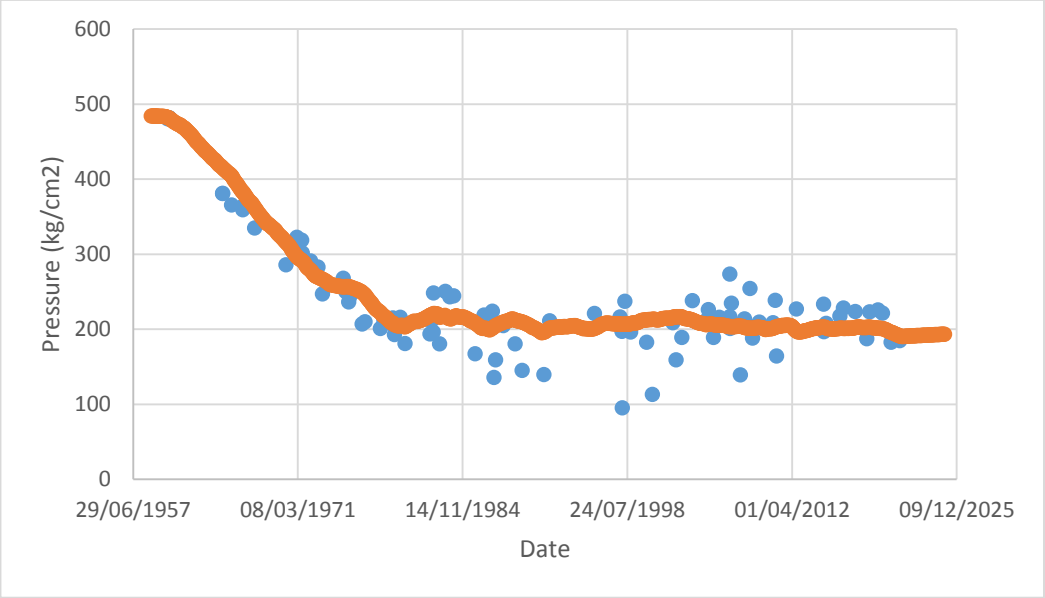

Figure IV. 15: pressure forecast of pattern 2 (fourth scenario)

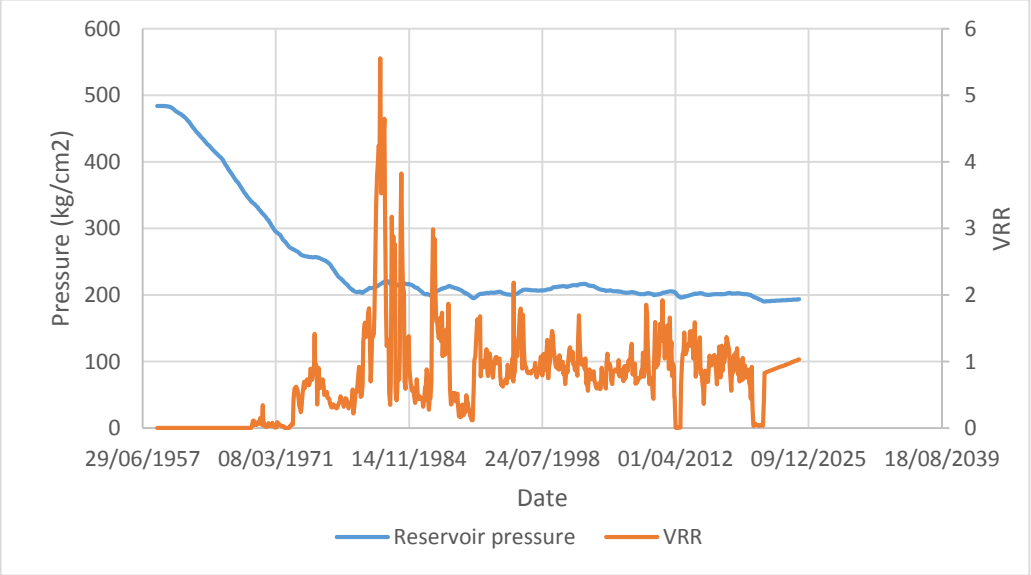

Figure IV. 16: forecast of VRR and the average pressure curves of the pattern 2 (fourth scenario)

IV.3. Breakthrough problem diagnostic:

IV.3.1. The well MD193:

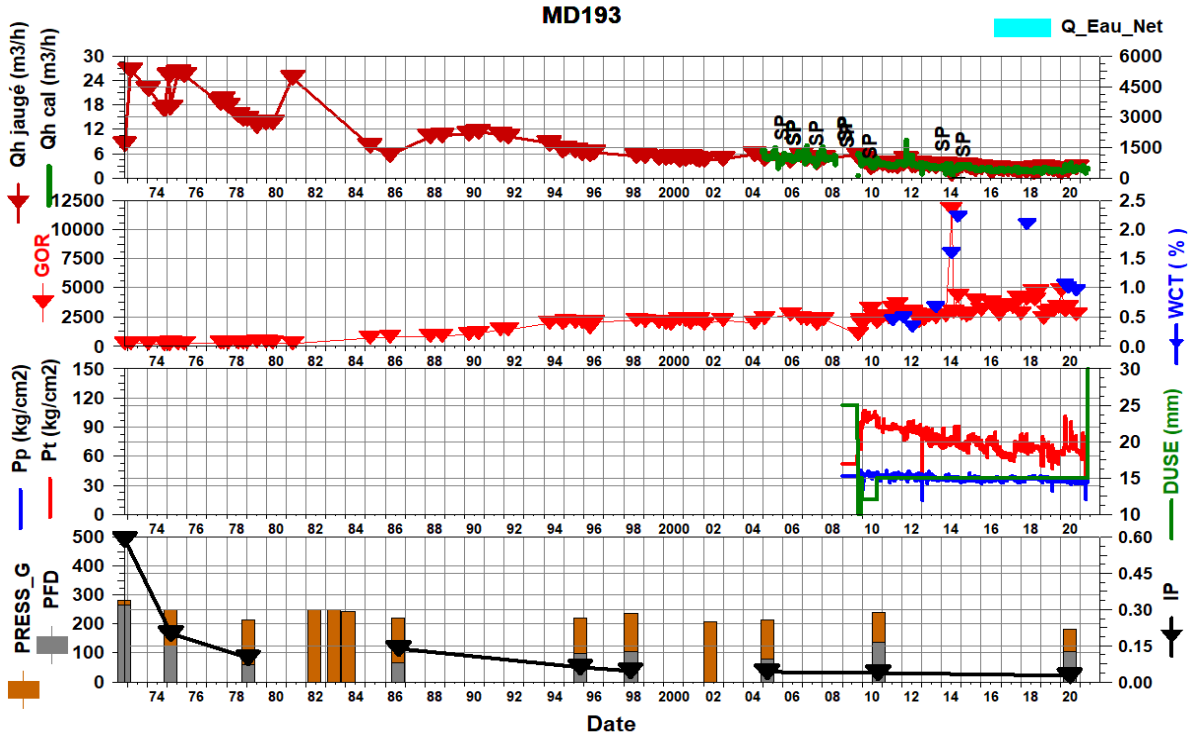

Figure IV. 17: Reservoir pressure, oil flow rate, GOR, water cut, wellhead pressure and pipeline pressure curves of the well MD193 [17].

.

This well was drilled in September 1972 in the west part of the inter-zone 17-19 and was put on production in December 1972. In the first years of its exploitation, this well was characterized by a high flow of 28 m^3/h of oil.

According to the graphs above the well starts producing with a high rate and a reservoir pressure of 283 kg/cm^2.

Quantitative interpretation of the PLT shows gas breakthroughs at the following intervals:

- The interval (3402.3-3409.2m) in the ID with about 8% gas.
- The interval (3411.9-3426.6m) in the D1 with about 18% gas and 41% oil.

The majority of the production comes from the zone (3399.6-3401.5m) with a percentage of 73% gas and 33% oil.

NB: the percentages of oil and gas flows are calculated in ratio to the total flow of each phase

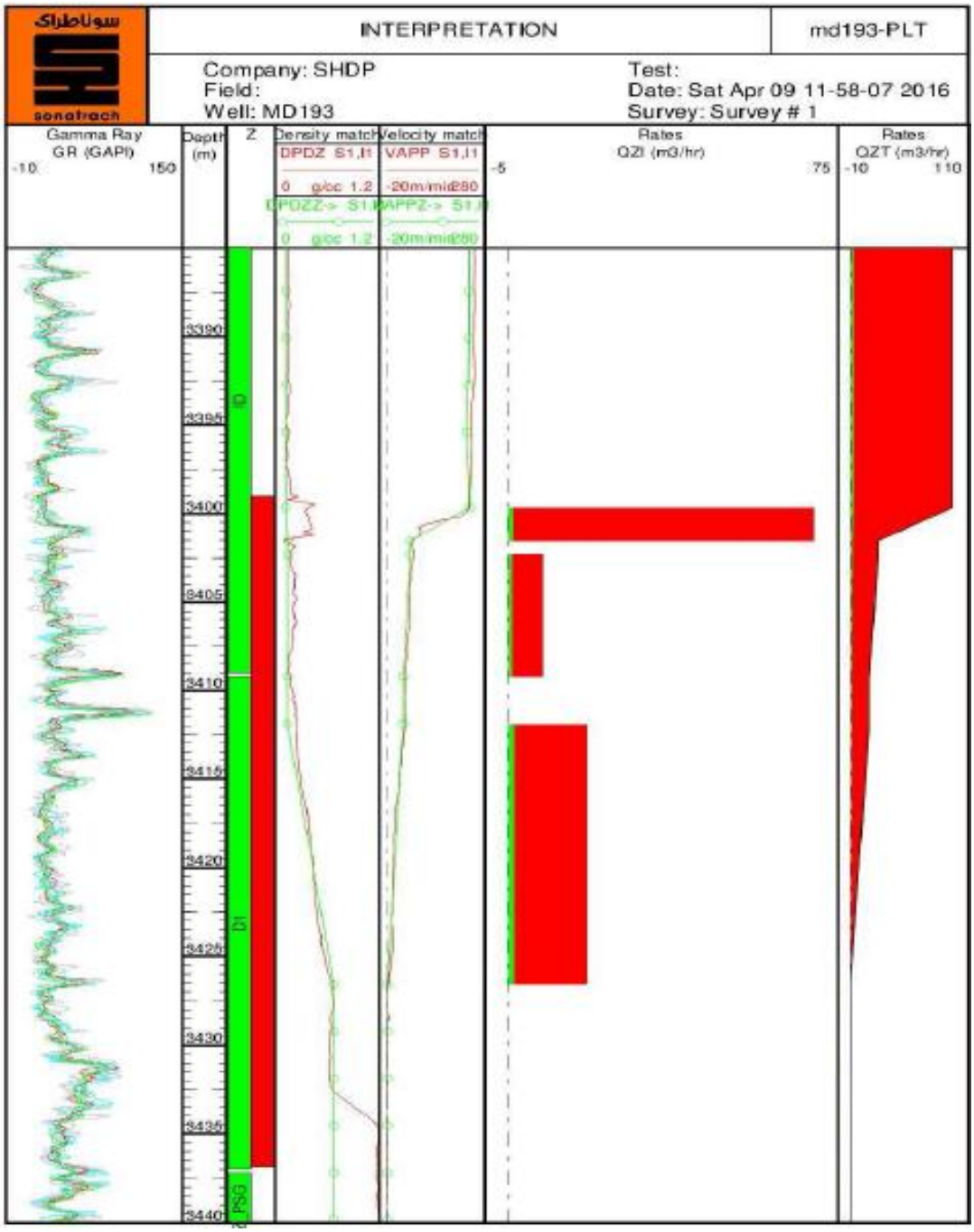

Figure IV. 18: PLT result of the well MD193 [17].

IV.3.2. The well MD45:

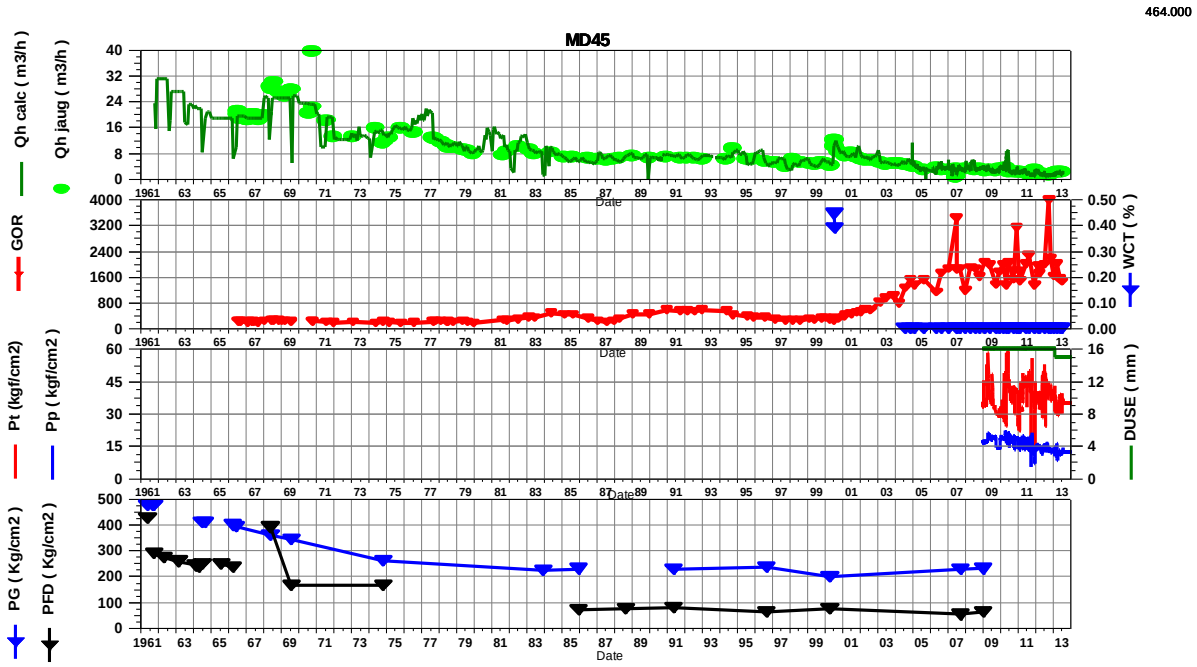

Figure IV. 19: Reservoir pressure, oil flow rate, GOR, water cut, wellhead pressure and pipeline pressure curves of the well MD45 [17].

This well was drilled in May 1961 in the southwestern part of the inter-zone 17-19 and was put on production in October 1961. In the first years of its exploitation, this well was characterized by a high flow of 15 m^3/h of oil.

According to these graphs the well starts producing with a high rate and a reservoir pressure of 475 kg/cm^2.

By the year 2003 the gas breakthrough problem starts to occur in this well and the GOR reaches 1800 m^3/m^3 and was closed in 2013

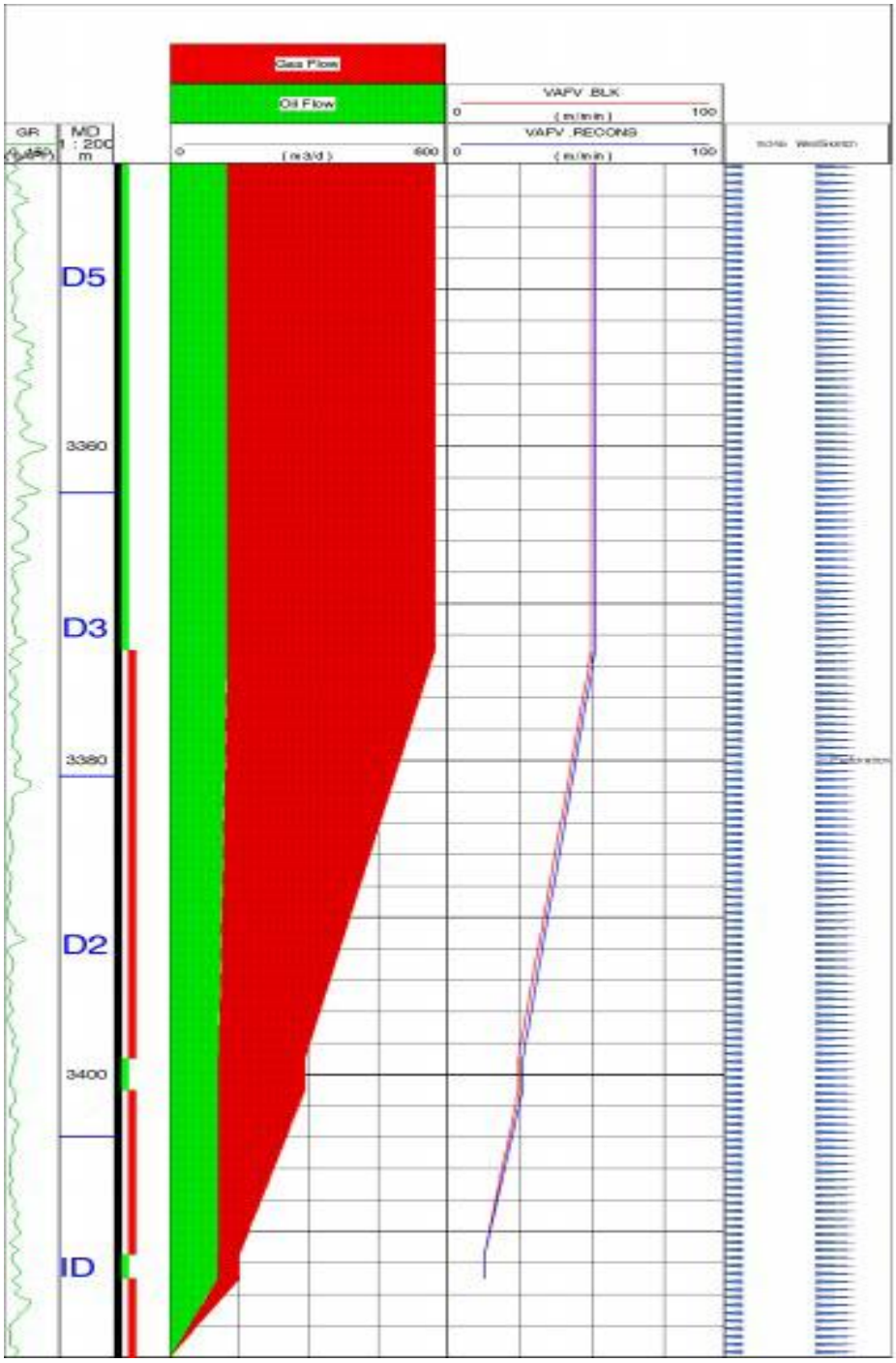

Figure IV. 20: PLT result of the well MD45 [17].

The majority of the oil production comes from the 3413 - 3418 interval (ID). Gas is present in all drains, however D3 and D2 contain the largest portion: 58.58% in interval 3373 - 3399 and 31% in interval 3410 - 3411.5m.

IV.3.3. The well MD231:

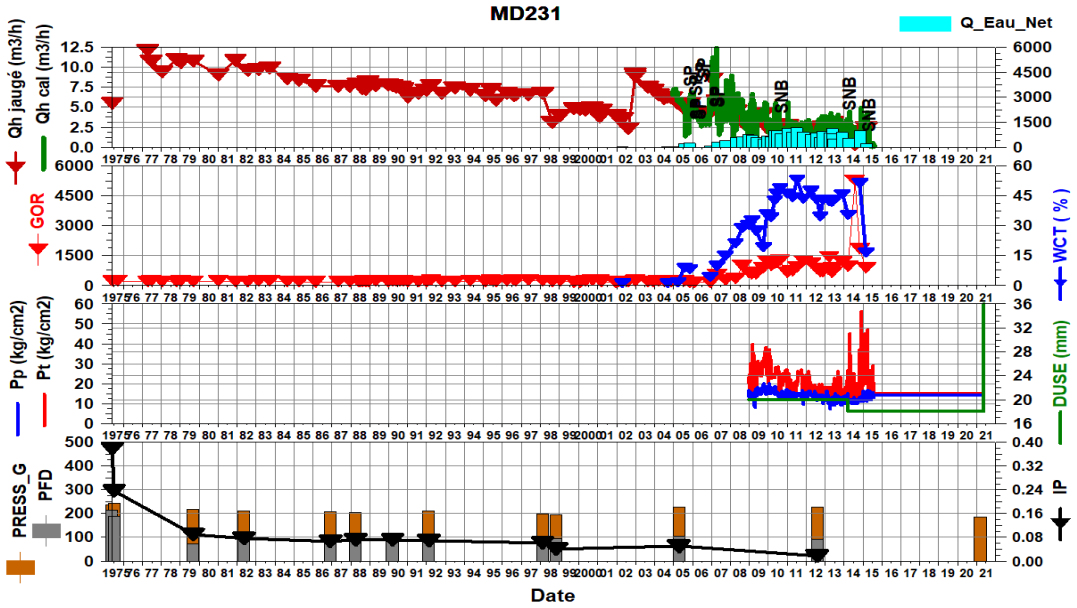

Figure IV. 21: Reservoir pressure, oil flow rate, GOR, water cut, wellhead pressure and pipeline pressure curves of the well MD231 [17].

This well starts producing in 1975 with an average rate of 10 m^3/h of oil, and at an average reservoir pressure of 300 kg/cm^2.

The water breakthrough problem starts to occur in this well in 2006, and the water cut reaches to 50% which ends up to closing the well in 2015.

IV.3.4. The well MD126:

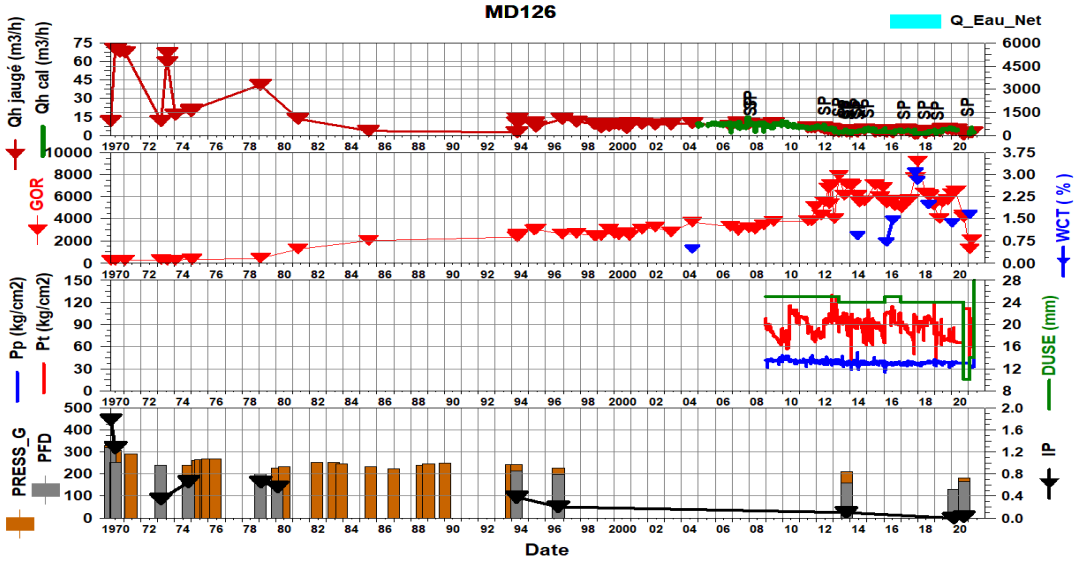

Figure IV. 22: Reservoir pressure, oil flow rate, GOR, water cut, wellhead pressure and pipeline pressure curves of the well MD126 [17].

This well was drilled in march 1970 in the southwestern part of the inter-zone 17-19 and was put in production in September 1970.

According to these graphs the well starts producing with a high rate and a reservoir pressure of 307 kg/cm^2.

Gas breakthrough problem starts to occur in this well and the 2011, and it causes the increase of the GOR from 3860 m^3/m^3 on 15/10/2011 to 7110 m^3/m^3 on 15/12/2012.

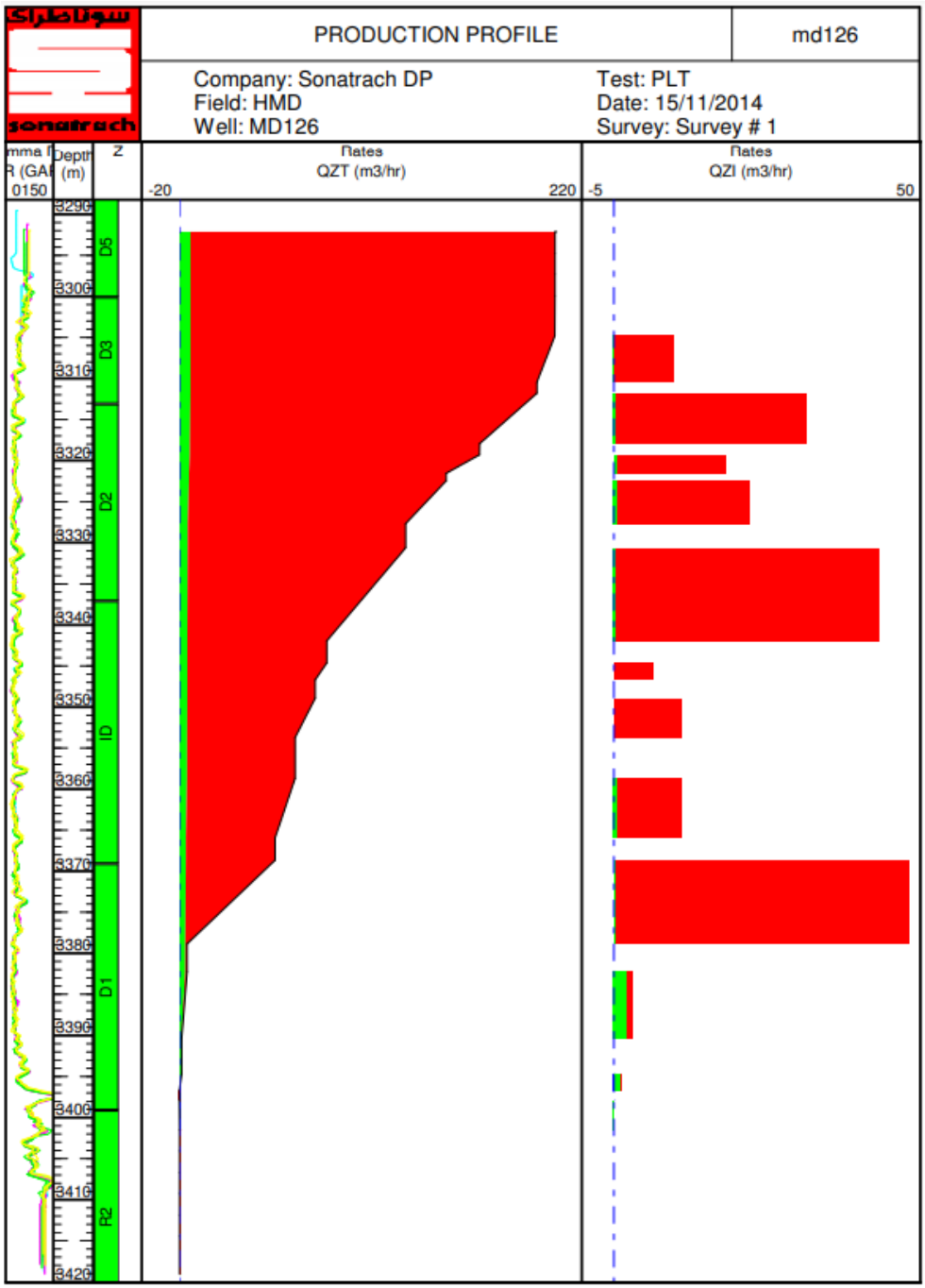

Figure IV. 23: PLT result of the well MD126 [17].

The interpretation of this PLT shows that the gas breakthroughs are located in the following areas:

- [3311.8m - 3317.9m].
- [3330.6m - 3341.9m].
- [3368.7m - 3378.9m].

Due to the difficulties of exploitation of this well because of the gas breakthrough, a decision was made in April 2020 to do SIDE Track operation on this well which result a decrease in the GOR to 4242 m^3/m^3

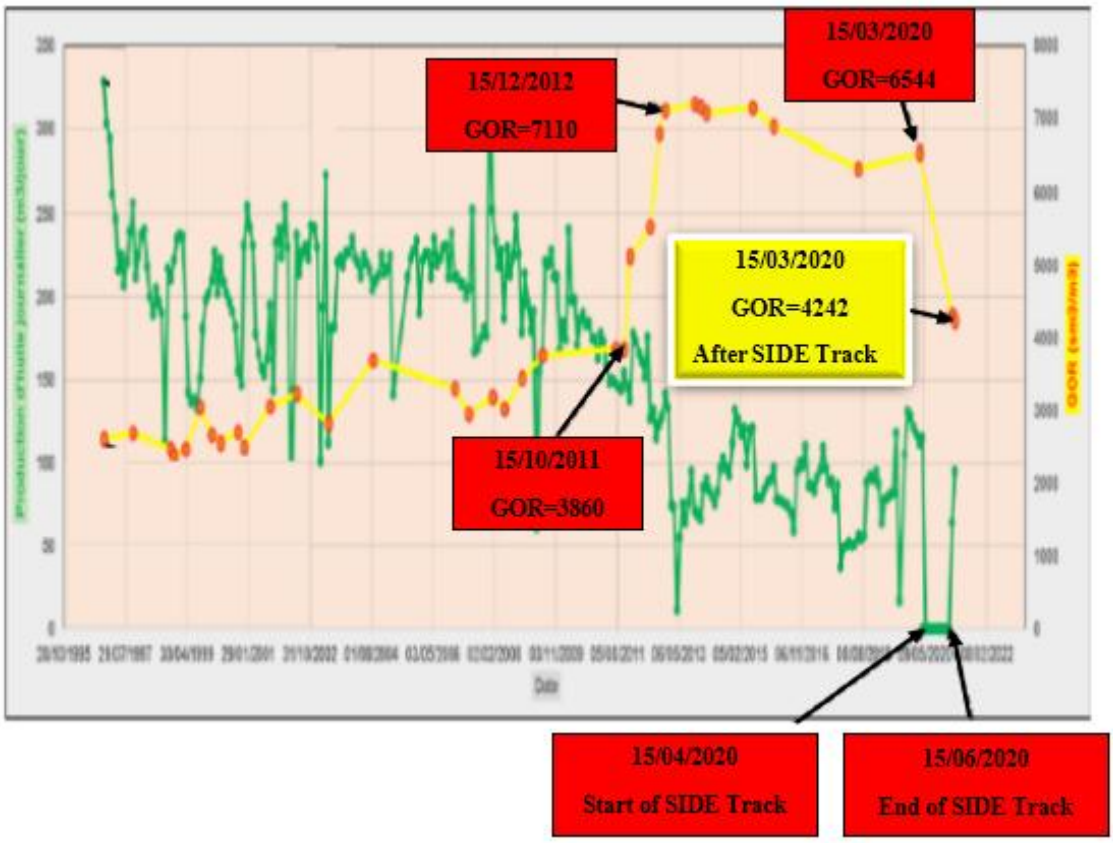

Figure IV. 24: Production history and GOR curves of the well MD126 [17].

IV.4. Conclusion:

The injection in the inter-zone 17-19 has had mixed results in terms of improved production and recovery. While it has helped to maintain reservoir pressure, in these early years, it causes a rapid decline in the production due to breakthrough problems.

The SIDE Track operation in the well MD126 shows an efficient result in solving the breakthrough problem which clear the way in reopening the injector wells and keep the pressure maintenance.

GENERAL CONCLUSION

General conclusion:

The presented work allowed us to reach the following conclusions:

- The natural drainage mechanisms in this area are the expansion of the oil and its dissolved gas (more than 70%) and the expansion of the rock (less than 30%).
- The application of the material balance method allowed us to re-evaluate the initial oil in-place reserves of the inter zone 17-19 (60 810 000 Stm^3).
- The recovery factor before the start of injection was 5.52%, currently it reaches 36% after injecting HCPVI= 57.9%.
- The inter-zone 17-19 has known a reservoir pressure maintenance above 200 kg/cm^2 since 1972 to this day.
- The pressure restitution method of MBAL software, allowed us to define the injection patterns and evaluate the participation factors of each well in the patterns to which it belongs.
- The proposed injection pattern configuration for the inter-zone 17-19 takes into consideration the existence of faults and barriers, which has increasingly allowed injection control.
- The performance of the injection at the patterns depends strongly on the void replacement ratio. Keeping this ratio close to or slightly above 1 is necessary to ensure stable production.
- The low ratio of injector and producer wells makes the closure of any injector well particularly damaging to the injection-withdrawal balance.
- The gas breakthrough caused a significant drop in production of the wells MD193 and MD45.
- The water breakthrough caused the closing of the wells MD231.
- The gas and water breakthrough problems causes the closing of most injector wells (only MD18 still injecting).
- The SIDE Track operation was an efficient solution to gas breakthrough problem in the well MD126.

Recommendations:

- ✓ Stop drilling in the inter-zone 17-19 due to the drop in reservoir pressure.
- ✓ Increase the frequency of gauging for the wells with gas breakthroughs problem for a better monitoring of the evolution of the gas production.
- ✓ Continuous monitoring of the wells and the reservoir with the pattern monitoring to maintain a good condition of the reservoir.
- ✓ Examine the possibility of doing a SIDE Track operation on the wells MD45 and MD193 to solve the gas breakthrough problem.
- ✓ Perform a PLT on the well MD231 to locate the water producing zones and find a solution to the water breakthrough problem.
- ✓ Study the possibility of converting the injector wells into WAG to see the efficiency of this technique in this zone.
- ✓ The necessity to reopen the injector wells to avoid the pressure drop below the bubble pressure.
- ✓ Focus the injection in the pattern 1 to recover the maximum of oil.
- ✓ Use interference tests to reveal the distribution of faults.

References

[1]. Abubaker H. Alagorni, Zulkefli Bin Yaacob, and Abdurahman H. Nour An Overview of Oil Production Stages: Enhanced Oil Recovery Techniques and Nitrogen Injection September 2015

[2]. AdnanAjam Abed Mohammed Jawad Zeinalabideen, Integrated approach of fluid modeling using material balance technique to estimate oil in place, case study: Northern IRAQ May 2021

[3]. Ahmed, T. (2019). Principles of Waterflooding. Reservoir Engineering Handbook, 901–1107.

[4]. Ahmed, T. (2019). Oil Recovery Mechanisms and the Material Balance Equation. Reservoir Engineering Handbook, 751–818.

[5]. Alamooti, A. M., & Malekabadi, F. K. (2018). An Introduction to Enhanced Oil Recovery. Fundamentals of Enhanced Oil and Gas Recovery from Conventional and Unconventional Reservoirs, 1–40.

[6]. Bailey B, Crabtree M, Tyrie J, Elphick J, Kuchuk F, Romano C, Roodhart L ; „„Water control", Oilfield review (2000)

[7]. Darvishnezhad, M. J., Moradi, B., Zargar, G., Jannatrostami, A., & Montazeri, G. H. (2010). Study of Various Water Alternating Gas Injection Methods in 4- and 5-Spot Injection Patterns in an Iranian Fractured Reservoir. Proceedings of Trinidad and Tobago Energy Resources Conference.

[8]. Gyan, P. S., Xie, C., Brantson, E. T., & Atuahene, S. (2019). Computer modeling and simulation for undersaturated primary drive recovery mechanism. Advances in Mechanical Engineering,

[9]. L.P. Dake Fundamentals of Reservoir Engineering Elsevier (1978)

[10]. Mohammed A Samba 1, Mahmoud O. Elsharafi Literature Review of Water Alternation Gas Injection 03 November 2018

[11]. P. Glover, Formation Evaluation MSc Course Notes, Aberdeen University, pp. 19-26, 2001

[12]. Richard O. Baker, ... Jerry L. Jensen, in Practical Reservoir Engineering and Characterization, 2015

[13]. Romero-Zern, L. (2012). Advances in Enhanced Oil Recovery Processes. Introduction to Enhanced Oil Recovery (EOR) Processes and Bioremediation of Oil-Contaminated Sites.

[14]. S. Kokal and A. Al-Kaabi, Enhanced Oil Recovery: Challenges & Opportunities, World Petroleum Council: Official Publication, 2010

[15]. Satter, A., & Iqbal, G. M. (2016). Primary recovery mechanisms and recovery efficiencies. Reservoir Engineering, 185–193.

[16]. Secondary and Tertiary Recovery Methods. (2018). Geophysical Monograph Series, 459–502.

[17]. SONATRACH DATA base

[18]. Speight, J. G. (2016). General Methods of Oil Recovery. Introduction to Enhanced Recovery Methods for Heavy Oil and Tar Sands, 253–322

[19]. T. Ahmed, N. Meehan. Advanced Reservoir Management and Engineering. s.l. : Gulf Professional Publishing , 2011

[20]. Temizel, C., Kirmaci, H., Wijaya, Z., Balaji, K., Suhag, A., Ranjith, R., … Aminzadeh, F. (2016). Production Optimization through Voidage Replacement using Triggers for Production Rate. SPE Heavy Oil Conference and Exhibition.

[21]. Vipin Gupta, Petroleum Development of Oman; Saadi Faisal ; Petroleum Development of Oman, Abdul Aziz Belushi, Petroleum development of Oman Active Water Flood (Pattern) Management Through Modern Online Production Data Base Systems Using Classical Techniques: A Case Study On Heavy Oil Fields In South Oman December 2009

[22]. Vishnyakov, V., Suleimanov, B., Salmanov, A., & Zeynalov, E. (2020). Oil recovery stages and methods. Primer on Enhanced Oil Recovery, 53–63.

[23]. Vishnyakov, V., Suleimanov, B., Salmanov, A., & Zeynalov, E. (2020). Water altering gas injection. Primer on Enhanced Oil Recovery, 127–139.

[24]. Xia, J., Liu, P., Jiao, Y., Dong, M., Zhang, J., & Zhang, J. (2018). Characteristics and quantitative study on gas breakthrough in developing Yaha-2 condensate gas reservoir in Tarim Basin, China. Energy Exploration & Exploitation, 36(4), 787–800.

[25]. S. Pramanik, G. L. Kulukuru, M. Mishra, Miscible Viscous Fingering: Application in Chromatographic Columns and Aquifers (2012).

[26]. https://www.britannica.com/technology/petroleum-production/Recovery-of-oil-and-gas consulted 13/05/2021

[27]. https://www.rigzone.com/training/insight.asp?insight_id=345&c_id consulted 19/05/2021

[28]. Princewill Ikpeka, Mbagwu Chinedu, Effect of initial Gas-Oil ratio, produced Gas Re-Injection and Formation Compressibility on predicted production performance of a Depletion Drive Reservoir December 2018.

[29]. https://www.petropedia.com/understanding-reservoir-drive-mechanisms/2/9856 consulted 10/05/2021.

[30]. https://petroinfo.weebly.com/production.html consulted 07/05/2021.

[31]. Okotie, S., & Ikporo, B. (2018). Linear Form of Material Balance Equation. Reservoir Engineering, 245–288

ANNEXES

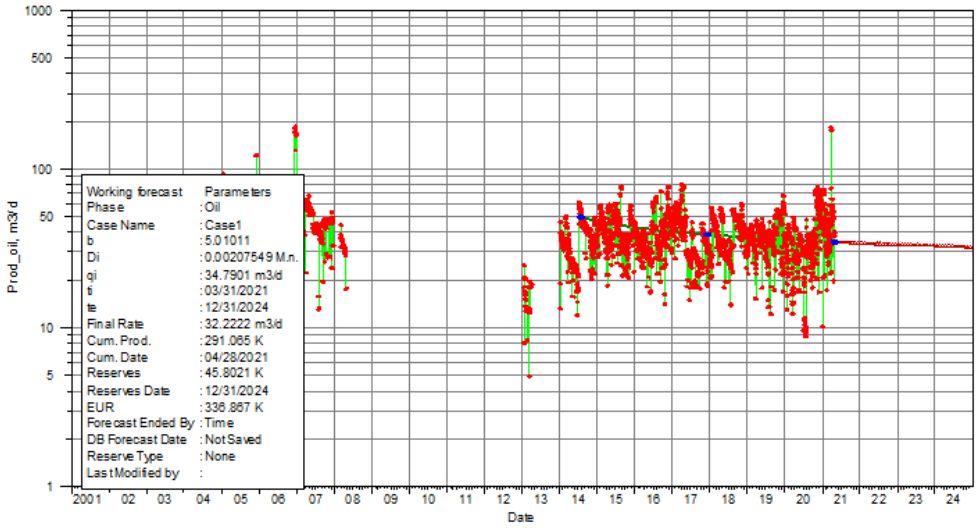

Annexe1: DCA of the well MDZ534

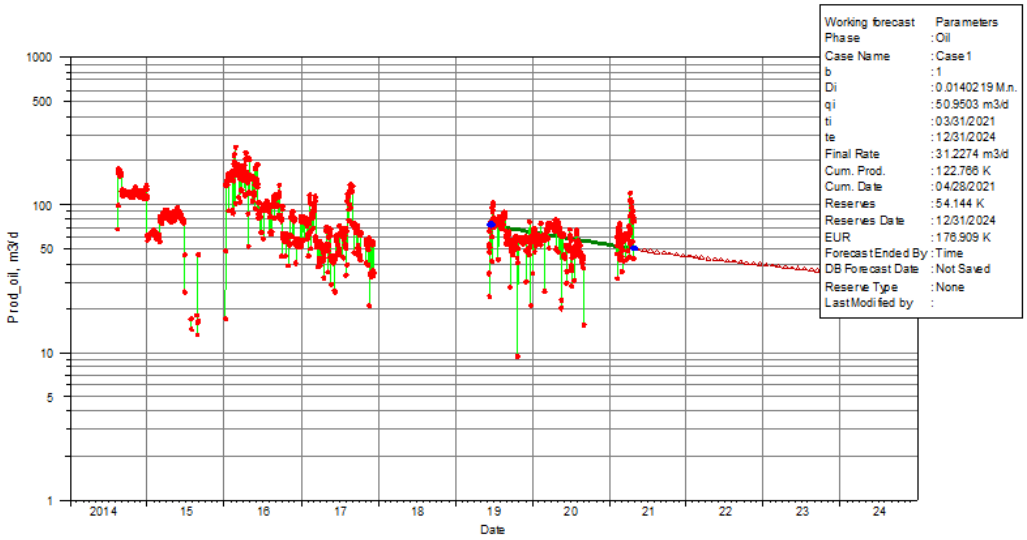

Annexe2: DCA of the well MD653

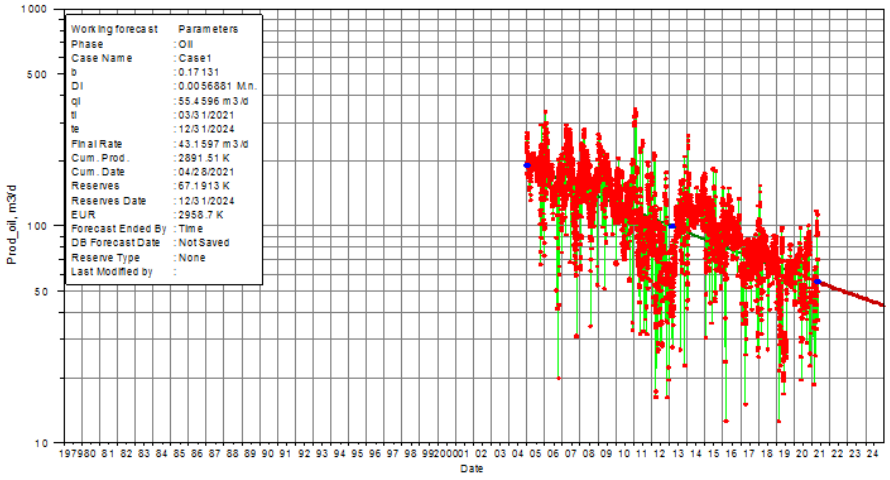

Annexe3: DCA of the well MD318

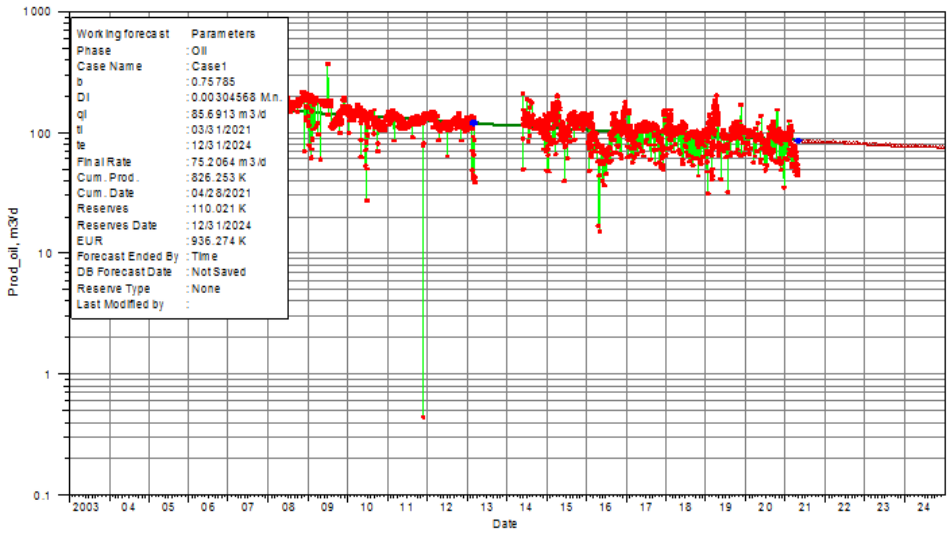

Annexe4: DCA of the well MD254

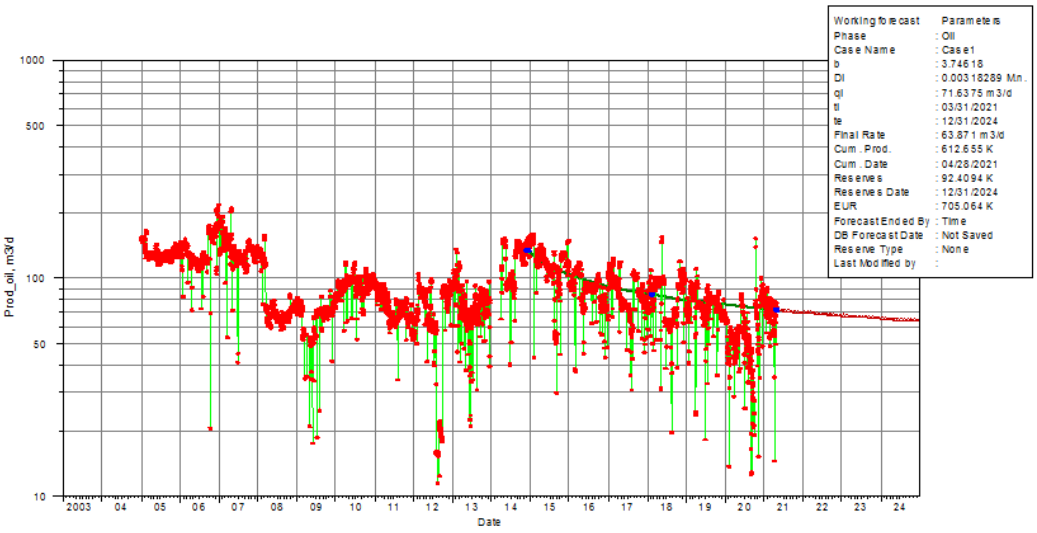

Annexe5: DCA of the well MDZ548

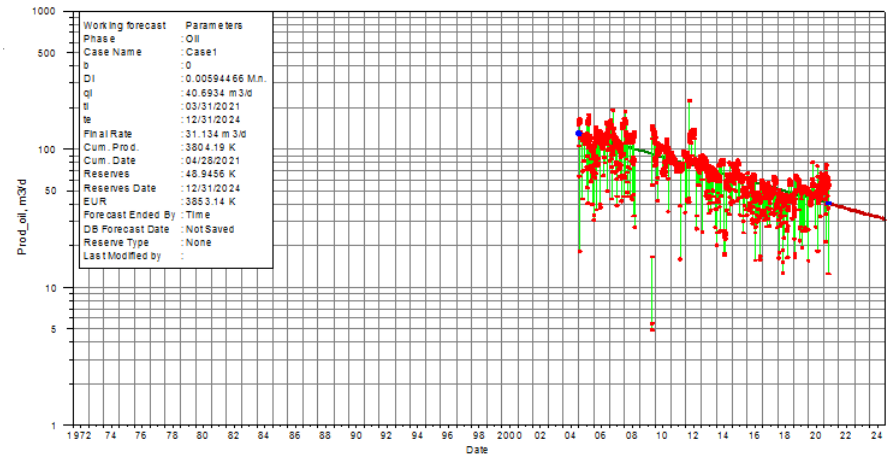

Annexe6: DCA of the well MD193

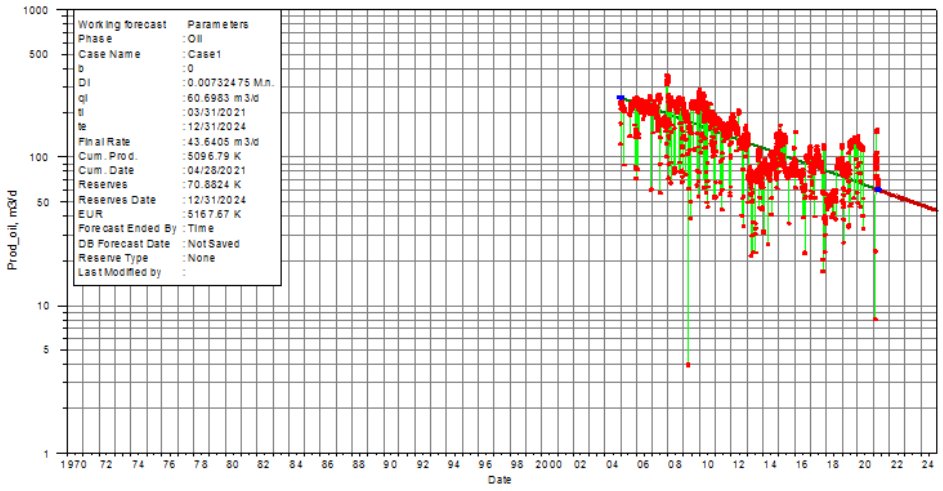

Annexe7: DCA of the well MD126

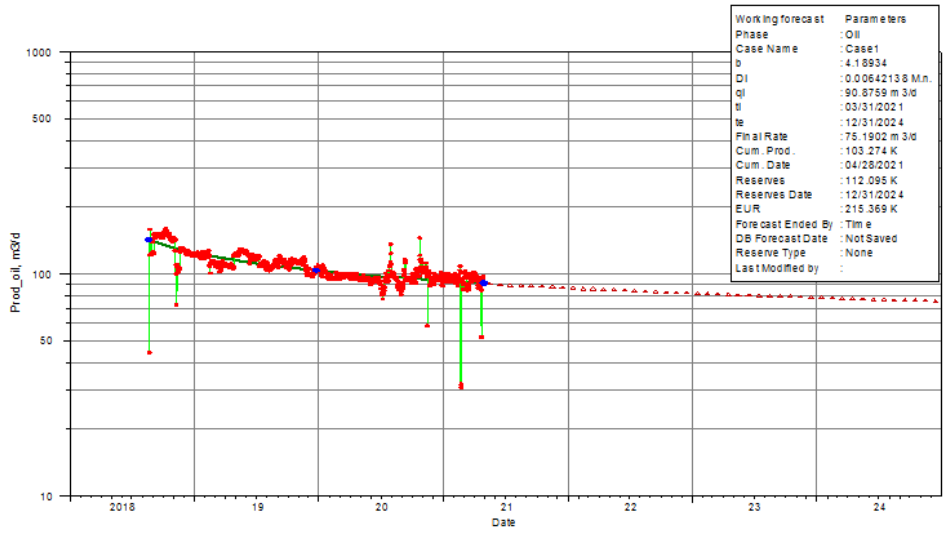

Annexe8: DCA of the well MDZ703

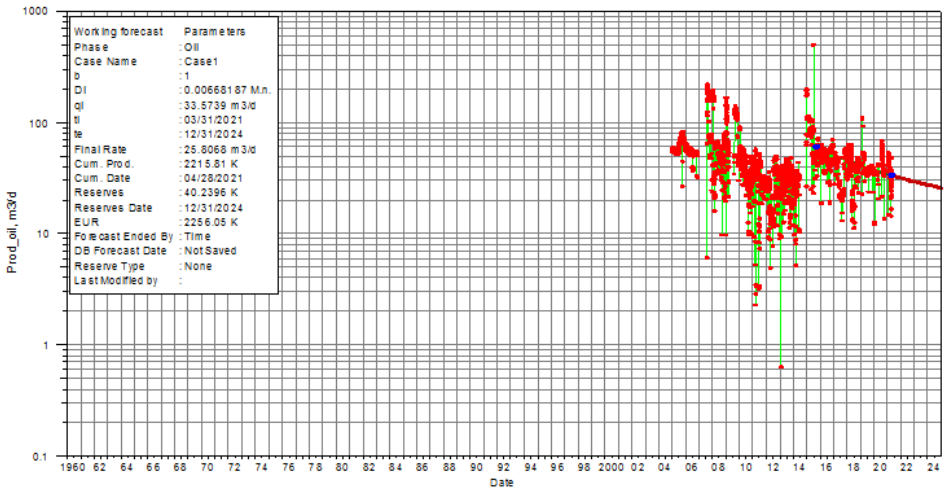

Annexe9: DCA of the well MD33

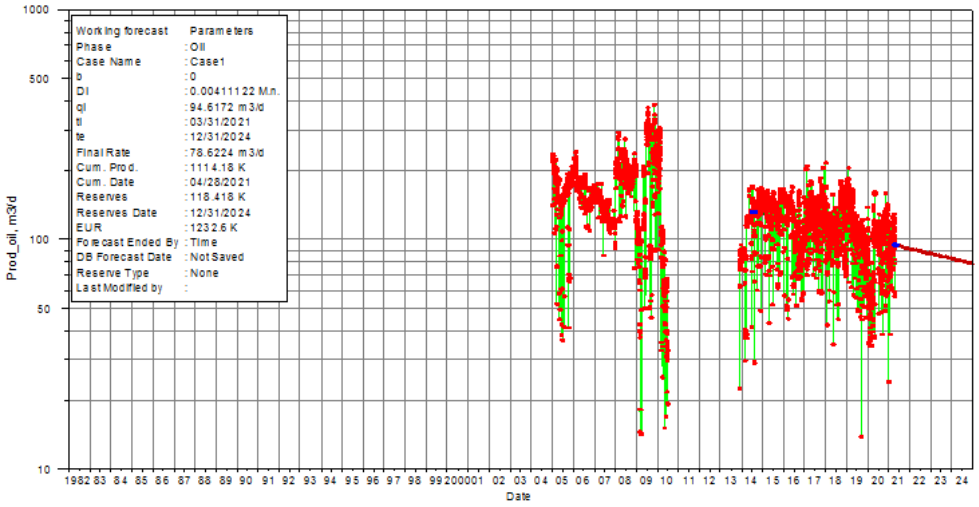

Annexe10: DCA of the well MD358

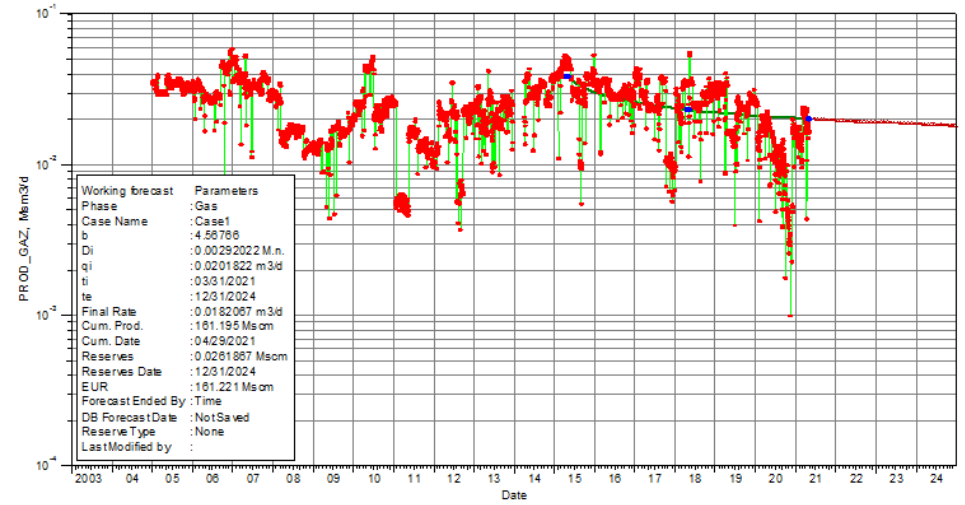

Annexe11: DCA of the well MDZ548 gas production

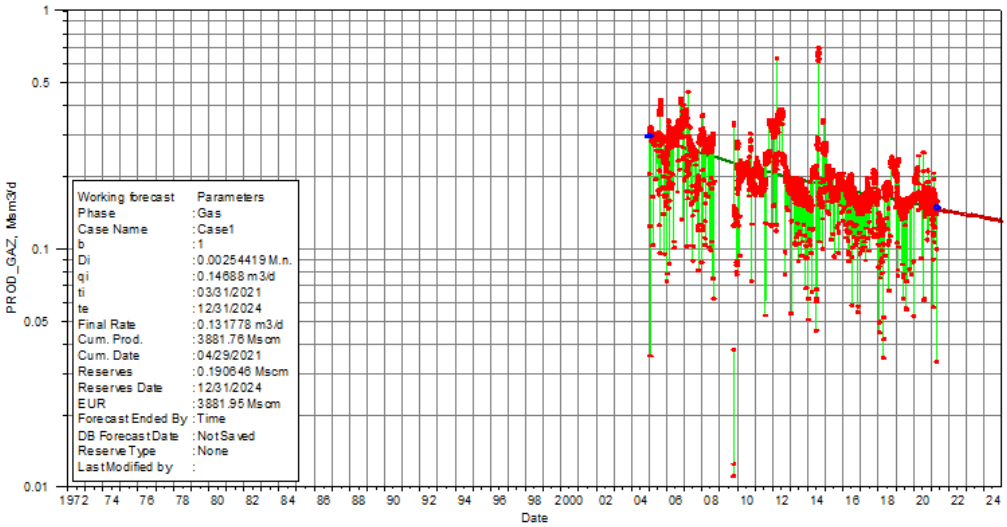

Annexe12: DCA of the well MD193 gas production

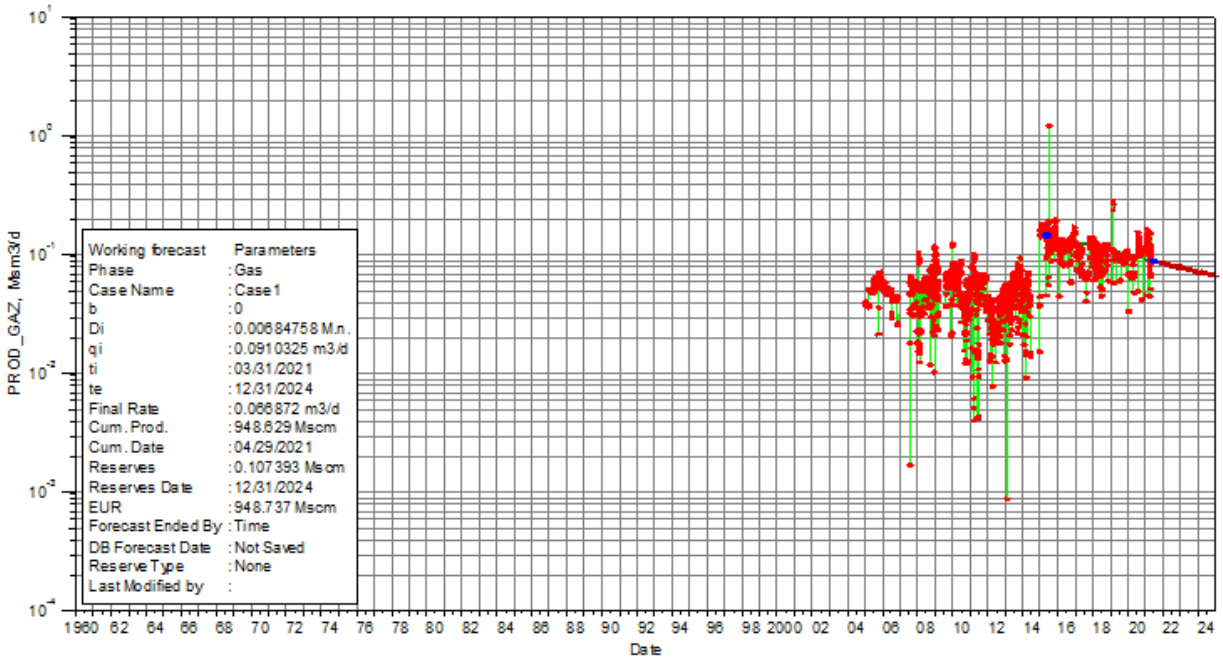

Annexe13: DCA of the well MD33 gas production

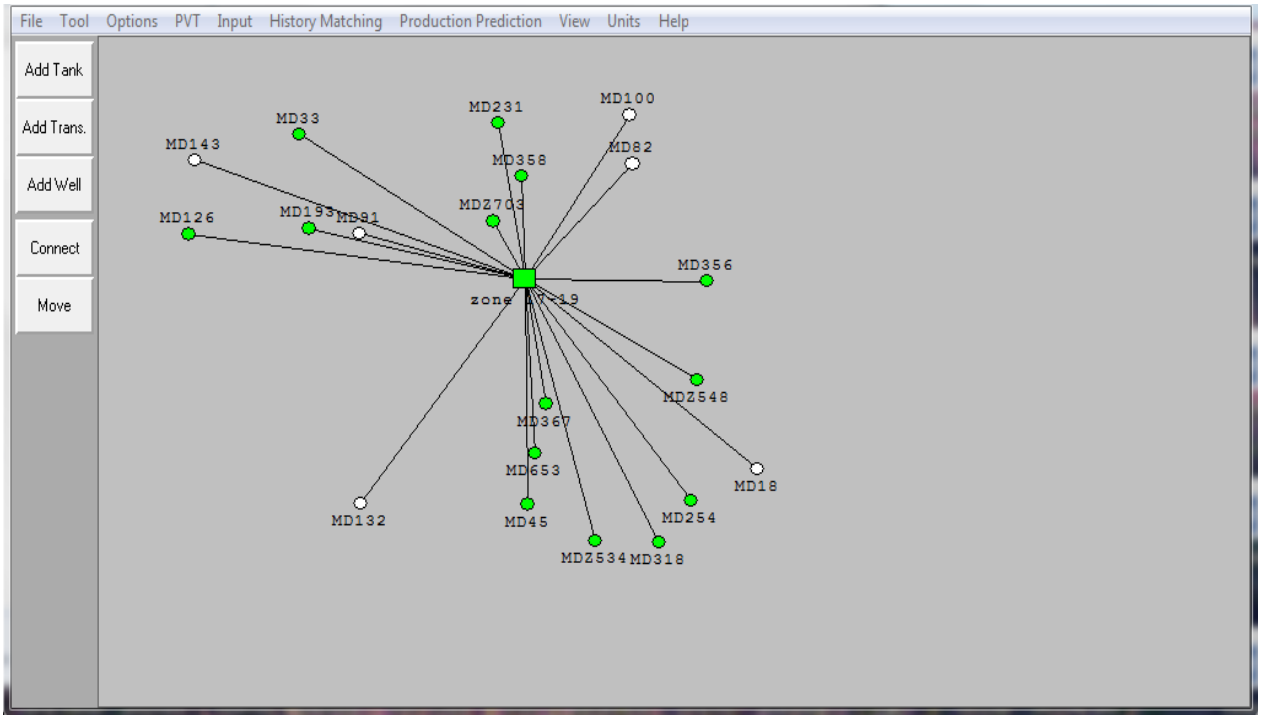

Annexe14: Interface of MBAL software of the inter-zone17-19

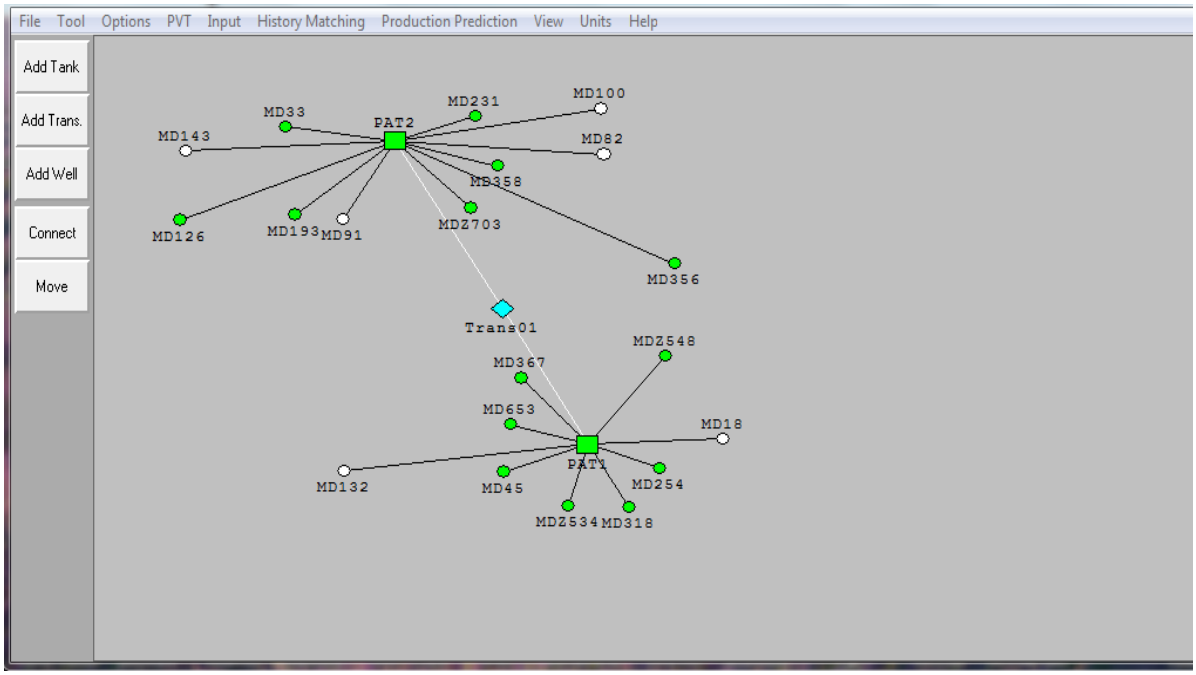

Annexe15: Interface of MBAL software: patterns of the inter-zone17-19

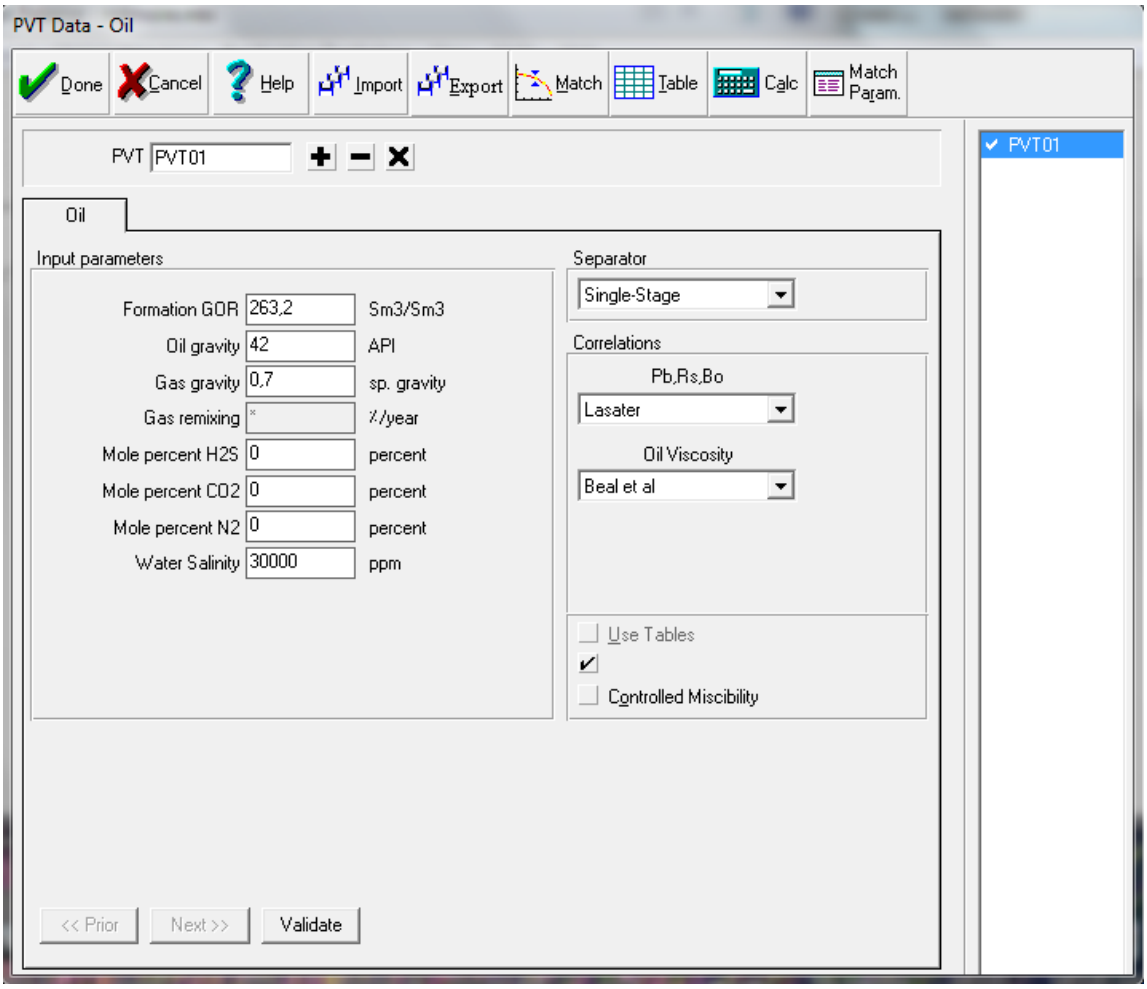

Annexe16: Interface of MBAL software: PVT data of the inter-zone17-19

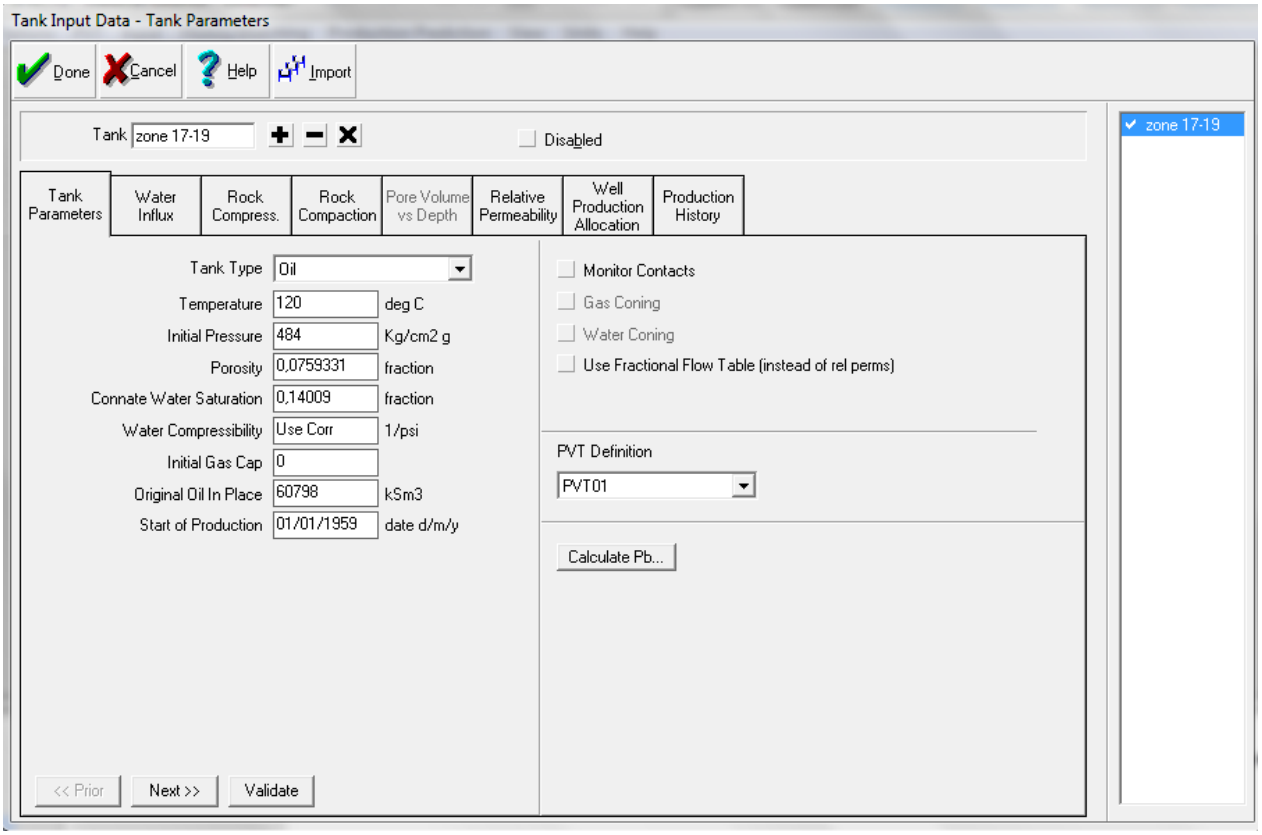

Annexe17: Interface of MBAL software: data of the inter-zone17-19

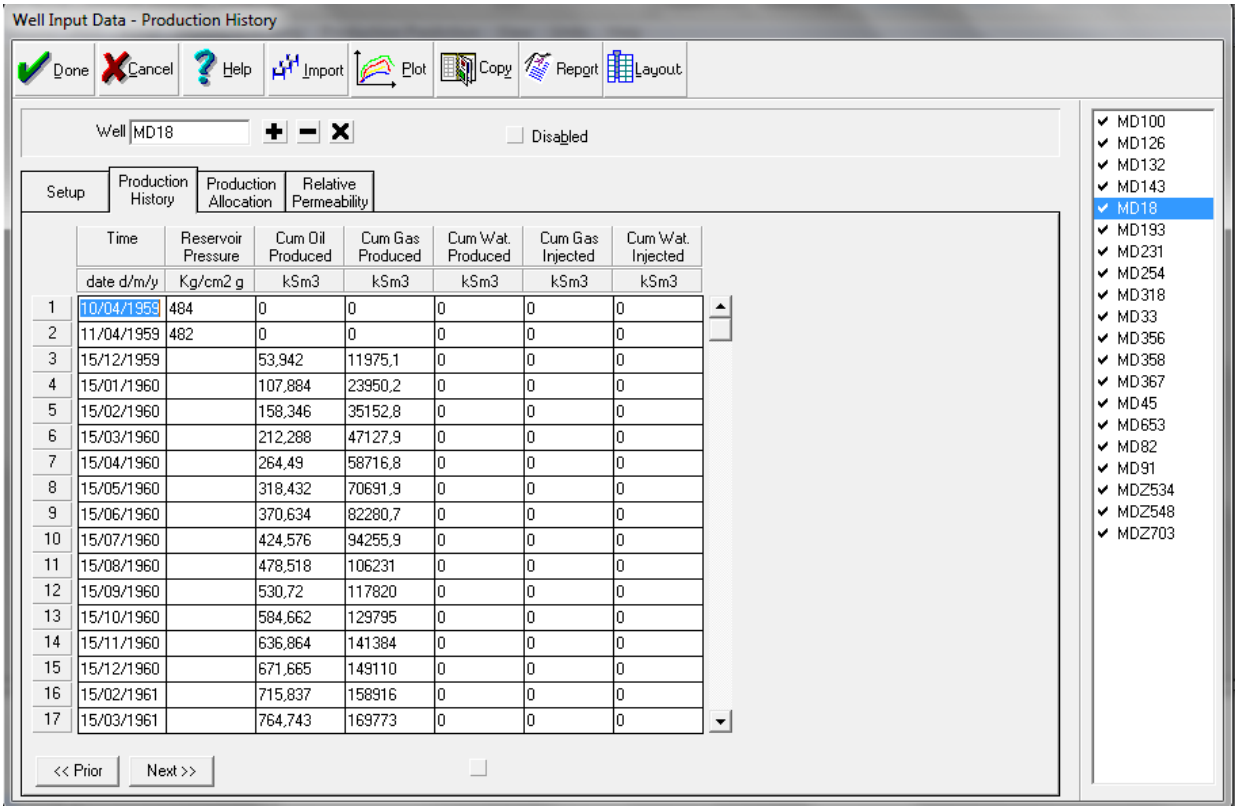

	Time	Reservoir Pressure	Cum Oil Produced	Cum Gas Produced	Cum Wat. Produced	Cum Gas Injected	Cum Wat. Injected
	date d/m/y	Kg/cm2 g	kSm3	kSm3	kSm3	kSm3	kSm3
1	10/04/1959	484	0	0	0	0	0
2	11/04/1959	482	0	0	0	0	0
3	15/12/1959		53,942	11975,1	0	0	0
4	15/01/1960		107,884	23950,2	0	0	0
5	15/02/1960		158,346	35152,8	0	0	0
6	15/03/1960		212,288	47127,9	0	0	0
7	15/04/1960		264,49	58716,8	0	0	0
8	15/05/1960		318,432	70691,9	0	0	0
9	15/06/1960		370,634	82280,7	0	0	0
10	15/07/1960		424,576	94255,9	0	0	0
11	15/08/1960		478,518	106231	0	0	0
12	15/09/1960		530,72	117820	0	0	0
13	15/10/1960		584,662	129795	0	0	0
14	15/11/1960		636,864	141384	0	0	0
15	15/12/1960		671,665	149110	0	0	0
16	15/02/1961		715,837	158916	0	0	0
17	15/03/1961		764,743	169773	0	0	0

Annexe18: Interface of MBAL software: data wells of the inter-zone17-19